

## **INFORMATION TO USERS**

**This manuscript has been reproduced from the microfilm master. UMI films the text directly from the original or copy submitted. Thus, some thesis and dissertation copies are in typewriter face, while others may be from any type of computer printer.**

**The quality of this reproduction is dependent upon the quality of the copy submitted. Broken or indistinct print, colored or poor quality illustrations and photographs, print bleedthrough, substandard margins, and improper alignment can adversely affect reproduction.**

**In the unlikely event that the author did not send UMI a complete manuscript and there are missing pages, these will be noted. Also, if unauthorized copyright material had to be removed, a note will indicate the deletion.**

**Oversize materials (e.g., maps, drawings, charts) are reproduced by sectioning the original, beginning at the upper left-hand corner and continuing from left to right in equal sections with small overlaps.**

**Photographs included in the original manuscript have been reproduced xerographically in this copy. Higher quality 6" x 9" black and white photographic prints are available for any photographs or illustrations appearing in this copy for an additional charge. Contact UMI directly to order.**

**ProQuest Information and Learning  
300 North Zeeb Road, Ann Arbor, MI 48106-1346 USA  
800-521-0600**

**UMI<sup>®</sup>**





Université d'Ottawa • University of Ottawa



**THE DISPLACEMENT OF OIL BY AQUEOUS SOLUTIONS  
IN POROUS MEDIA**

**By**

**MARIAME SAKANOKO**

**A thesis submitted to the Faculty of Graduate and Postdoctoral Studies  
in partial fulfilment of the requirements for the  
Degree of Master of Applied Science  
in Chemical Engineering**

**DEPARTMENT OF CHEMICAL ENGINEERING  
UNIVERSITY OF OTTAWA  
OTTAWA, ONTARIO**

**August 2001**



**National Library  
of Canada**

**Acquisitions and  
Bibliographic Services**

**395 Wellington Street  
Ottawa ON K1A 0N4  
Canada**

**Bibliothèque nationale  
du Canada**

**Acquisitions et  
services bibliographiques**

**395, rue Wellington  
Ottawa ON K1A 0N4  
Canada**

*Your file Votre référence*

*Our file Notre référence*

**The author has granted a non-exclusive licence allowing the National Library of Canada to reproduce, loan, distribute or sell copies of this thesis in microform, paper or electronic formats.**

**The author retains ownership of the copyright in this thesis. Neither the thesis nor substantial extracts from it may be printed or otherwise reproduced without the author's permission.**

**L'auteur a accordé une licence non exclusive permettant à la Bibliothèque nationale du Canada de reproduire, prêter, distribuer ou vendre des copies de cette thèse sous la forme de microfiche/film, de reproduction sur papier ou sur format électronique.**

**L'auteur conserve la propriété du droit d'auteur qui protège cette thèse. Ni la thèse ni des extraits substantiels de celle-ci ne doivent être imprimés ou autrement reproduits sans son autorisation.**

0-612-67207-7

**Canada**

## **ABSTRACT**

The immiscible displacement of oil by water in a petroleum reservoir has been simulated in the laboratory using a consolidated porous medium constructed out of silica sand particles. Four distinct displacement flow modes were employed, namely horizontal, vertical upward, vertical downward, and transverse. Experiments were carried out by displacing the oil phase (heavy paraffin oil) by the aqueous phase (dyed glycerol solution) at different oil/water viscosity ratios, at different flow rates, and in the presence and absence of connate water (connate water is the name given to the very small amount of water that occurs naturally in petroleum reservoirs). The objective of this study was to investigate the effects of viscosity ratio, flow rate, and flow mode on the oil recovery efficiency. In the absence of connate water, a decrease in the oil recovery is observed when the oil/water viscosity ratio increases for all four flow modes but the displacement patterns are different for each flow mode. In the presence of connate water, the dependence of oil recovery on viscosity ratio is similar although in this case the displacement patterns are almost indistinguishable for the four different flow modes on account of coalescence of the connate water phase with the displacing aqueous phase. Without connate water, the highest recovery is obtained in the vertical upward mode where the buoyancy forces stabilize the displacement process. Conversely, in the vertical downward flow mode, the instability promoted by gravity leads to a low recovery. Comparison of the results obtained with and without connate water shows that connate water has a negative effect on the recovery and, moreover, that the synergistic effect between the viscosity ratio and the connate water reduces the oil recovery efficiency significantly.

**Keywords:** Oil recovery, viscous fingering, connate water, porous medium

## RÉSUMÉ

Le déplacement non-miscible du pétrole par l'eau dans le réservoir de pétrole a été simulé au laboratoire à l'aide d'une cellule poreuse consolidée, construite à partir de particules de sable de silice. Les déplacements ont été effectués dans quatre modes d'écoulement: horizontal, vertical ascendant, vertical descendant et transversal. Les expériences ont été réalisées en présence et en absence de l'eau conée (l'eau conée désigne la toute petite quantité d'eau présente dans les réservoirs de pétrole) en déplaçant la phase huileuse (huile de paraffine lourde) par la phase aqueuse (solution de glycérol colorée), à des rapports de viscosité huile/eau et des débits différents. L'objectif de cette recherche est d'étudier les effets du rapport de viscosité, du débit et du mode d'écoulement sur le taux de récupération de l'huile. En absence de l'eau conée, une diminution du taux de récupération est observée lorsque le rapport de viscosité huile/eau augmente pour les quatre modes d'écoulement mais, les modèles de déplacement sont différents pour chaque mode d'écoulement. En présence de l'eau conée et pour les quatre différents modes, la dépendance du taux de récupération du rapport de viscosité est similaire bien que dans ce cas, les modèles de déplacement soient presque indiscernables à cause de l'eau conée qui se mélange à la phase aqueuse. Le taux de récupération le plus élevé est obtenu en absence de l'eau conée et en mode d'écoulement vertical ascendant où les facteurs de flottabilité stabilisent le déplacement. Par contre, en mode d'écoulement vertical descendant, l'instabilité engendrée par l'effet de la gravité conduit à une faible récupération. Il ressort de la comparaison des résultats obtenus en présence et en absence de l'eau conée que l'eau conée exerce un effet négatif sur la récupération de l'huile. Bien plus, l'effet de synergie

**entre le rapport de viscosité et l'eau conée réduit considérablement le taux de récupération de l'huile.**

**Mots-clés:** Récupération du pétrole, digitation, milieu poreux, eau conée.

## **ACKNOWLEDGEMENTS**

**I would like to thank my research supervisor Dr. Graham Henry Neale for his guidance and assistance during the preparation of this thesis as well as the experimental work.**

**My thanks go to the technical staff of the Chemical Engineering Department for the technical assistance they provided.**

## TABLE OF CONTENTS

ABSTRACT.....	i
RÉSUMÉ.....	iii
ACKNOWLEDGEMENTS.....	v
TABLE OF CONTENTS.....	vi
LIST OF FIGURES.....	ix
LIST OF TABLES.....	xiv
NOMENCLATURE.....	xv
INTRODUCTION.....	1
CHAPTER I	
LITERATURE SURVEY.....	2
1.1 Oil Formation.....	2
1.2 Oil recovery.....	4
1.2.1 Primary recovery.....	4
1.2.2 Secondary recovery.....	4
1.2.3 Tertiary recovery.....	8
1.3 Displacement by fingering.....	9
1.3.1 Viscous fingering.....	9
1.3.2 Overview of fingering phenomena.....	9
1.4 Connate water.....	12
1.5 Theory.....	14
1.5.1 Dimensional analysis.....	14
1.5.2 Viscous forces.....	17

1.5.3	Gravity forces.....	18
1.5.4	Pressure difference.....	18
1.5.5	Permeability.....	19
1.5.6	Porosity.....	20
<b>CHAPTER II</b>		
<b>EXPERIMENTAL STUDIES.....</b>		<b>21</b>
2.1	Experimental materials.....	21
2.1.1	Cell properties.....	21
2.1.2	Apparatus.....	23
2.2	Experimental method.....	26
2.2.1	Saturation process.....	26
2.2.2	Displacement process.....	27
2.2.3	Cleaning and drying processes.....	27
2.3	Experiments performed.....	28
2.3.1	Homogeneity of the consolidated porous medium.....	28
2.3.2	Reproducibility of the experiments.....	28
2.3.3	Immiscible displacements.....	31
<b>CHAPTER III</b>		
<b>RESULTS AND DISCUSSION.....</b>		<b>36</b>
3.1	Effects of time on fingering patterns.....	36
3.2	Displacements in the absence of connate water.....	46
3.2.1	Horizontal flow mode.....	46
3.2.2	Vertical upward flow mode.....	54
3.2.3	Vertical downward flow mode.....	62

3.2.4	Transverse flow mode.....	70
3.3	Displacements in the presence of connate water.....	78
3.4	Effects of flow mode.....	89
3.5	Comparison with and without connate water.....	90
	CONCLUSIONS.....	94
	RECOMMENDATIONS.....	95
	REFERENCES.....	96

## LIST OF FIGURES

1.1	Oil formation.....	3
1.2	Displacement process.....	5
1.3	Primary recovery.....	6
1.4	Water flooding process.....	7
1.5	Displacement by fingering.....	10
1.6	Connate water.....	13
2.1	Experimental set-up.....	24
2.2	Schematic of the experimental set-up.....	24
2.3	Specific orientations of the cell.....	25
2.4	Homogeneity test.....	29
2.5	Reproducibility experiments for glycerol solution (75%) displacing heavy paraffin oil at $Q = 0.78\text{ml/min}$ in horizontal mode.....	30
3.1	Development of the fingering patterns without connate water in the horizontal flow mode.....	38
3.2	Development of the fingering patterns without connate water in the vertical upward flow mode.....	39
3.3	Development of the fingering patterns without connate water in the vertical downward flow mode.....	40
3.4	Development of the fingering patterns without connate water in the transverse flow mode.....	41
3.5	Development of the fingering patterns with connate water in the horizontal flow mode.....	42

3.6	Development of the fingering patterns with connate water in the vertical upward flow mode.....	43
3.7	Development of the fingering patterns with connate water in the vertical downward flow mode.....	44
3.8	Development of the fingering patterns with connate water in the transverse flow mode.....	45
3.9	Effects of flow rate on the horizontal flow mode patterns at a given viscosity ratio $\mu_o/\mu_w = 143.5$ .....	48
3.10	Effects of flow rate on the horizontal flow mode patterns at a given viscosity ratio $\mu_o/\mu_w = 49.0$ .....	49
3.11	Effects of flow rate on the horizontal flow mode patterns at a given viscosity ratio $\mu_o/\mu_w = 3.3$ .....	50
3.12	Effects of viscosity ratio on the horizontal flow mode patterns at a given flow rate $Q = 0.23\text{ml/min}$ .....	51
3.13	Effects of viscosity ratio on the horizontal flow mode patterns at a given flow rate $Q = 0.78\text{ml/min}$ .....	52
3.14	Recovery vs. viscosity ratio (Horizontal mode-without connate water).....	53
3.15	Effects of flow rate on the vertical upward flow mode patterns at a given viscosity ratio $\mu_o/\mu_w = 143.5$ .....	56
3.16	Effects of flow rate on the vertical upward flow mode patterns at a given viscosity ratio $\mu_o/\mu_w = 49.0$ .....	57
3.17	Effects of flow rate on the vertical upward flow mode patterns at a given viscosity ratio $\mu_o/\mu_w = 3.3$ .....	58

3.18	Effects of viscosity ratio on the vertical upward flow mode patterns at a given flow rate $Q = 0.23\text{ml/min}$ .....	59
3.19	Effects of viscosity ratio on the vertical upward flow mode patterns at a given flow rate $Q = 0.78\text{ml/min}$ .....	60
3.20	Recovery vs. viscosity ratio (Vertical upward-without connate water).....	61
3.21	Effects of flow rate on the vertical downward flow mode patterns at a given viscosity ratio $\mu_o/\mu_w = 143.5$ .....	64
3.22	Effects of flow rate on the vertical downward flow mode patterns at a given viscosity ratio $\mu_o/\mu_w = 49.0$ .....	65
3.23	Effects of flow rate on the vertical downward flow mode patterns at a given viscosity ratio $\mu_o/\mu_w = 3.3$ .....	66
3.24	Effects of viscosity ratio on the vertical downward flow mode patterns at a given flow rate $Q = 0.23\text{ml/min}$ .....	67
3.25	Effects of viscosity ratio on the vertical downward flow mode patterns at a given flow rate $Q = 0.78\text{ml/min}$ .....	68
3.26	Recovery vs. viscosity ratio (Vertical downward-without connate water)...	69
3.27	Effects of flow rate on the transverse flow mode patterns at a given viscosity ratio $\mu_o/\mu_w = 143.5$ .....	72
3.28	Effects of flow rate on the transverse flow mode patterns at a given viscosity ratio $\mu_o/\mu_w = 49.0$ .....	73
3.29	Effects of flow rate on the transverse flow mode patterns at a given viscosity ratio $\mu_o/\mu_w = 3.3$ .....	74

3.30	Effects of viscosity ratio on the transverse flow mode patterns at a given flow rate $Q = 0.23\text{ml/min}$ .....	75
3.31	Effects of viscosity ratio on the transverse flow mode patterns at a given flow rate $Q = 0.78\text{ml/min}$ .....	76
3.32	Recovery vs. viscosity ratio (Transverse-without connate water).....	77
3.33	Effects of flow rate on the horizontal flow mode patterns at a given viscosity ratio $\mu_o/\mu_w = 49.0$ (With connate water).....	80
3.34	Effects of flow rate on the vertical upward flow mode patterns at a given viscosity ratio $\mu_o/\mu_w = 49.0$ (With connate water).....	81
3.35	Effects of flow rate on the vertical downward flow mode patterns at a given viscosity ratio $\mu_o/\mu_w = 49.0$ (With connate water).....	82
3.36	Effects of flow rate on the transverse flow mode patterns at a given viscosity ratio $\mu_o/\mu_w = 49.0$ (With connate water).....	83
3.37	Effects of viscosity ratio on the vertical upward flow mode patterns at a given flow rate $Q = 0.78\text{ml/min}$ (With connate water).....	84
3.38	Recovery vs. viscosity ratio (Horizontal mode-with connate water).....	85
3.39	Recovery vs. viscosity ratio (Vertical upward mode-with connate water)...	86
3.40	Recovery vs. viscosity ratio (Vertical downward mode-with connate water).....	87
3.41	Recovery vs. viscosity ratio (Transverse mode-with connate water).....	88
3.42	Effects of flow mode in the absence of connate water for $\mu_o/\mu_w = 143.5$ and $Q = 0.23\text{ml/min}$ .....	91

<b>3.43</b>	<b>Effects of flow mode in the absence of connate water</b>	
	for $\mu_o/\mu_w = 3.3$ and $Q = 0.23\text{ml/min}$ .....	<b>92</b>
<b>3.44</b>	<b>Effects of flow mode in the presence of connate water</b>	
	for $\mu_o/\mu_w = 3.3$ and $Q = 0.23\text{ml/min}$ .....	<b>93</b>

## **LIST OF TABLES**

<b>2.1</b>	<b>Specification of the system.....</b>	<b>22</b>
<b>2.2</b>	<b>Cell properties.....</b>	<b>22</b>
<b>2.3</b>	<b>Properties of fluid systems employed.....</b>	<b>31</b>
<b>2.4</b>	<b>Results of experiments performed.....</b>	<b>32</b>

## **NOMENCLATURE**

<b>A</b>	<b>=</b>	<b>Area</b>
<b>Ca</b>	<b>=</b>	<b>Capillary number</b>
<b>D</b>	<b>=</b>	<b>Diameter</b>
<b>g</b>	<b>=</b>	<b>Gravitational acceleration</b>
<b>k</b>	<b>=</b>	<b>Absolute permeability</b>
<b>k<sub>e</sub></b>	<b>=</b>	<b>Effective permeability</b>
<b>k<sub>r</sub></b>	<b>=</b>	<b>Relative permeability</b>
<b>L</b>	<b>=</b>	<b>Length</b>
<b>ΔP</b>	<b>=</b>	<b>Pressure gradient</b>
<b>Q</b>	<b>=</b>	<b>Flow rate</b>
<b>t<sub>br</sub></b>	<b>=</b>	<b>Breakthrough time</b>
<b>U</b>	<b>=</b>	<b>Characteristic velocity of displacement front</b>
<b>V</b>	<b>=</b>	<b>Bulk volume</b>
<b>V<sub>g</sub></b>	<b>=</b>	<b>Grain volume</b>
<b>V<sub>p</sub></b>	<b>=</b>	<b>Pore volume</b>
<b>φ</b>	<b>=</b>	<b>Porosity</b>
<b>γ</b>	<b>=</b>	<b>Oil/water interfacial tension</b>
<b>ρ<sub>o</sub></b>	<b>=</b>	<b>Density of oil phase</b>
<b>ρ<sub>w</sub></b>	<b>=</b>	<b>Density of aqueous phase</b>
<b>μ</b>	<b>=</b>	<b>Fluid viscosity</b>
<b>μ<sub>o</sub></b>	<b>=</b>	<b>Viscosity of oil phase</b>
<b>μ<sub>w</sub></b>	<b>=</b>	<b>Viscosity of aqueous phase</b>

## INTRODUCTION

Petroleum reservoirs consist of porous rocks saturated with oil, gas and water. A small amount of water called *connate water*, deposited during the prehistoric times when the oil was formed is dispersed within the oil phase or forms a thin film around the particles depending on whether the reservoir is water-wet or oil-wet. Due to its influence on the recovery efficiency, connate water should be taken into account when simulating the natural reservoir in the laboratory. In practice, the oil recovery involves the displacement of one fluid by another. Three processes known as primary recovery, secondary recovery and tertiary recovery are used to extract the oil from the rock pores. The highest potential recovery is difficult to attain because of hydrodynamic instabilities, which lead to a premature breakthrough and a low recovery. When a less viscous fluid displaces a more viscous fluid, the macroscopic interface between the two fluids becomes unstable and this hydrodynamic instability known as *viscous fingering* reduces the oil recovery efficiency. At this point, any process aimed at the suppression of the fingering phenomenon is of great interest to the petroleum recovery industry.

The objective of this study was to investigate the effects of flow rate, viscosity ratio and flow mode on the oil recovery efficiency. An immiscible displacement of the oil phase by the aqueous phase was carried out in a two-dimensional consolidated porous medium in four distinct flow modes, namely horizontal, vertical upward, vertical downward and transverse. The present investigation is a fundamental mechanistic study. Due to the complexity of natural reservoirs and their contents, the current study will be focused on the behaviour of a less viscous fluid displacing a more viscous fluid assuming that the reservoir formation is a homogeneous system.

## CHAPTER I

### LITERATURE REVIEW

#### 1.1 Oil formation

Oil occurs in nature within the tiny pores of sedimentary rocks formed during prehistoric times and this geological formation is called an *oil reservoir*. Oil formation is a long process, which can take millions of years. When marine creatures and plants died, their remains were deposited on the ocean floor. This organic matter was mixed with silt from erosion and buried farther downward. The decayed animals and plants were “cooked” and transformed into fluids under the pressure from the rocks above and heat from the earth’s crust. As the crust was warped, the oil migrated until it became trapped into rock formations like sandstone and limestone. Since the oil is relatively light, it remains above water, and depending on the wettability of the reservoir formation, part of the water called connate water is found within the oil phase or forms a thin film around rock particles. Figure 1.1 shows how oil is formed. The reservoir formation is a complex structure, which contains a mixture of a great number of compounds with varying proportions of carbon and hydrogen. In the book titled “ The properties of petroleum fluids”, McCain (1990) describes the liquids obtained from different petroleum reservoirs. According to the author, these liquids have widely different characteristics; some are black, heavy and thick, like tar while others are brown or nearly clear with low viscosity ratio and low specific gravity (Wheeler and Whited, 1985; Jenyon, 1990; McCain, 1990).

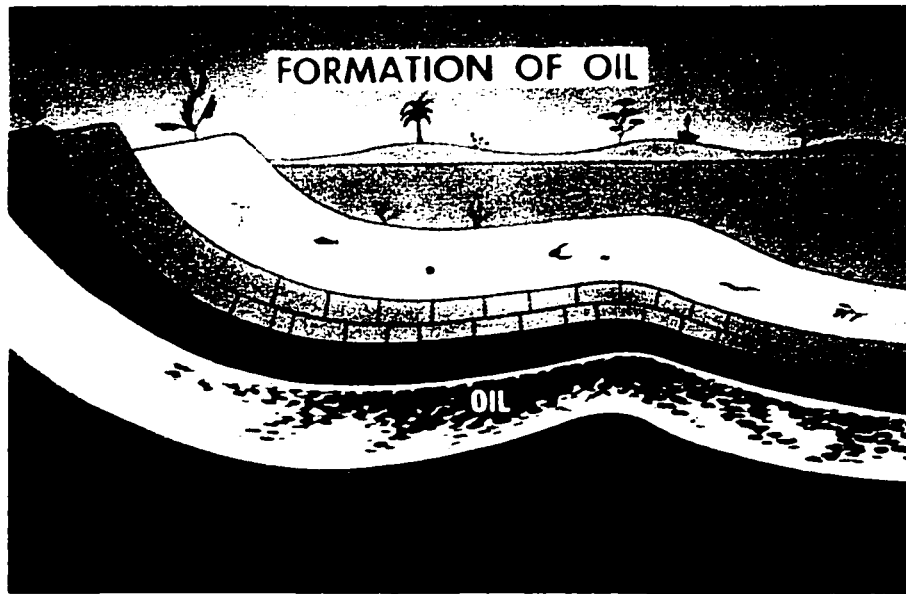


**Figure 1.1: Oil formation (Society of Petroleum Engineers, 1983)**

## **1.2 Oil recovery**

Oil recovery is a displacement process where one fluid displaces another one. Several fluids are used to squeeze oil out of the pores. Figure 1.2 is a visualization of the displacement process at a microscopic level.

### **1.2.1 Primary recovery**

Primary recovery is the conventional method used to produce oil; once a production well has been drilled, the water exerting an upward pressure pushes the oil to the surface (Figure 1.3). When the pressure is low in the reservoir formation, the oil cannot flow naturally. At this point, the reservoirs were abandoned in the past. A different technique is therefore required to force the oil out of the pores. The recovery efficiency varies from reservoir to reservoir depending on the type of reservoir, rock properties and the arrangement of production and injection wells. Only 10-30% of the original oil is recovered with primary recovery (Neale et al., 1981). Gas cap drive and water drive are the two processes that do not require an external force to extract the oil from the reservoir (Mayer-Gürr, 1976; Berger and Anderson, 1981).

### **1.2.2 Secondary recovery**

To improve the recovery efficiency after primary recovery, water or natural gas is introduced into the partially depleted reservoir through the injection well. Water flooding and water drive processes are similar except that in the case of water flooding processes, an artificial force is needed to displace the oil. Water is injected into the reservoir through an injection well and the oil is recovered at the production well as can be seen in Figure 1.4. The water injected displaces the oil until it breaks through at the production well.

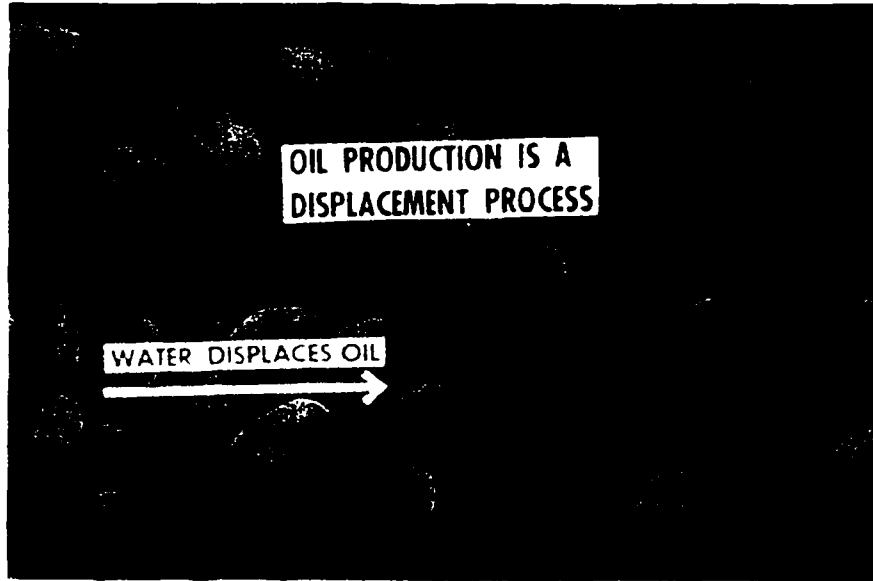


**Figure 1.2: Displacement process (Society of Petroleum Engineers, 1983)**

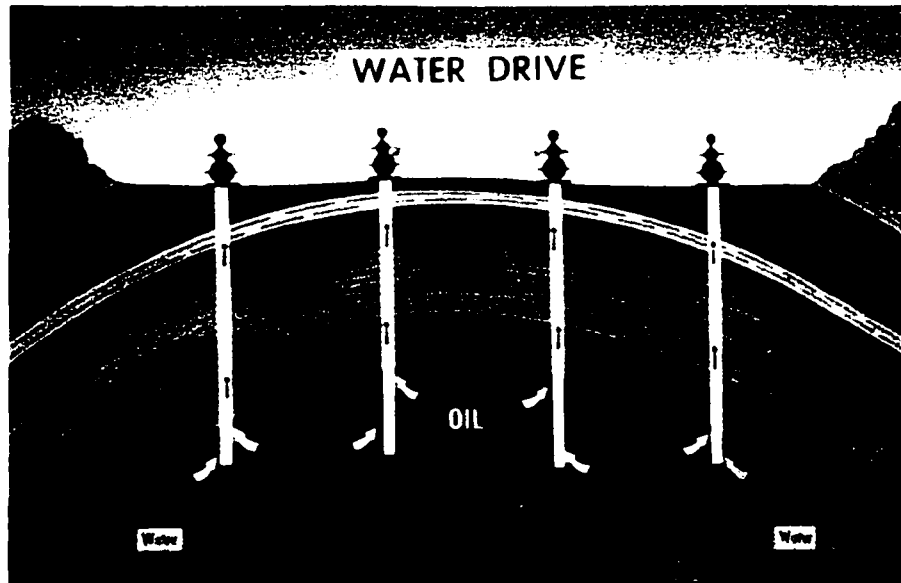


**Figure 1.3: Primary recovery (Society of Petroleum Engineers, 1983)**

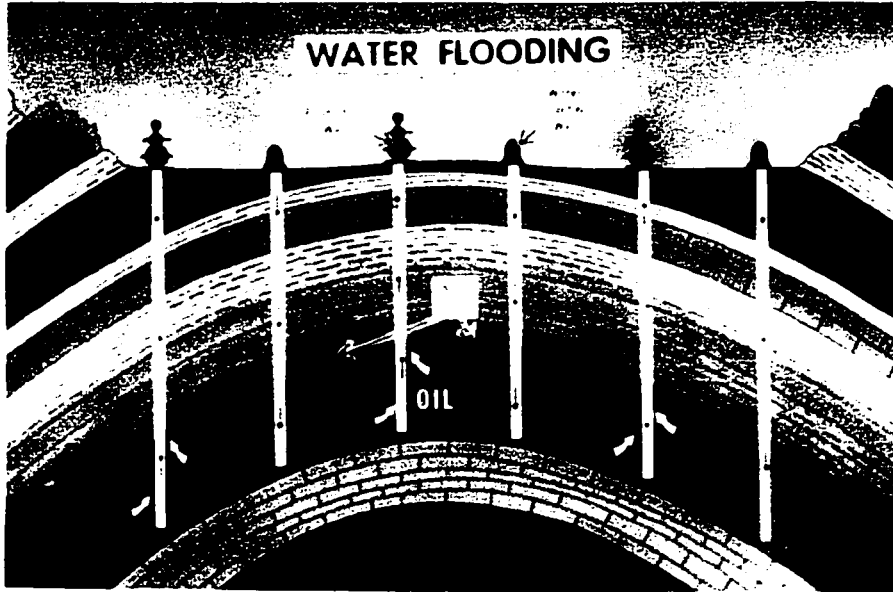


**Figure 1.4: Water flooding process (Society of Petroleum Engineers, 1983)**

Consequently, the recovery is low after the breakthrough. The instability of the macroscopic interface between the two fluids, due to the difference of viscosity and known as *viscous fingering* causes a significant decrease in the recovery efficiency. Any process that reduces the fingering phenomenon is of great interest in the oil production field. 10-30% of the original oil is recovered with secondary recovery. The recovery of the 40-80% of the original oil remaining in the reservoir represents a major challenge for the oil production industry.

### **1.2.3 Tertiary recovery**

Tertiary recovery encompasses various techniques used to recover the oil remaining in the reservoir formation after the primary and secondary recovery processes. These methods are subdivided into three major groups known as (Van Poolen and Associates Inc., 1980; Berger and Anderson, 1981; Okandan, 1984):

- Thermal recovery, which involves steam injection, steam stimulation and combustion in situ
- Chemical flooding, which includes surfactant-polymer injection, polymer flooding and caustic flooding. Chemicals are injected in order to lower the interfacial tension and mobilize the unrecoverable oil
- Miscible flooding, which includes hydrocarbon displacement, carbon dioxide injection and inert gas injection

The Enhanced Oil Recovery (EOR) techniques are any method that involves an artificial drive to squeeze the oil out of the rocks. From this definition, EOR includes both secondary and tertiary processes (Latil, 1980).

### **1.3 Displacement by fingering**

#### **1.3.1 Viscous fingering**

Fingering occurs when a less viscous fluid displaces a more viscous fluid. The less viscous one tends to channel through the more viscous one leading to an unstable interface between the two fluids. The channelling phenomenon is called *viscous fingering* since the displacement pattern looks like fingers (Perkins and Johnston, 1969; Paterson et al., 1982; Hu et al., 1985; Homsy, 1987; Manickam and Homsy, 1995). The width of the fingers depends on the viscosity ratio, the flow rate, the wettability and the permeability of the porous medium. The wider the fingers are, and the closer they are to each other, the more stable the displacement is and the recovery is high. Figure 1.5 is an example of a displacement by fingering in a vertical upward mode and at a high flow rate.

#### **1.3.2 Overview of fingering phenomena**

Many techniques have been developed to recover the 40-80% of the oil remaining in the reservoir. The Hele-Shaw cell, named after its inventor and first introduced in 1898 is made of two parallel glass plates separated by a narrow gap. It was first used to visualize a two-dimensional non-rotational flow. Since the 1950's, Hele-Shaw cells have been used to study viscous fingering (Franchi and Christiansen, 1989; Hornof and Bernard, 1992; Baig et al., 2000).

The chaotic motion that characterizes a hydrodynamic instability (viscous fingering) is extremely sensitive to initial conditions making difficult the reproducibility of experiments. If experiments are repeated many times, the results for each experiment will be somewhat different due to the imperfections present in the experimental set-up (Peters and Cavalero, 1990).

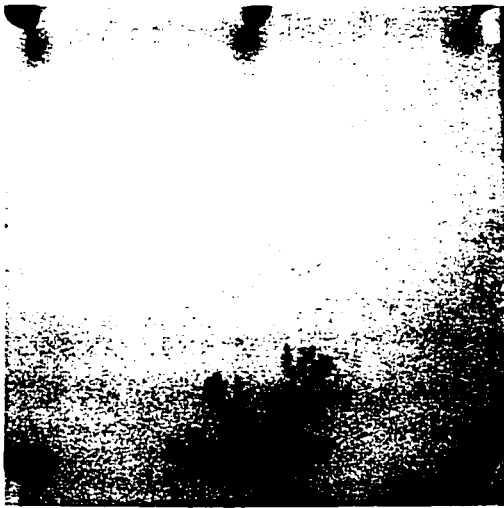


**Figure 1.5: Displacement by fingering (Glycerol solution displacing heavy paraffin oil)**

In 1993, Christie et al. investigated the impact and importance of three-dimensional effects on viscous fingering computations. Simulations were carried out with a 3D simulator for linear flow and, the viscous and gravity forces were controlled by the injection rate. Results obtained are similar in both 2D and 3D computations at high rates but when the density difference increases, the 3D computations give a low recovery compared to the 2D calculations. Importance should be accorded to 3D effects when viscous forces and gravitational forces are significant.

Viscous fingering responsible for a decrease in the sweep efficiency has been studied by Homsy in 1987 (Peters et al., 1984; Ni et al., 1986; Nasr-El-Din et al., 1987; Baker and Mcclernon, 1998). In their study in 1984, Jerault et al. described the theory of instability of plane saturation fronts in immiscible displacements. A decrease in capillary number can stabilize the displacement in a porous medium of restricted width. The capillary number ( $Ca$ ) based on the linear frontal velocity ( $U$ ) is expressed as:

$$Ca = \frac{U\mu_w}{\gamma} \quad [1]$$

Where

$\mu_w$  = Viscosity of aqueous phase

$U$  = Characteristic velocity of displacement front

$\gamma$  = Oil/water interfacial tension

Recent developments in EOR technology in China based on polymer (Polyacrylamide, PAM) flooding methods in different oil fields of various types show that

polymer solution can apparently reduce the water cut in these reservoirs of heterogeneous geological conditions and can consequently increase the oil recovery efficiency. At present, in China, the polymer flooding technology has been fully industrialized and its achievements are very promising (Han et al., 1999).

#### **1.4 Connate water**

Connate water is the name given to the small amount of water found in natural reservoirs, which was deposited simultaneously with the oil during prehistoric times when the bed of sediments was formed. Despite its volume, which is relatively small, about 5% of pore volume, connate water has a significant effect on the recovery efficiency, and should always be taken into account when simulating a natural reservoir rock in the laboratory. Although connate water has the tendency to accumulate at the bottom of the pool, it is dispersed within the oil phase or forms a thin film around rock particles depending on whether the reservoir is oil-wet or water-wet (Berger and Anderson, 1981).

Although many studies have shown the negative effects of connate water on the recovery, it also plays an important role in the oil recovery industry especially during the early stage of the production when the oil flows under the high pressure in the rock formations. The low recovery should be attributed to the water present within the oil phase. Figure 1.6, a picture published by the Society of Petroleum Engineers, shows the reservoir rocks containing connate water. In water-wet porous media connate water exists in pendular form and in insular form in an oil-wet system (Paterson et al., 1984; Thibodeau et al., 1997). Connate water influences the displacement patterns and is also responsible for a decrease in the recovery efficiency (Thibodeau and Neale, 1998).

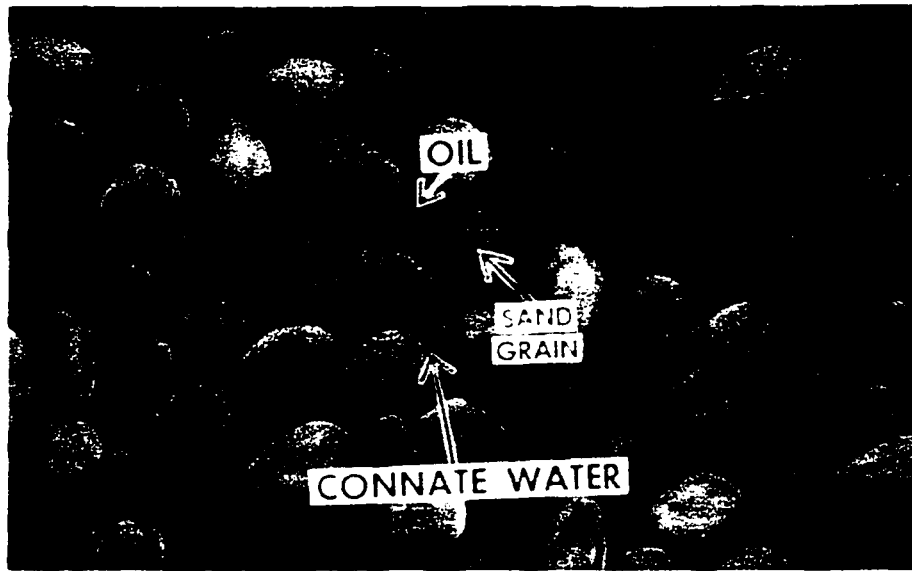


**Figure 1.6: Connate water (Society of Petroleum Engineers, 1983)**

## 1.5 Theory

### 1.5.1 Dimensional analysis

The dimensional analysis using Rayleigh's Method for an immiscible system where glycerol solution displaces heavy paraffin oil is determined as followed:

#### 1. R = Fractional oil recovery

The system is defined by the following variables, which characterize the displacement process, the porous media and the parameters of the cell's geometry:

$$R = C (Q)^a (\mu_o)^b (\mu_w)^c (\rho_o)^d (\rho_w)^e (\gamma)^f (g)^g (D)^h \quad [2]$$

Where

Q = Flow rate

$\mu_o$  = Viscosity of oil phase

$\mu_w$  = Viscosity of aqueous phase

$\rho_o$  = Density of oil phase

$\rho_w$  = Density of aqueous phase

$\gamma$  = oil/water interfacial tension

D = Diameter

g = Gravitational acceleration

#### 2. Dimensional form:

$$[M^0 L^0 T^0] = C [L^3 T^{-1}]^a [ML^{-1} T^{-1}]^b [ML^{-1} T^{-1}]^c [ML^{-3}]^d [ML^{-3}]^e [MT^{-2}]^f [LT^{-2}]^g [L]^h \quad [3]$$

3. Equate exponents of M, L and T:

$$M: 0 = b + c + d + e + f \quad [4]$$

$$L: 0 = 3a - b - c - 3d - 3e + g + h \quad [5]$$

$$T: 0 = -a - b - c - 2f - 2g \quad [6]$$

There are eight variables and three dimensions, so three of the eight unknowns may be eliminated and expressed in terms of the five remaining unknowns (arbitrary unknowns)

$$\text{Number of dimensionless groups} = 8 - 3 = 5$$

4. Select a, b, c, d and e as the arbitrary unknowns

5. Solution for f, g, and h

$$a = a, b = b, c = c, d = d, e = e \quad [7]$$

$$\therefore M: f = -b - c - d - e \quad [8]$$

$$L: g = -\frac{1}{2}a + \frac{1}{2}b + \frac{1}{2}c + d + e \quad [9]$$

$$T: h = -\frac{5}{2}a + \frac{1}{2}b + \frac{1}{2}c + 2d + 2e \quad [10]$$

The oil recovery may therefore be expressed as:

$$R = C (Q)^a (\mu_o)^b (\mu_w)^c (\rho_o)^d (\rho_w)^e (\gamma)^{-b-c-d-e} (g)^{-\frac{1}{2}a + \frac{1}{2}b + \frac{1}{2}c + d + e} (D)^{-\frac{5}{2}a + \frac{1}{2}b + \frac{1}{2}c + 2d + 2e} \quad [11]$$

6. Group together common exponents:

$$R = C \left[ \left( \frac{Q}{g^{1/2} D^{5/2}} \right)^a \left( \frac{\mu_o g^{1/2} D^{1/2}}{\gamma} \right)^b \left( \frac{\mu_w g^{1/2} D^{1/2}}{\gamma} \right)^c \left( \frac{\rho_o g D^2}{\gamma} \right)^d \left( \frac{\rho_w g D^2}{\gamma} \right)^e \right] \quad [12]$$

$$R = f \left[ \left( \frac{Q}{g^{1/2} D^{5/2}} \right), \left( \frac{\mu_o g^{1/2} D^{1/2}}{\gamma} \right), \left( \frac{\mu_w g^{1/2} D^{1/2}}{\gamma} \right), \left( \frac{\rho_o g D^2}{\gamma} \right), \left( \frac{\rho_w g D^2}{\gamma} \right) \right] \quad [13]$$

For an immiscible system the five independent groups as expected are:

$$(a) \frac{Q}{g^{1/2} D^{5/2}}$$

$$(b) \frac{\mu_o g^{1/2} D^{1/2}}{\gamma}$$

$$(c) \frac{\mu_w g^{1/2} D^{1/2}}{\gamma}$$

$$(d) \frac{\rho_o g D^2}{\gamma}$$

$$(e) \frac{\rho_w g D^2}{\gamma}$$

These five dimensionless groups can be manipulated and rearranged in order to obtain three conventional groups, i.e., a Reynolds Number, a Capillary Number and a Bond Number, as follows:

$$\frac{(a)(e)}{(c)} = \frac{\rho_w Q}{\mu_w D} = \text{Reynolds Number based on the displacing phase} \quad [14]$$

$$(a)(c) = \frac{\mu_w Q}{\gamma D^2} = \text{Capillary Number based on the displacing phase} \quad [15]$$

$$(e) = \frac{\Delta \rho g D^2}{\gamma \left(1 - \frac{\rho_o}{\rho_w}\right)} = \text{Bond Number, where } \Delta \rho = \rho_w - \rho_o \quad [16]$$

$$\frac{(b)}{(c)} = \frac{\mu_o}{\mu_w} = \text{Viscosity ratio} \quad [17]$$

$$\frac{(d)}{(e)} = \frac{\rho_o}{\rho_w} = \text{Density ratio} \quad [18]$$

$$R = f \left[ \frac{\rho_w Q}{\mu_w D}, \frac{\mu_w Q}{\gamma D^2}, \frac{\Delta \rho g D^2}{\gamma \left(1 - \frac{\rho_o}{\rho_w}\right)}, \frac{\mu_o}{\mu_w}, \frac{\rho_o}{\rho_w} \right] \quad [19]$$

### 1.5.2 Viscous forces

The forces required whenever one layer of fluid slides past another or when a surface slides past another with a layer of fluid between the surfaces are called *viscous forces*. These forces result in friction between the fluid phases and are related to the viscosity, which by definition is associated with the internal friction within a moving fluid (Francis et al., 1987).

### **1.5.3 Gravity forces**

Hydrostatic equilibrium is maintained in a fluid by an upward pressure force that balances the weight of the fluid volume. When the fluid volume is replaced by another fluid of different density the remaining fluid continues to exert an upward force whose magnitude is equivalent to the weight of the original volume of the fluid displaced. This force is called the *buoyancy force*. If the replacing fluid has a lower density, the net force is upward, and downward if the density is higher (Wolfson and Pasachoff, 1987; Frayers and Newley, 1988). Visualization of the effects of buoyancy forces has been undertaken in porous medium cells. It is convenient to carry out the displacement processes in a two-dimensional consolidated porous medium aligned in the vertical plane in which the fluids are not impeded to move vertically or transversely (Page et al., 1993; Guo and Neale, 1995; Thirunavu and Neale, 1995).

### **1.5.4 Pressure difference**

When a displacing fluid is injected into a cell by means of a constant flow rate syringe pump, a pressure difference is created between the inlet and the outlet ports of the cell. This pressure difference force causes the oil to flow toward the outlet port. Since the injection takes place at one port and the recovery at the opposite port, the flow may be divergent (decreasing velocity) near the inlet port and convergent (increasing velocity) at the outlet port.

### 1.5.5 Permeability

The permeability of a rock is a measure of the ease with which fluid can flow through it. If only one fluid is present in the rock, and the rock does not react with the fluid, the permeability of the rock is known as the “*absolute permeability*” or “*specific permeability*”. In a rock that contains more than one fluid (which is always the case in a hydrocarbon reservoir), there is a tendency for each fluid to interfere with the flow of the other fluids. This reduction in ability of a fluid to flow through a permeable material is called a *relative permeability* effect (Jha, 1982; Koederitz et al., 1989).

Effective permeability and absolute permeability are related by the equation:

$$k_e = k k_r \quad [20]$$

Where

$k_e$  = Effective permeability

$k$  = Absolute permeability

$k_r$  = Relative permeability to the fluid for which  $k_e$  is specified, dimensionless

The unit of  $k$  and  $k_e$  is the darcy, d

$$1d = 0.987 \times 10^{-12} \text{m}^2$$

$$k = \frac{Q L}{A \Delta P} \mu \quad [21]$$

Where

$Q$  = Flow rate ( $\text{m}^3/\text{s}$ )

$A$  = Area ( $\text{m}^2$ )

**L = Length (m)**

**$\Delta P$  = Pressure gradient (Pa/m)**

**$\mu$  = Fluid viscosity (Pa.s)**

### **1.5.6 Porosity**

The porosity is a measure of the storage capacity of a reservoir. It is defined as the ratio of void space to bulk volume, and it may be expressed as either a percentage or a fraction.

$$\phi = \frac{V_p}{V} = \frac{(V - V_g)}{V} \quad [22]$$

**Where**

**$V_p$  = Pore volume (void space)**

**V = Bulk volume**

**$V_g$  = Grain volume**

## **CHAPTER II**

### **EXPERIMENTAL STUDIES**

#### **2.1 Experimental materials**

The consolidated porous medium used consisted of sintered glass beads sandwiched between two parallel glass plates of 0.4cm thickness. The sintering process was performed by, slowly heating the medium (between the plates) to 660°C and maintaining this temperature for two hours. The sand had been previously treated with 50% nitric acid in order to remove any possible organic contamination, then washed with distilled water and dried. After cooling, the cell edges were sealed with an epoxy resin and two sets of three equally spaced ports were drilled into opposite sides of the cell. Any of the six ports could be used for the injection and recovery of the fluids.

The dimensions of the cell were 15 x 15 x 1.1 cm. The resulting porous medium had a porosity of 0.23 and a pore volume of 15.6ml. Table 2.1 shows the specification of the system used.

##### **2.1.1 Cell properties**

Table 2.2 summarizes the properties of the consolidated porous medium used in this project.

**Table 2.1: Specification of the system**

<b>Material/Equipment</b>	<b>Specification</b>
Glycerol	BDH, Analytical reagent
Heavy paraffin oil	BDH, Analytical reagent
Water	Distilled
Methylene blue dye	Fisher Scientific Co.
Propanol-2	BDH, Analytical reagent
Acetone	BDH, Analytical reagent
Syringe pump	Sage Instrument Model
Glass beads	Rouville Inc.

**Table 2.2: Cell properties**

Space between plates (porous medium)	0.3 cm
Thickness of cell	1.1 cm
Porosity of porous medium	0.23
Pore volume	15.6 ml
Size of glass plates	15 x 15 x 0.4 cm

### **2.1.2 Apparatus**

The main components of the experimental set-up are listed below:

1. Porous medium cell
2. Camera
3. Constant flow rate syringe pump
4. 50 ml syringe
5. Timer
6. Vacuum tubing
7. Vacuum pump
8. 50 ml burette
9. Fluorescent light source
10. 10 ml container

For experiments performed in the horizontal mode, the camera was located overhead and the cell was laid above the light source. In the vertical and transverse modes, the camera was mounted on a tripod and a wooden holder in the front of the light source supported the cell. Figures 2.1 and 2.2 show the experimental set-up while Figure 2.3 displays the specific orientations of the cell.

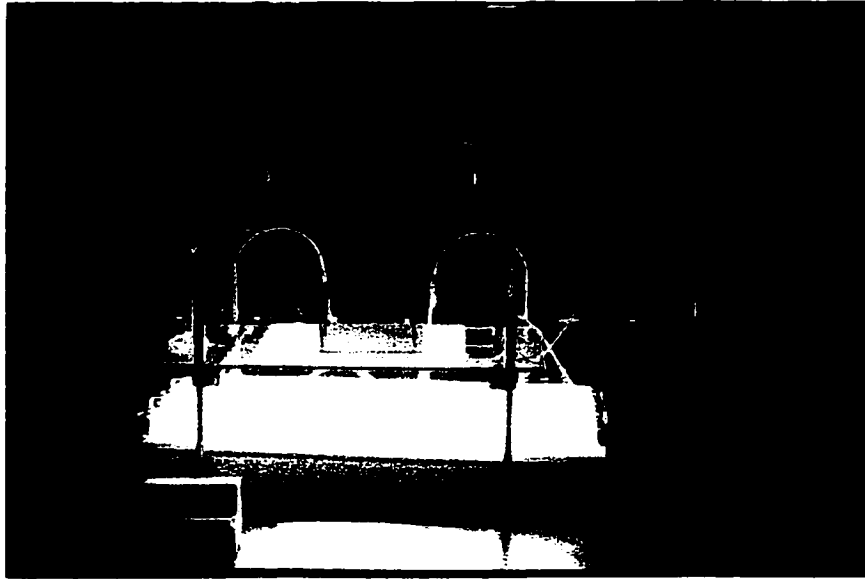


**Figure 2.1: Experimental set-up**

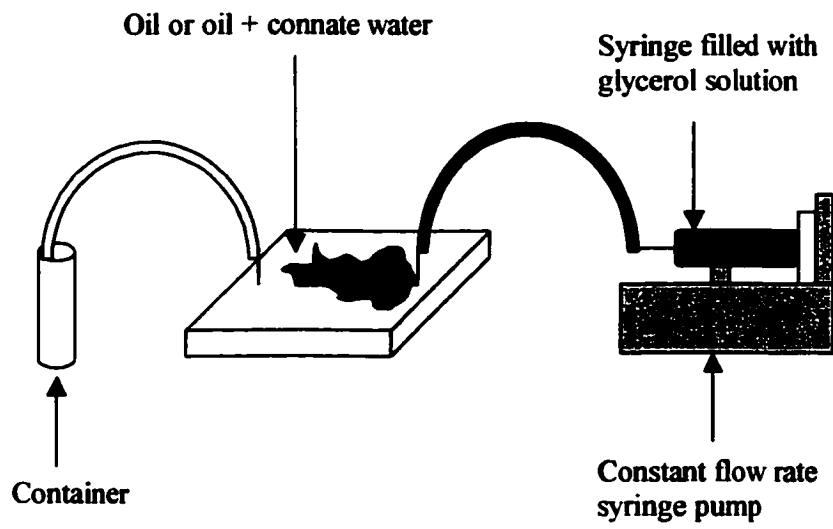


**Figure 2.2: Schematic of the experimental set-up**

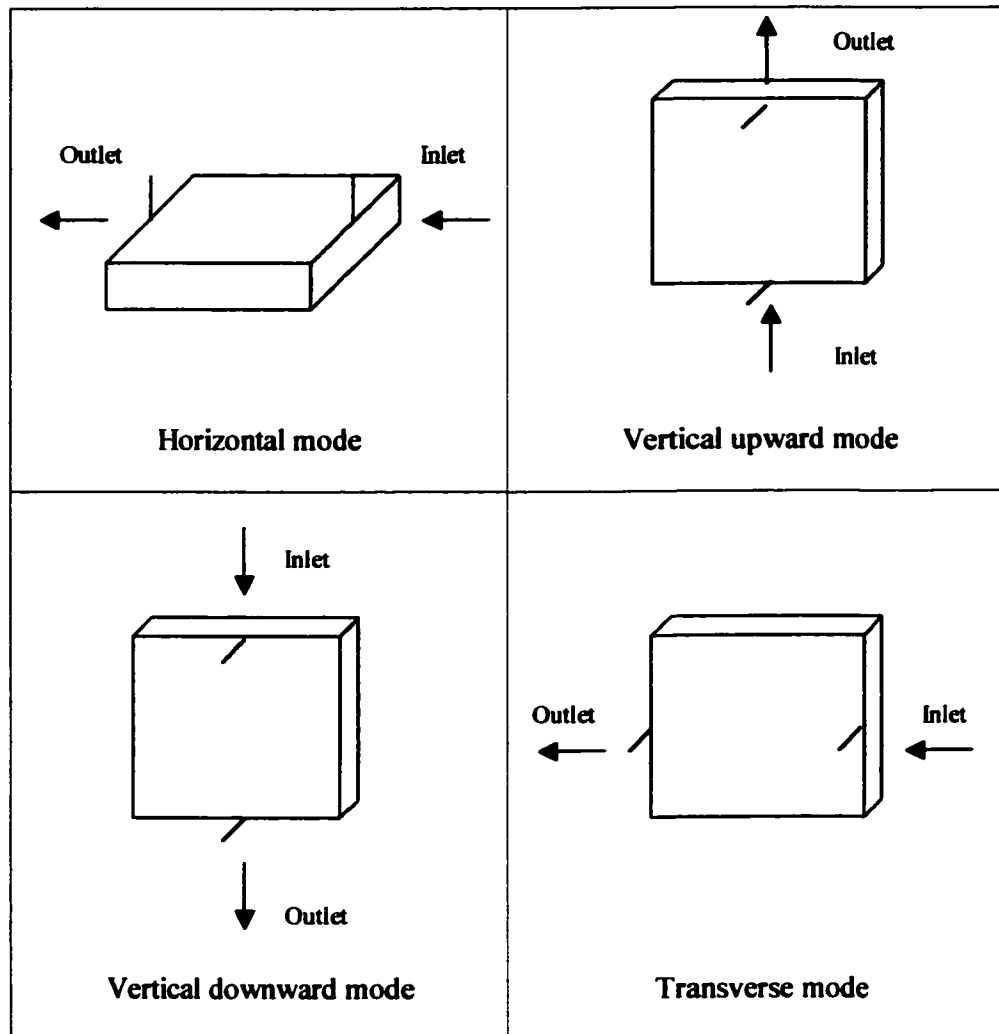


**Figure 2.3: Specific orientations of the cell**

## **2.2 Experimental method**

### **2.2.1 Saturation process**

For the experiments performed without connate water, the cell was evacuated using a vacuum pump in order to remove the air in the cell, and was then completely saturated with heavy paraffin oil. After the filling process, the pump was disconnected and the cell was ready for the experiment. The displaced fluid in this study was heavy paraffin oil and the displacing fluid was glycerol solution (mixture of glycerol and distilled water dyed with 0.025 wt.% methylene blue to make visualization easier). If the cell is 100% saturated with paraffin oil, the amount of oil required to fill completely the cell gives the pore volume of the porous medium.

For the experiments performed with connate water, the cell was first filled under vacuum with distilled water. After the cell was 100% saturated with distilled water, the pump was released. The paraffin oil was then introduced under vacuum into the cell using the inlet port. Since the viscosity of the oil is higher than that of water, the displacement is very stable. A plug flow is obtained; as a result, the bulk of the water is removed. The small amount of water remaining in the cell constituted the connate water. In principle, the fractional volume (saturation) of the connate water phase can be measured but, in practice, saturation is difficult to measure accurately because of its low value.

### **2.2.2 Displacement process**

A syringe filled with the glycerol solution was kept in a constant flow rate syringe pump. The flow rate selector was set to a certain value and the pump was connected to the inlet port of the cell through a tube. The outlet port was connected to a container in order to collect the oil displaced during the displacement process. The cell represents the reservoir and the several inlet/outlet ports represent the production and injection wells.

To study the behaviour of the fingering, photographs were taken and the time recorded as the glycerol solution displaced the paraffin oil until the fingers of the displacing fluid reached the outlet port. At this point, the so-called breakthrough time was recorded and used in the calculation of the recovery. Using the breakthrough time, the fractional oil recovery could be calculated using the equation:

$$R = \frac{Qt_{br}}{V_p} \quad [23]$$

Where  $Q$  denotes the volumetric injection flow rate,  $V_p$  the pore volume of the cell and  $t_{br}$  the breakthrough time.

### **2.2.3 Cleaning and drying processes**

To ensure good reproducibility of the experiments the cell was cleaned and dried after each experiment. About 100ml of propanol-2 and acetone were used under vacuum to remove all traces of glycerol, dye and paraffin oil present in the cell. The cell was then flushed with distilled water and dried with air for 1 hour. All of the six ports were used during the cleaning and drying processes.

## **2.3 Experiments performed**

### **2.3.1 Homogeneity of the consolidated porous medium**

Before use, the cell was tested to confirm its homogeneity. The test was carried out, by performing displacement experiments with a viscosity ratio of one. Distilled water was displaced by distilled water dyed with methylene blue at an injection flow rate of 0.44ml/min. As shown in Figure 2.4, there was no fingering; the displacement front was smooth indicating good homogeneity and uniformity. This test does not prove that the cell is microscopically homogeneous but it does indicate that it is free of major heterogeneities, which could lead to false fingering behaviour in water/oil displacements.

### **2.3.2 Reproducibility of the experiments**

To test the reproducibility of wetting characteristics of the porous medium, two experiments were performed at the same flow rate of 0.78ml/min in the horizontal displacement mode. The heavy paraffin oil was displaced with glycerol solution (75%). Figure 2.5 shows the patterns of these displacements at the breakthrough condition. As can be observed, the two patterns are almost the same; the breakthrough recovery differs slightly by an absolute amount of 0.34% (or relative amount of 1%), which is entirely acceptable. With regard to the displacement experiments reported later, a similar relative reproducibility was observed.

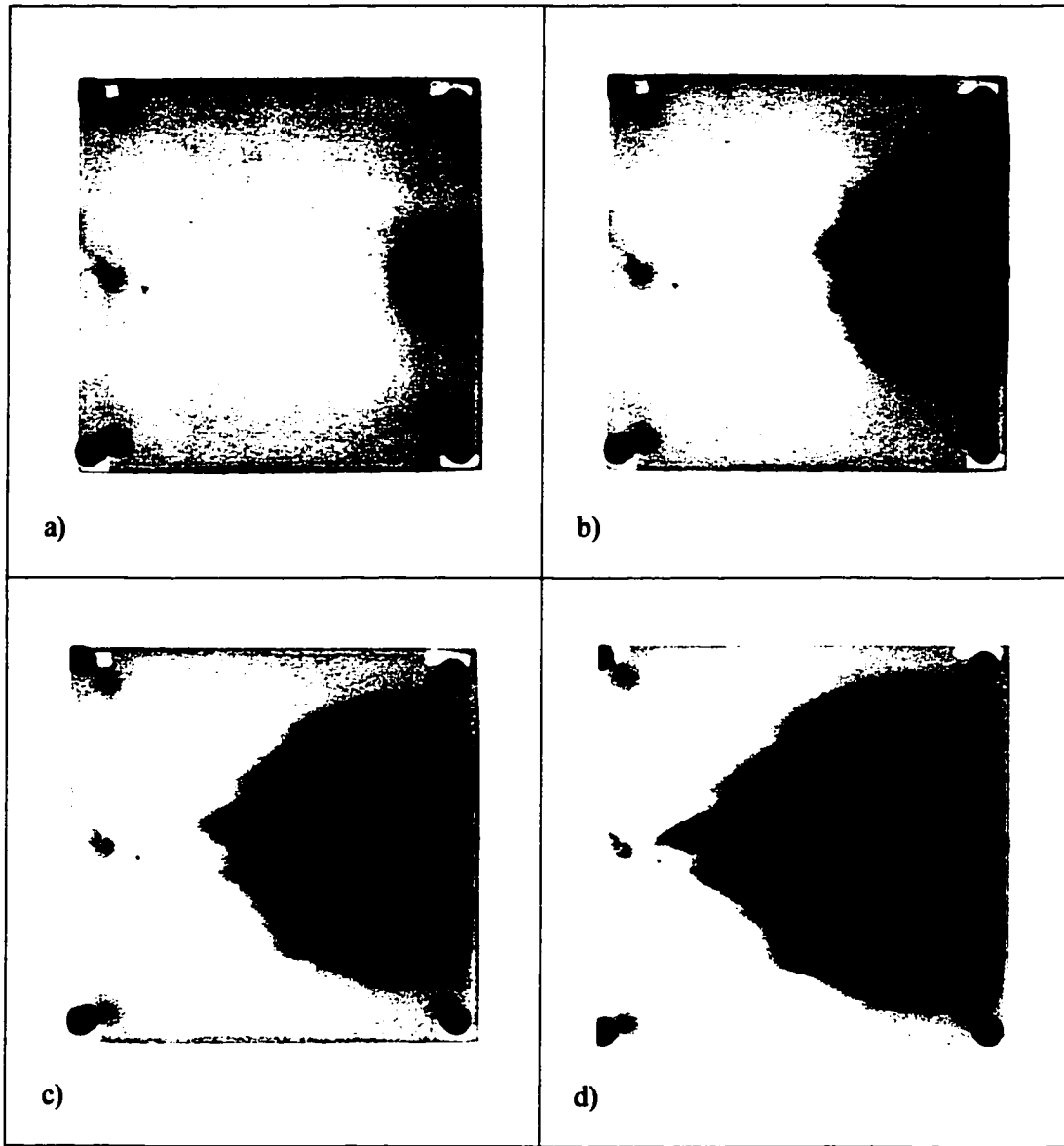


**Figure 2.4: Homogeneity test; Dyed distilled water displacing distilled water at  $Q = 0.44$  ml/min in the horizontal flow mode. a)  $t_{br} = 100$  sec, b)  $t_{br} = 520$  sec, c)  $t_{br} = 850$  sec, d)  $t_{br} = 1113$  sec**

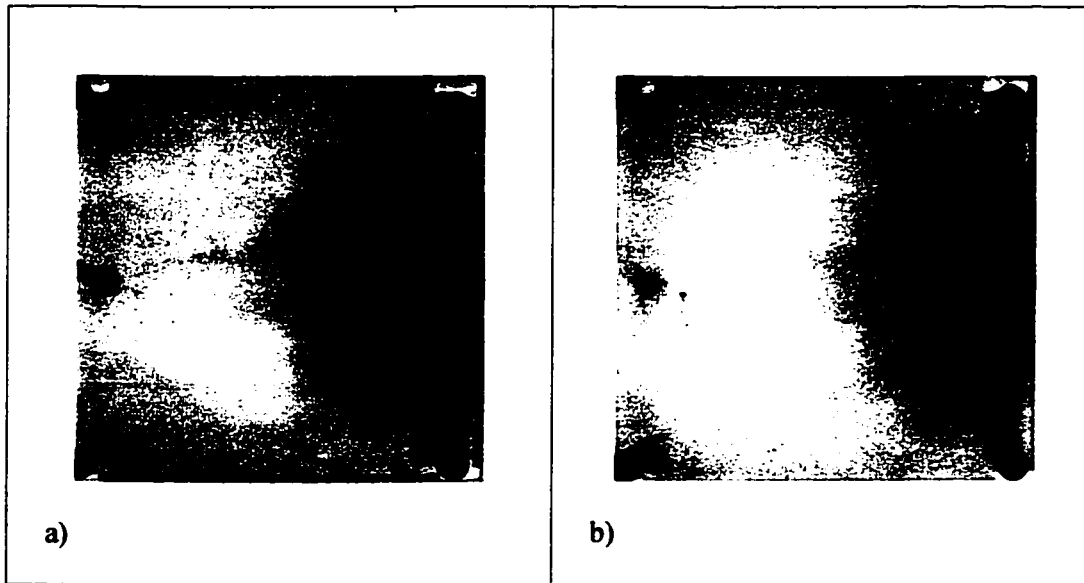


**Figure 2.5: Reproducibility experiments for glycerol solution (75%) displacing heavy paraffin oil at  $Q = 0.78\text{ml/min}$  in the horizontal flow mode. a)  $t_{br} = 403\text{sec}$ ,  $R = 33.58\%$ ; b)  $t_{br} = 407\text{sec}$ ,  $R = 33.92\%$**

### 2.3.3 Immiscible displacements

Two sets of experiments were performed, the first one in the absence of connate water and the second one in the presence of connate water. The different variables are the flow rate, viscosity ratio and flow mode. Table 2.3 displays the properties of the fluid systems employed at 25°C. As the glycerol concentration increases, the density ratio and the viscosity ratio decrease, but the variation is small in the case of the density ratio. The change in the recovery efficiency may be attributed to the viscosity ratio rather than to the density ratio. Table 2.4 displays the detailed results of the experiments performed.

**Table 2.3: Properties of fluid systems employed**

System	Glycerol concentration (vol./vol.)	Density ratio ( $\rho_o/\rho_w$ )	Viscosity ratio ( $\mu_o/\mu_w$ )
A	0.00 % (pure water)	0.877	143.5
B	30 %	0.814	49.0
C	60 %	0.750	11.11
D	75 %	0.737	3.3

Properties of paraffin oil:  $\mu_o = 153.55\text{mPa.s}$

at 25°C  $\rho_o = 0.877\text{g/ml}$

Properties of pure water:  $\mu_w = 1.07\text{mPa.s}$

at 25°C  $\rho_w = 1.00\text{g/ml}$

**Table 2.4: Results of experiments performed****Experiments without connate water**

Experiment	Fluid system	Flow mode	Flow rate (ml/min)	Recovery (%)
1	A	Horizontal	0.23	11.99
2	A	Horizontal	0.44	12.83
3	A	Horizontal	0.78	11.75
4	B	Horizontal	0.23	15.85
5	B	Horizontal	0.44	17.44
6	B	Horizontal	0.78	17
7	C	Horizontal	0.23	25.48
8	C	Horizontal	0.44	23.78
9	C	Horizontal	0.78	25.17
10	D	Horizontal	0.23	36.51
11	D	Horizontal	0.44	34.79
12	D	Horizontal	0.78	33.75
13	A	Vertical Upward	0.23	13.26
14	A	Vertical Upward	0.44	12.41
15	A	Vertical Upward	0.78	13.04
16	B	Vertical Upward	0.23	17.54
17	B	Vertical Upward	0.44	14.57
18	B	Vertical Upward	0.78	17.83
19	C	Vertical Upward	0.23	29.02
20	C	Vertical Upward	0.44	27.69
21	C	Vertical Upward	0.78	27.83
22	D	Vertical Upward	0.23	38.41
23	D	Vertical Upward	0.44	37.37
24	D	Vertical Upward	0.78	38.33

25	A	Vertical Downward	0.23	10.41
26	A	Vertical Downward	0.44	9.85
27	A	Vertical Downward	0.78	9.84
28	B	Vertical Downward	0.23	13.54
29	B	Vertical Downward	0.44	13.35
30	B	Vertical Downward	0.78	13.58
31	C	Vertical Downward	0.23	20.15
32	C	Vertical Downward	0.44	18.33
33	C	Vertical Downward	0.78	18.92
34	D	Vertical Downward	0.23	32.01
35	D	Vertical Downward	0.44	31.12
36	D	Vertical Downward	0.78	30.42
37	A	Transverse	0.23	11.75
38	A	Transverse	0.44	10.53
39	A	Transverse	0.78	10.58
40	B	Transverse	0.23	16.98
41	B	Transverse	0.44	15
42	B	Transverse	0.78	14.87
43	C	Transverse	0.23	23.47
44	C	Transverse	0.44	22.38
45	C	Transverse	0.78	21.25
46	D	Transverse	0.23	36.66
47	D	Transverse	0.44	34.69
48	D	Transverse	0.78	33.58

### Experiments with connate water

Experiment	Fluid system	Flow mode	Flow rate (ml/min)	Recovery (%)
49	A	Horizontal	0.23	15.33
50	A	Horizontal	0.44	14.76
51	A	Horizontal	0.78	16
52	B	Horizontal	0.23	18.06
53	B	Horizontal	0.44	17.11
54	B	Horizontal	0.78	18.67
55	C	Horizontal	0.23	23.84
56	C	Horizontal	0.44	22.85
57	C	Horizontal	0.78	20.92
58	D	Horizontal	0.23	26.1
59	D	Horizontal	0.44	25.08
60	D	Horizontal	0.78	26
61	A	Vertical Upward	0.23	14.22
62	A	Vertical Upward	0.44	15.51
63	A	Vertical Upward	0.78	15.5
64	B	Vertical Upward	0.23	17.35
65	B	Vertical Upward	0.44	19.13
66	B	Vertical Upward	0.78	17.67
67	C	Vertical Upward	0.23	21.97
68	C	Vertical Upward	0.44	22.61
69	C	Vertical Upward	0.78	22.33
70	D	Vertical Upward	0.23	26.32
71	D	Vertical Upward	0.44	25.57
72	D	Vertical Upward	0.78	25.25
73	A	Vertical Downward	0.23	14.4
74	A	Vertical Downward	0.44	14.43
75	A	Vertical Downward	0.78	14.83

76	B	Vertical Downward	0.23	17.82
77	B	Vertical Downward	0.44	18.52
78	B	Vertical Downward	0.78	18.17
79	C	Vertical Downward	0.23	22.24
80	C	Vertical Downward	0.44	20.54
81	C	Vertical Downward	0.78	20.92
82	D	Vertical Downward	0.23	25.19
83	D	Vertical Downward	0.44	23.17
84	D	Vertical Downward	0.78	25.08
85	A	Transverse	0.23	14.6
86	A	Transverse	0.44	14.99
87	A	Transverse	0.78	14.42
88	B	Transverse	0.23	16.51
89	B	Transverse	0.44	16.41
90	B	Transverse	0.78	18.25
91	C	Transverse	0.23	23.69
92	C	Transverse	0.44	22.47
93	C	Transverse	0.78	21
94	D	Transverse	0.23	26.87
95	D	Transverse	0.44	26.18
96	D	Transverse	0.78	26.08

## **CHAPTER III**

### **RESULTS AND DISCUSSION**

#### **3.1 Effects of time on fingering patterns**

In the absence of connate water, as shown in Figures 3.1 - 3.4, fingers are developed during the displacement process. At the early stage of the process, the fingers are well defined and grow progressively until the displacing fluid reaches the outlet port. Many other small fingers are generated when the oil is displaced, but because of gravitational forces these fingers are suppressed. In the transverse flow mode case, the fluid has a tendency to move toward the bottom due to the gravity acting on the fluid, and then to move to the outlet port.

In the presence of connate water, the patterns are similar for all four flow modes but different from those without connate water. The coalescence of connate water with the displacing fluid (glycerol) leads to an “undistinguished” fingering pattern as the displacing fluid moves toward the outlet port. Due to the effect of dilution, the fingers are so small that they cannot be distinguished; only a thin tiny tongue reaches the outlet port, reducing the recovery efficiency. As a result, the patterns appear to be light and smooth (Figures 3.5 - 3.8). It should be mentioned that there are two methods to reproduce connate water. The first one consists of flushing the cell with water and then displacing the remaining water with oil. The second one as used in the present study is to displace slowly the water previously introduced into the cell under vacuum with oil. It is evident that in the second case the amount of the so-called connate water will be higher than that of the first procedure. So, the fingering patterns will be different from one case to another one.

The flow rate is one of the most important factors in the displacement process. Previous studies had shown that the amount of oil recovered is greatly affected by the flow rate (Thirunavu and Neale, 1995), but since the variation in the flow rate in the present study is very small, the recovery and the patterns do not change too much. Therefore, over the next sections, discussion will be focused on the viscosity ratio and the flow mode rather than the flow rate.

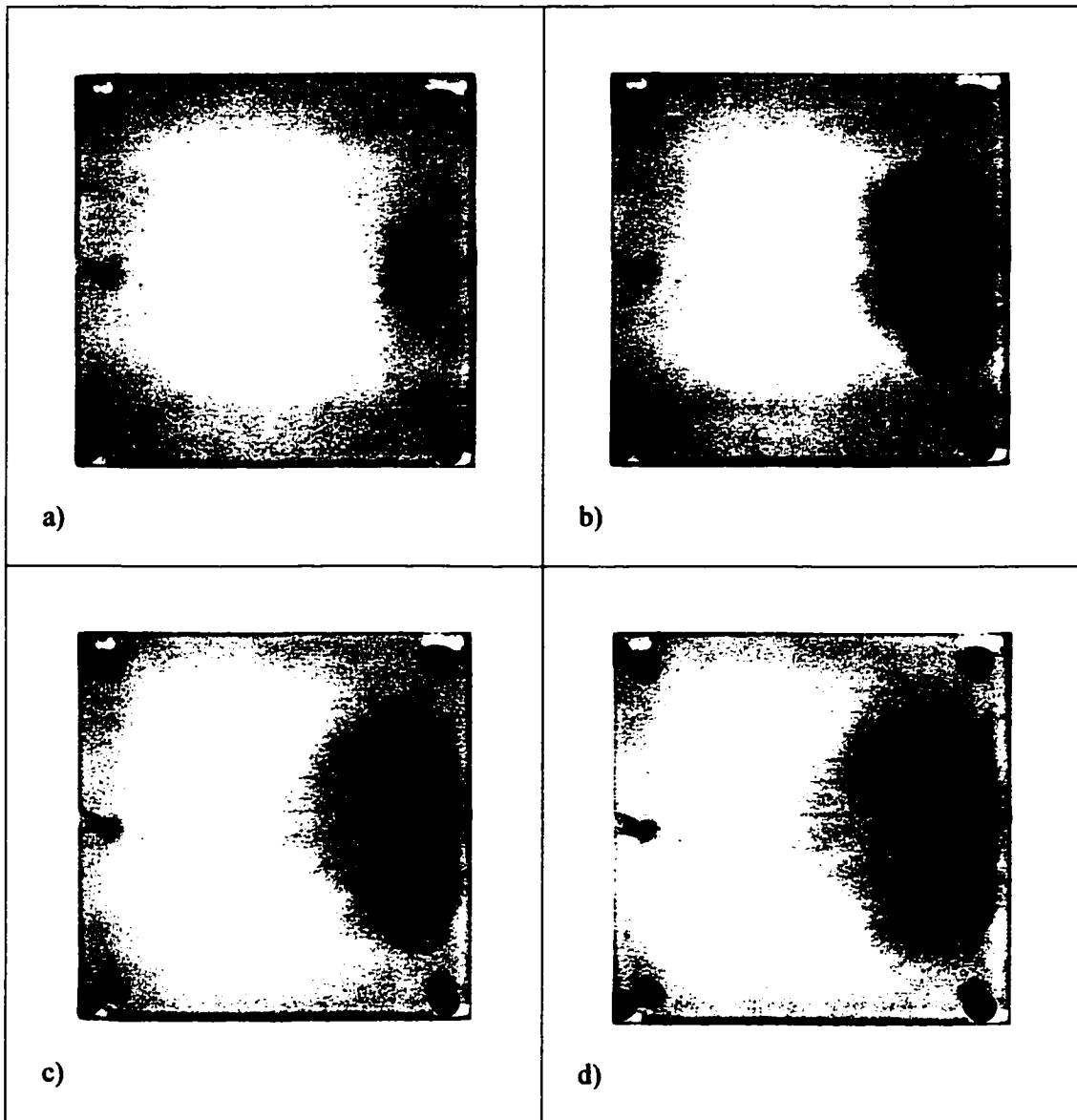


**Figure 3.1: Development of the fingering patterns without connate water in the horizontal flow mode.  $\mu_o/\mu_w = 11.11$ ,  $Q = 0.78$  ml/min, a)  $t = 70$ sec, b)  $t = 170$ sec, c)  $t = 250$ sec, d)  $t_{br} = 302$ sec**

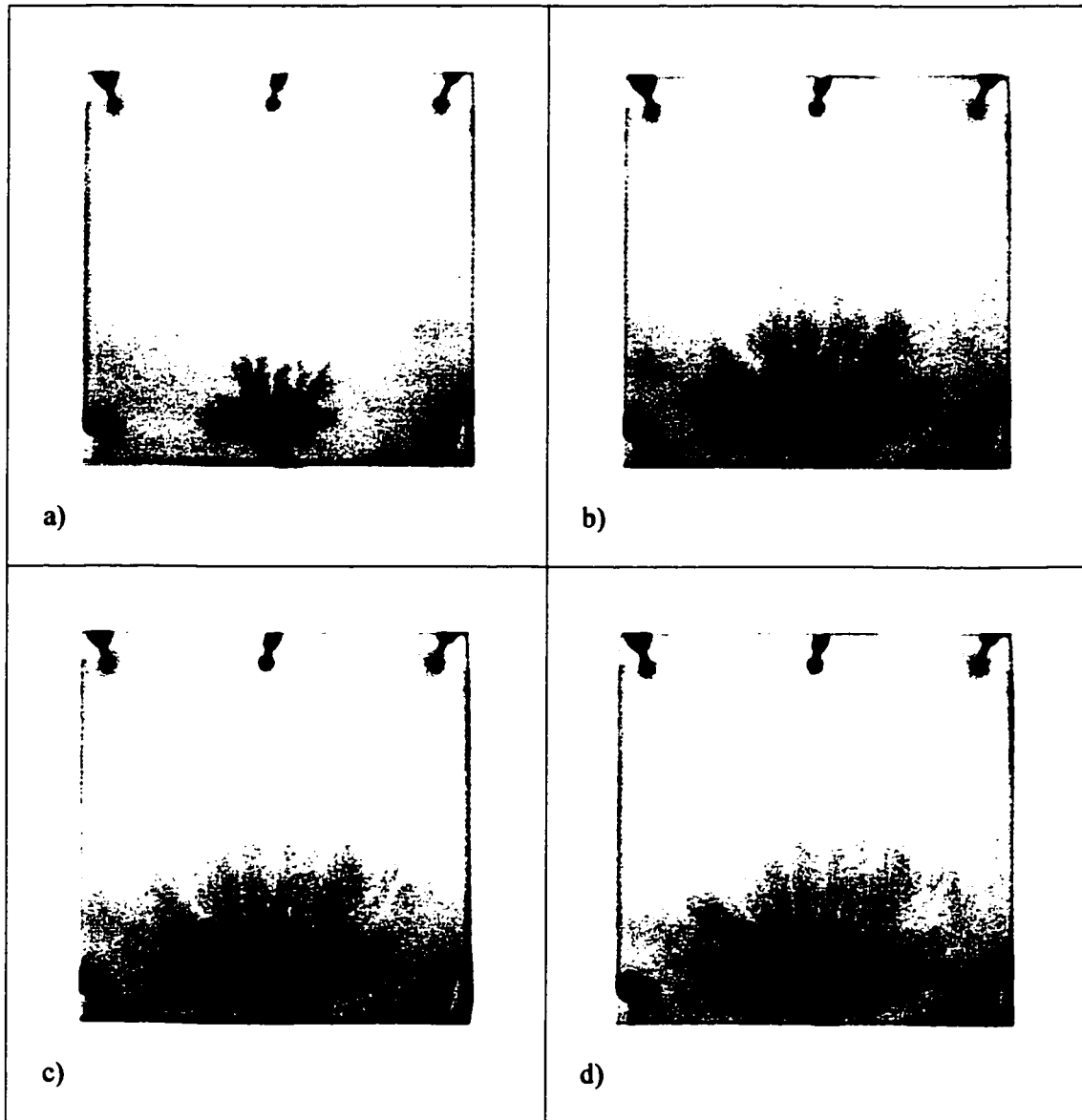


**Figure 3.2: Development of the fingering patterns without connate water in the vertical upward flow mode.  $\mu_o/\mu_w = 11.11$ ,  $Q = 0.78$ ml/min, a)  $t = 80$ sec, b)  $t = 240$ sec, c)  $t = 290$ sec, d)  $t_{br} = 334$ sec**

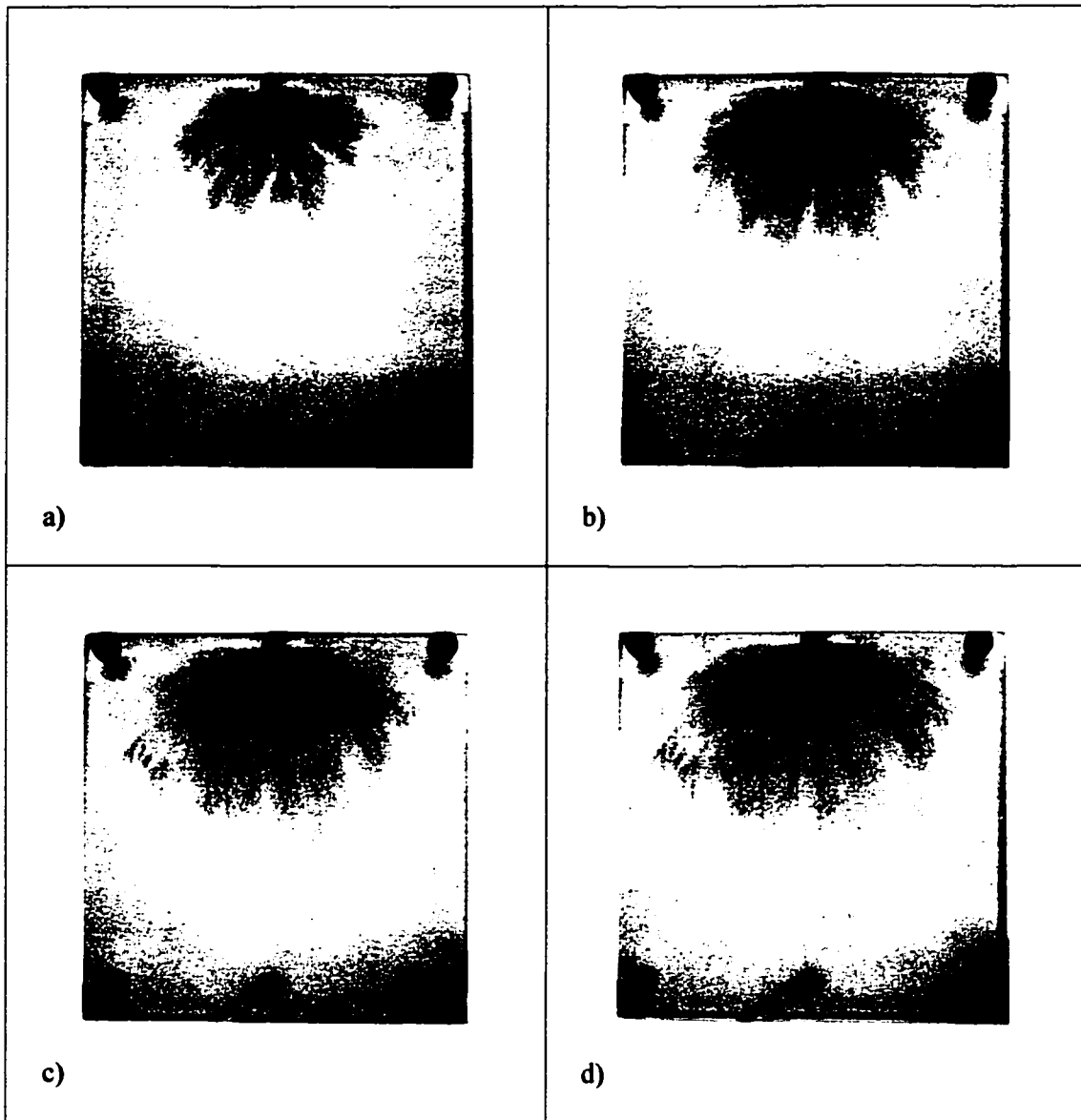


**Figure 3.3: Development of the fingering patterns without connate water in the vertical downward flow mode.  $\mu_o/\mu_w = 11.11$ ,  $Q = 0.78$  ml/min, a)  $t = 120$ sec, b)  $t = 170$ sec, c)  $t = 220$ sec, d)  $t_{br} = 227$ sec**

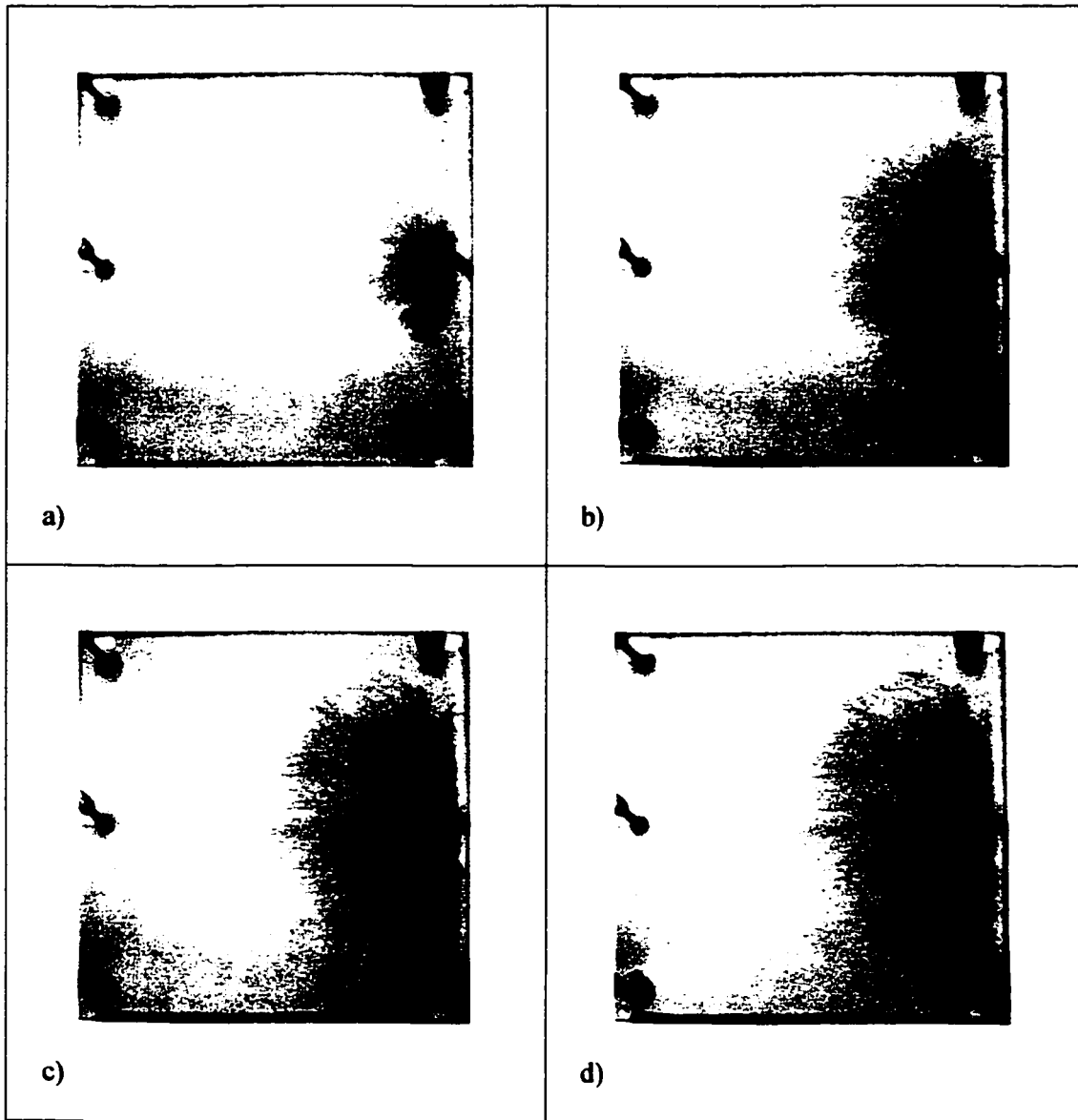


**Figure 3.4: Development of the fingering patterns without connate water in the transverse flow mode.  $\mu_o/\mu_w = 11.11$ ,  $Q = 0.78\text{ml/min}$ , a)  $t = 80\text{sec}$ , b)  $t = 180\text{sec}$ , c)  $t = 230\text{sec}$ , d)  $t_{br} = 255\text{sec}$**

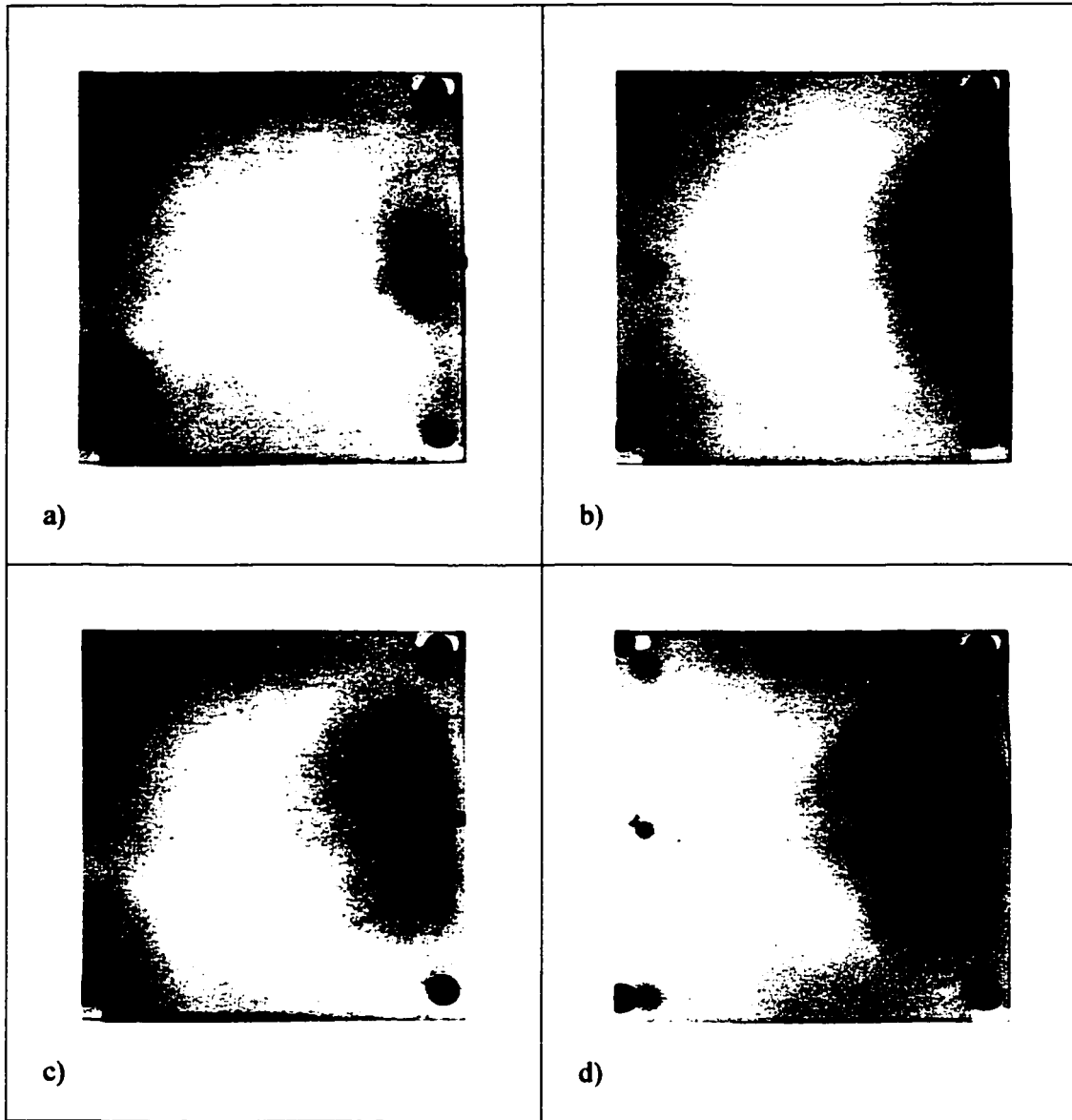


**Figure 3.5: Development of the fingering patterns with connate water in the horizontal flow mode.  $\mu_o/\mu_w = 11.11$ ,  $Q = 0.78$  ml/min, a)  $t = 60$ sec, b)  $t = 190$ sec, c)  $t = 230$ sec, d)  $t_{br} = 251$ sec**

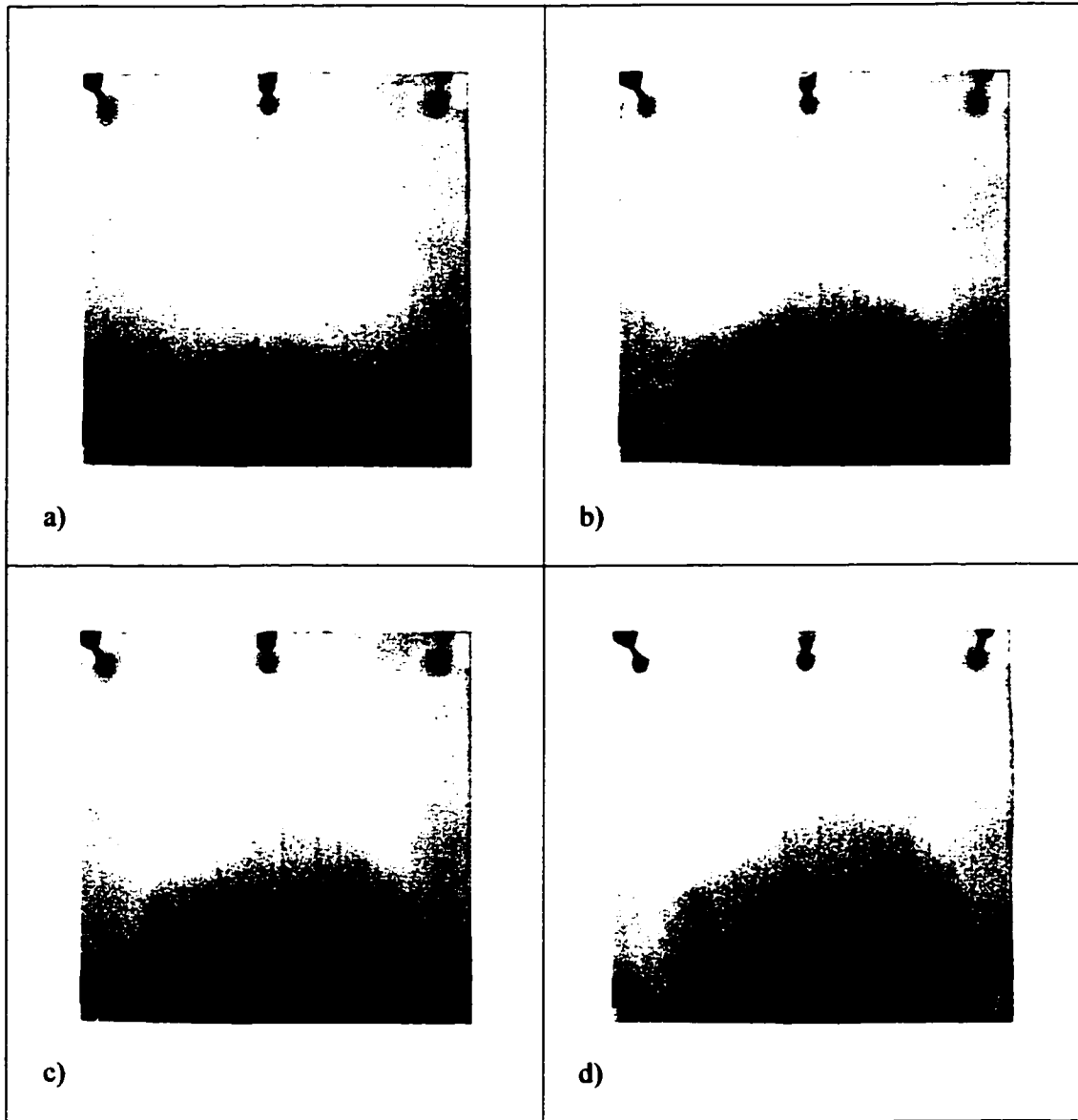


**Figure 3.6: Development of the fingering patterns with connate water in the vertical upward flow mode.  $\mu_o/\mu_w = 11.11$ ,  $Q = 0.78\text{ml/min}$ , (a)  $t = 120\text{sec}$ , (b)  $t = 220\text{sec}$ , (c)  $t = 240\text{sec}$ , (d)  $t_{br} = 268\text{sec}$**

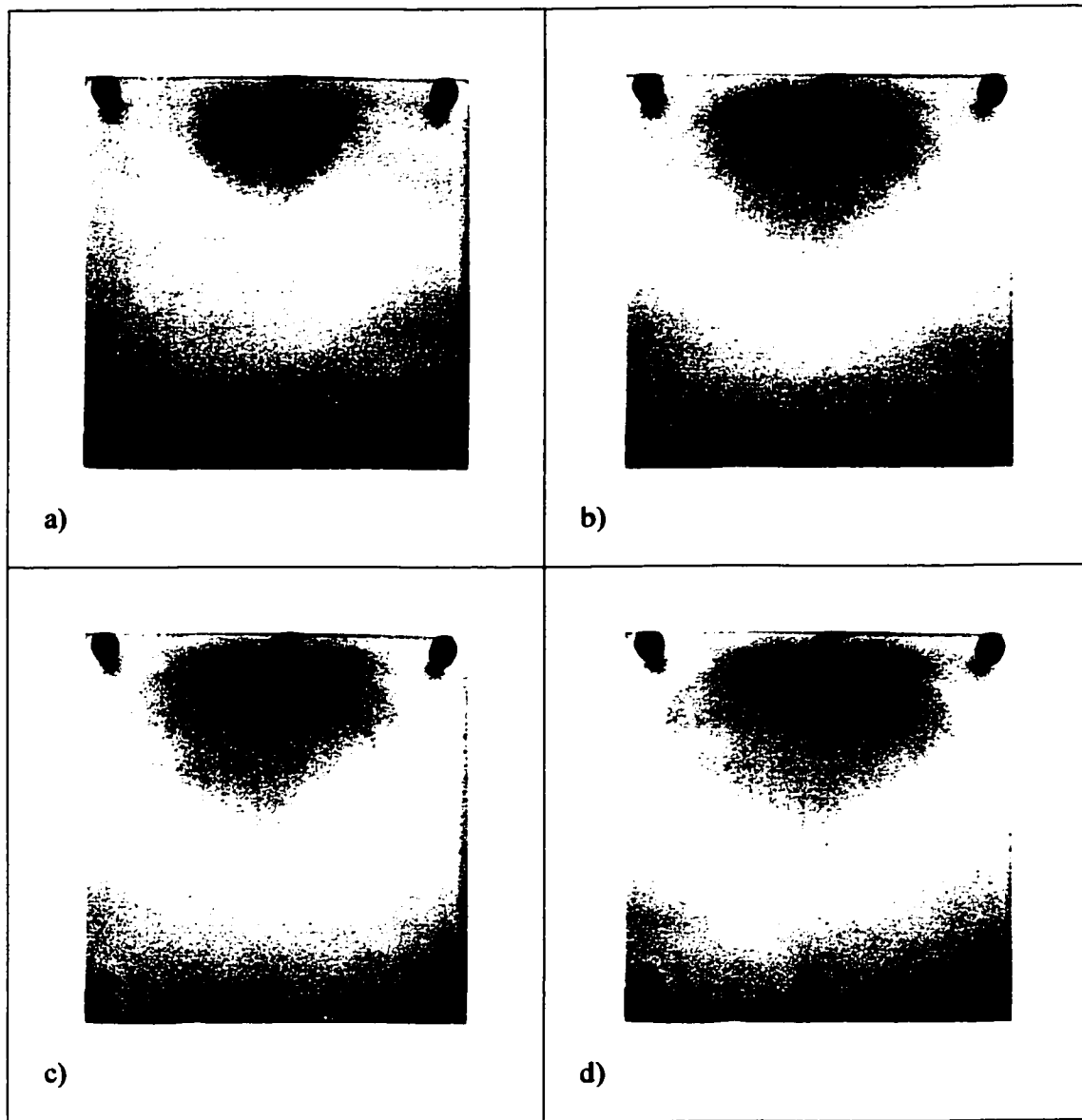


**Figure 3.7: Development of the fingering patterns with connate water in the vertical downward flow mode.  $\mu_o/\mu_w = 11.11$ ,  $Q = 0.78$  ml/min, a)  $t = 100$ sec, b)  $t = 200$ sec, c)  $t = 230$ sec, d)  $t_{br} = 251$ sec**

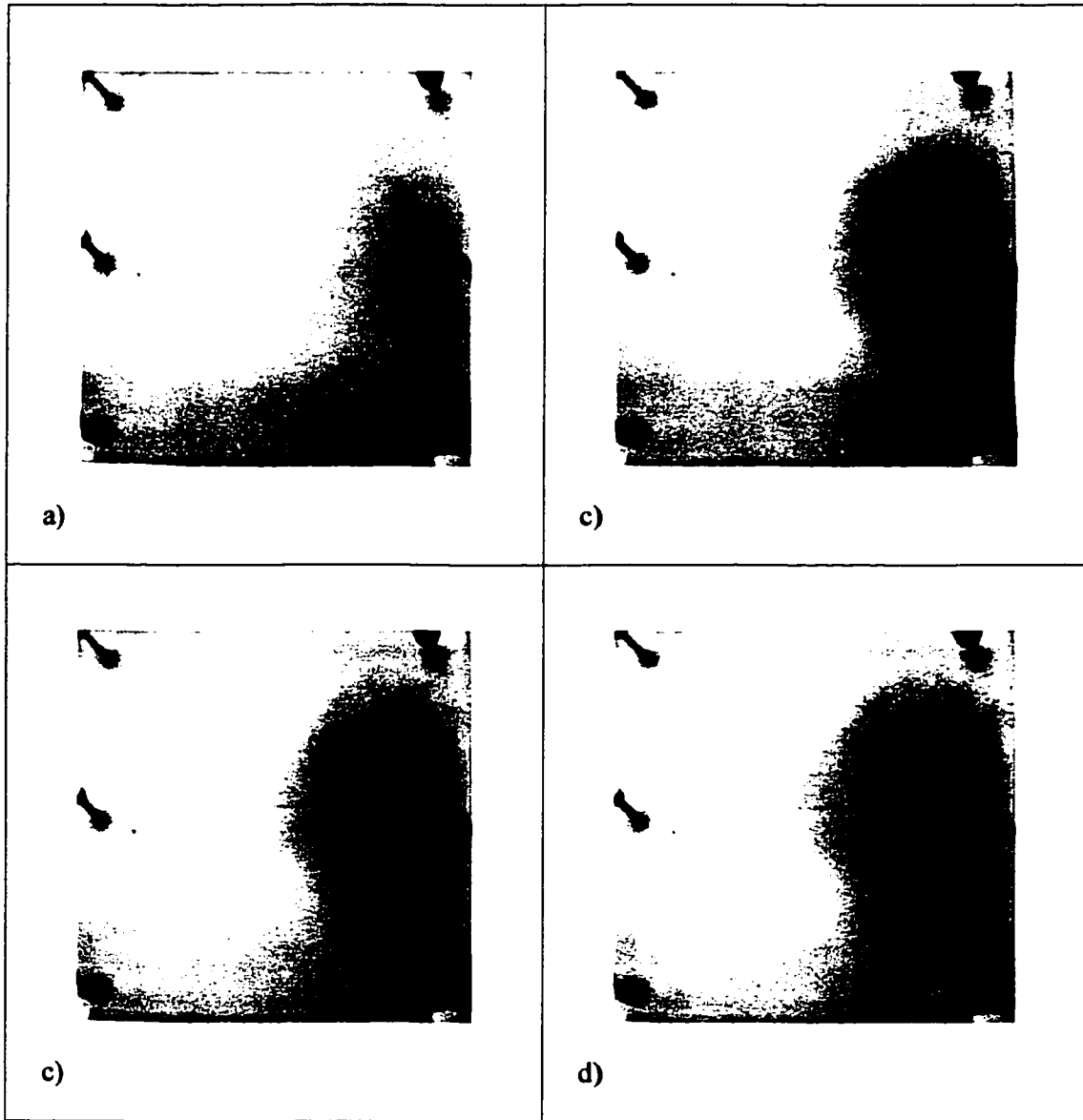


**Figure 3.8: Development of the fingering patterns with connate water in the transverse flow mode.  $\mu_o/\mu_w = 11.11$ ,  $Q = 0.78\text{ml/min}$ , a)  $t = 70\text{sec}$ , b)  $t = 210\text{sec}$ , c)  $t = 235\text{sec}$ , d)  $t_{br} = 252\text{sec}$**

## **3.2 Displacements in the absence of connate water**

### **3.2.1 Horizontal flow mode**

Experiments were carried out in the horizontal plane with glycerol solution displacing the heavy paraffin oil. Figures 3.9 - 3.11 display the results for the horizontal flow mode experiments at viscosity ratios  $\mu_o/\mu_w$  of 143.5, 49.0, and 3.3 respectively. From these figures, the flow rate seems not to affect the displacement patterns. Because of the very small variation in the flow rate, there is only a slight variation in the oil recovery efficiency.

Figures 3.12 and 3.13 depict the effects of viscosity ratio on the horizontal flow mode displacement. It is evident from these pictures that the viscosity ratio plays an important role in immiscible displacement in a porous medium. At a low viscosity ratio  $\mu_o/\mu_w = 3.3$ , the displacing fluid (dyed glycerol solution) covers a large area of the cell and the displacement patterns are smooth; hence, the recovery is high. The fingering at high viscosity ratio is non-uniform. As the viscosity ratio decreases, the fingers become closer to each other and the number diminishes leading to a smooth pattern and an increase in the recovery. For the same flow rate  $Q = 0.23\text{ml}/\text{min}$  the oil recovered is 11.99% for the viscosity ratio  $\mu_o/\mu_w = 143.5$ , and triples when the viscosity ratio reaches 3.3. From this observation, it is clear that a low viscosity ratio stabilizes the displacement pattern, leading to a high recovery.

The plot of the recovery versus the viscosity ratio (Figure 3.14) shows a decrease in the recovery efficiency as the viscosity ratio increases. This plot confirms the negative effects of the increasing viscosity ratio on the recovery. In the horizontal flow mode, gravity forces cannot be observed due to the very small space between the two parallel plates of the cell. These plates impede the fluids from moving freely up or down. In fact, gravity forces

do exist but the effects are negligible compared to the viscous forces responsible for the instability on the interface between the displacing and the displaced fluids. Viscous forces are predominant in the horizontal displacement at high viscosity ratios.

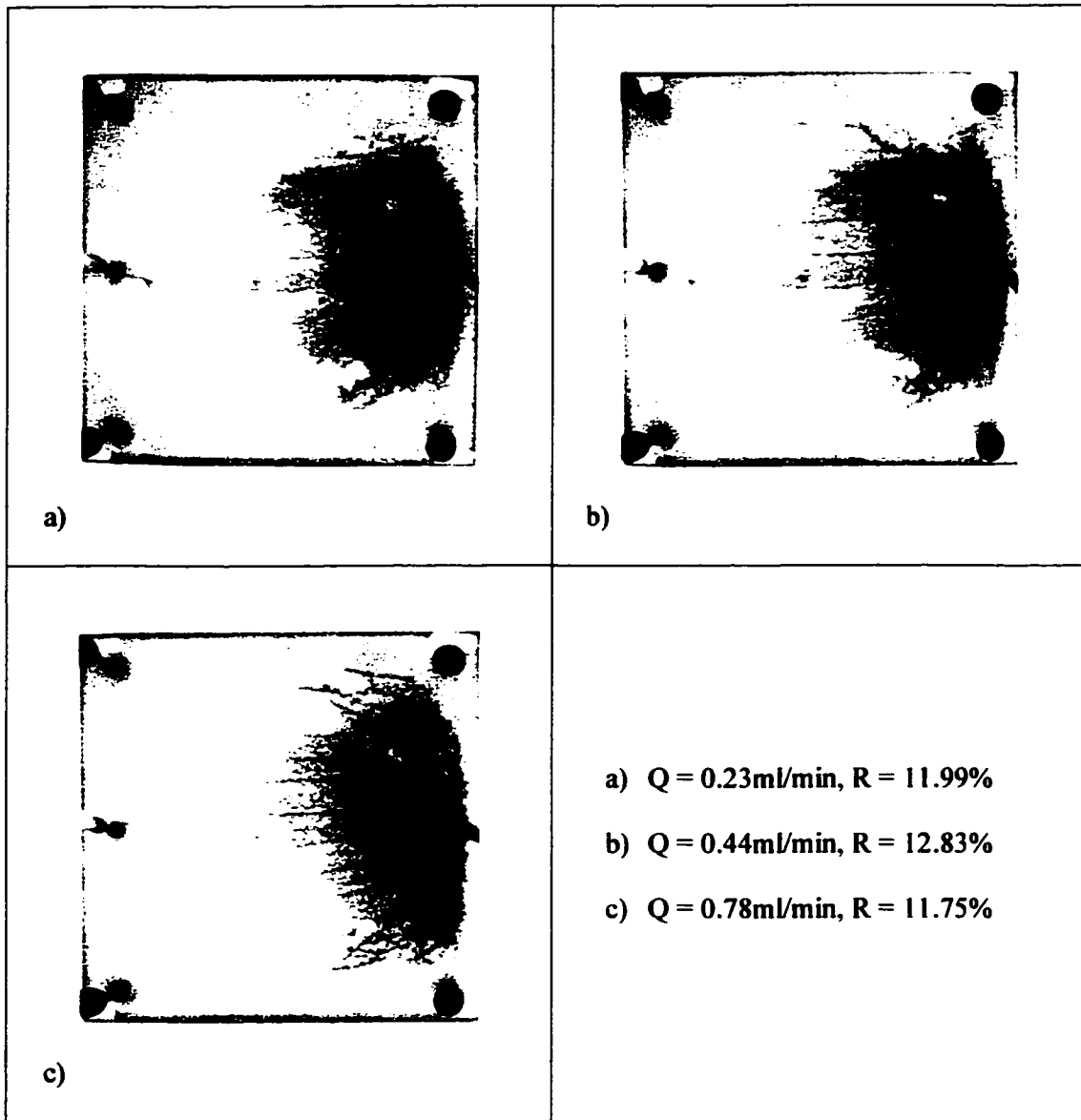


**Figure 3.9: Effects of flow rate on the horizontal flow mode patterns at a given viscosity ratio  $\mu_o/\mu_w = 143.5$**

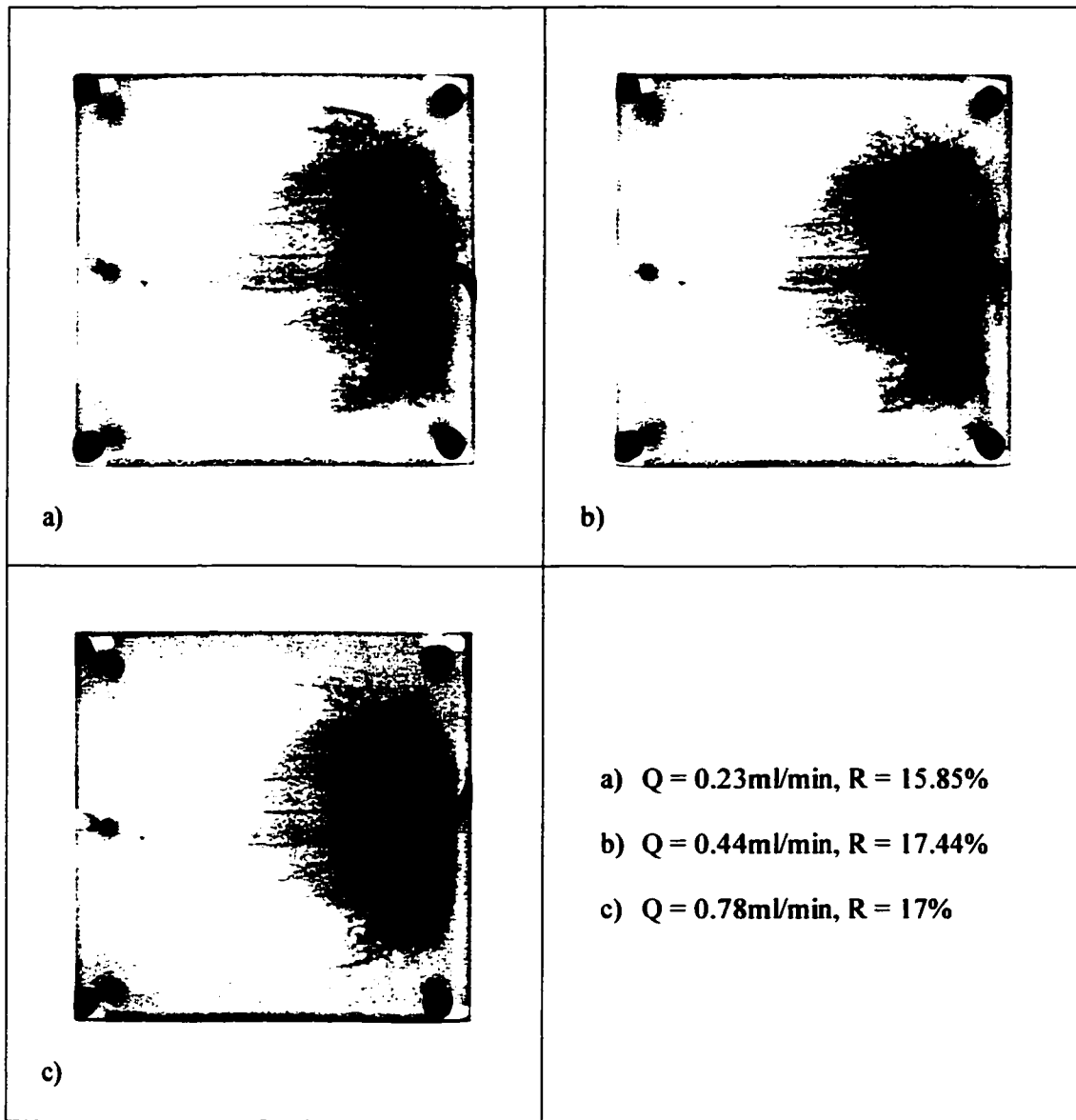


**Figure 3.10: Effects of flow rate on the horizontal flow mode patterns at a given viscosity ratio  $\mu_o/\mu_w = 49.0$**

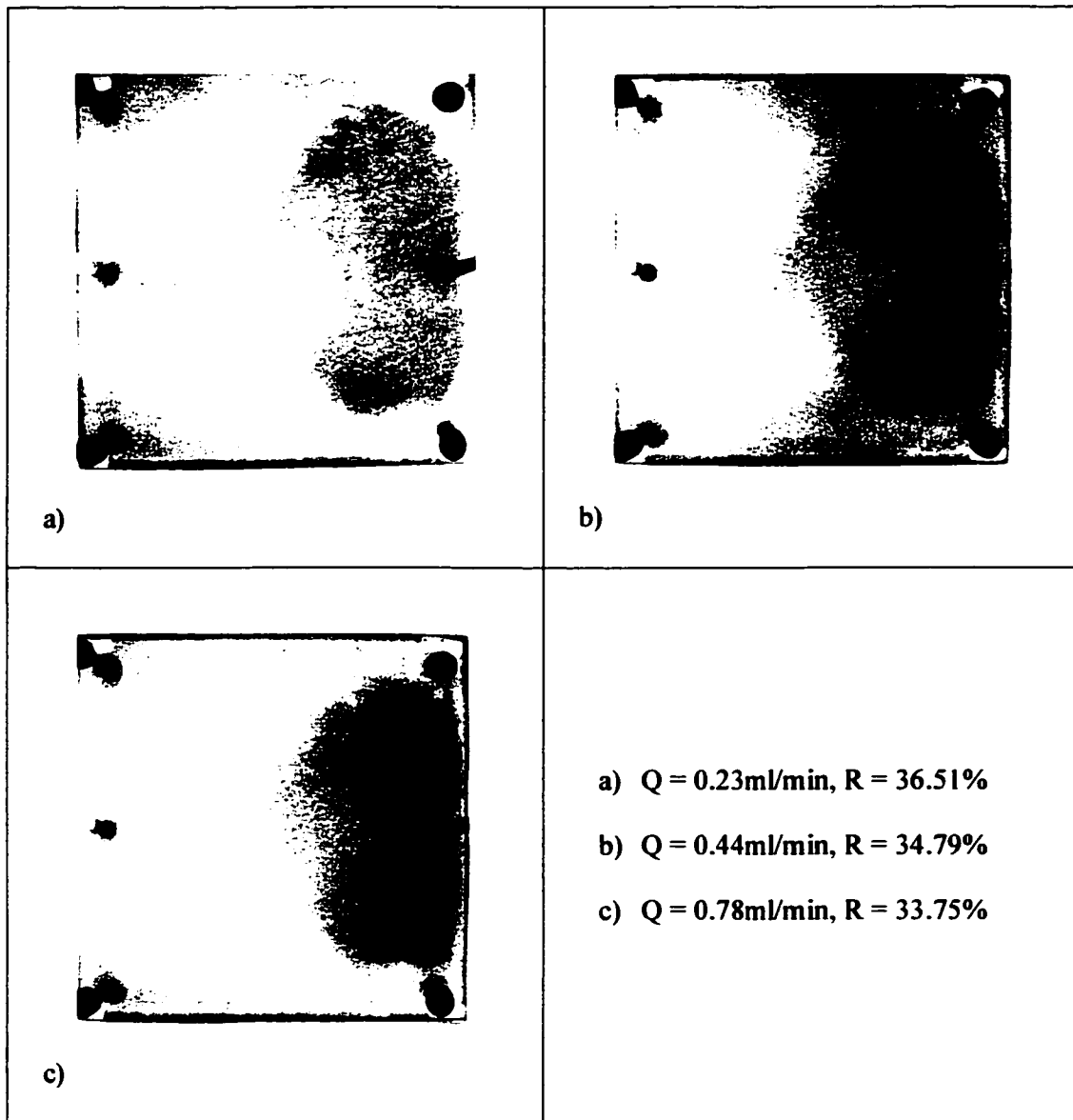


**Figure 3.11: Effects of flow rate on the horizontal flow mode patterns at a given viscosity ratio  $\mu_o/\mu_w = 3.3$**

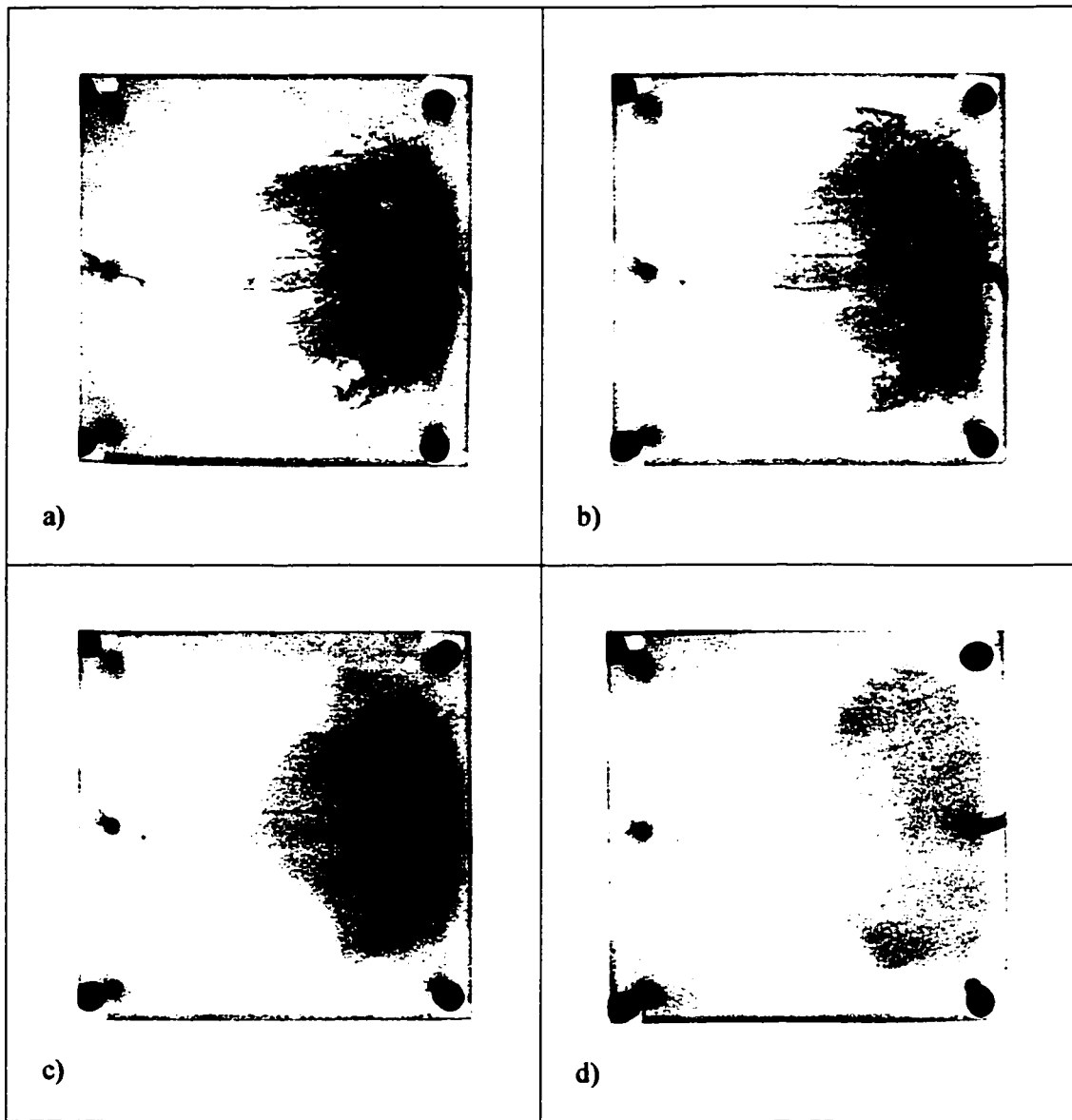


**Figure 3.12: Effects of viscosity ratio on the horizontal flow mode patterns at a given flow rate  $Q = 0.23\text{ml/min}$ . a)  $\mu_o/\mu_w = 143.5$ , b)  $\mu_o/\mu_w = 49.0$ , c)  $\mu_o/\mu_w = 11.11$ , d)  $\mu_o/\mu_w = 3.3$**

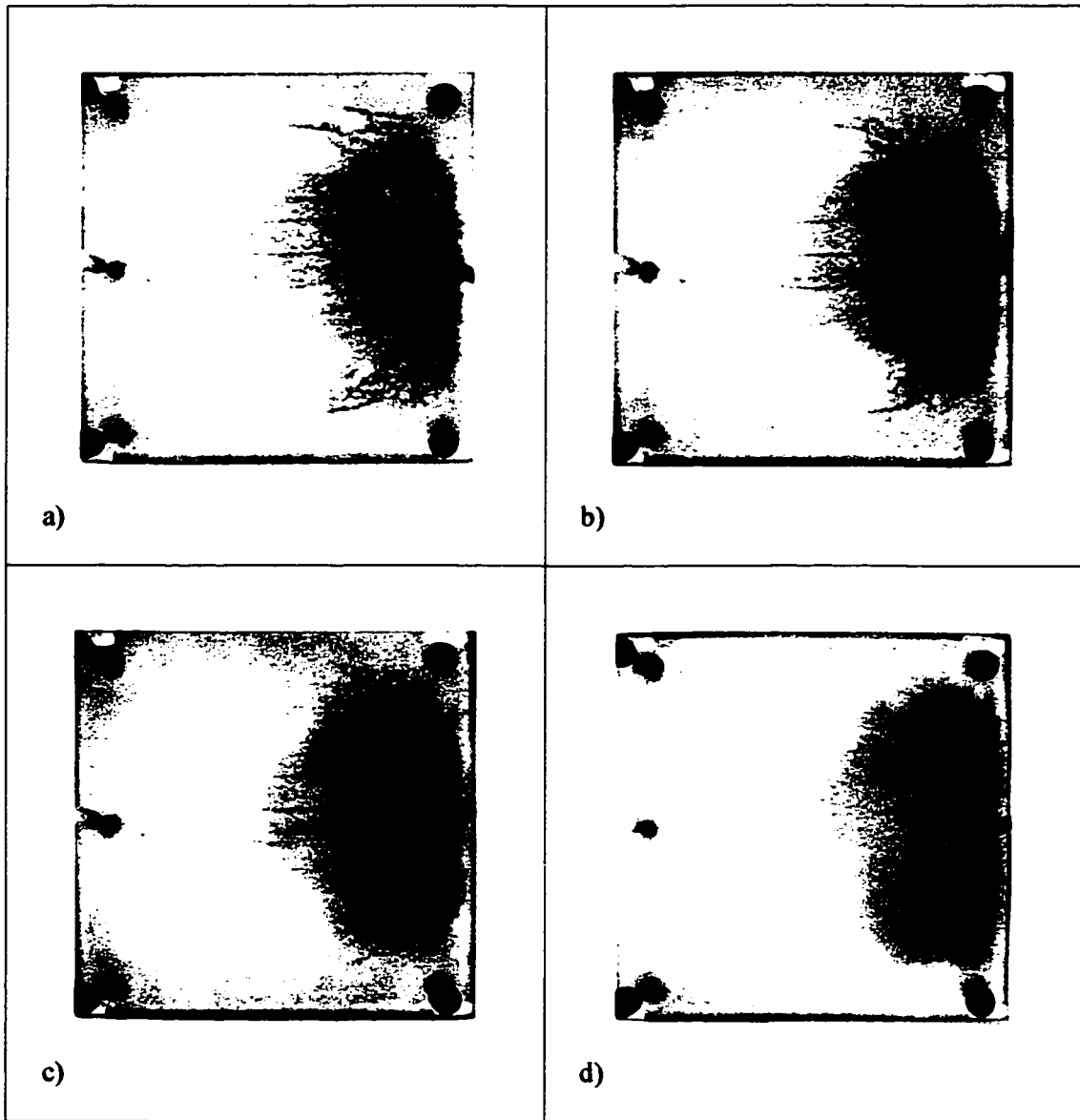


**Figure 3.13 Effects of viscosity ratio on the horizontal flow mode patterns at a given flow rate  $Q = 0.78\text{ml/min}$ . a)  $\mu_o/\mu_w = 143.5$ , b)  $\mu_o/\mu_w = 49.0$ , c)  $\mu_o/\mu_w = 11.11$ , d)  $\mu_o/\mu_w = 3.3$**

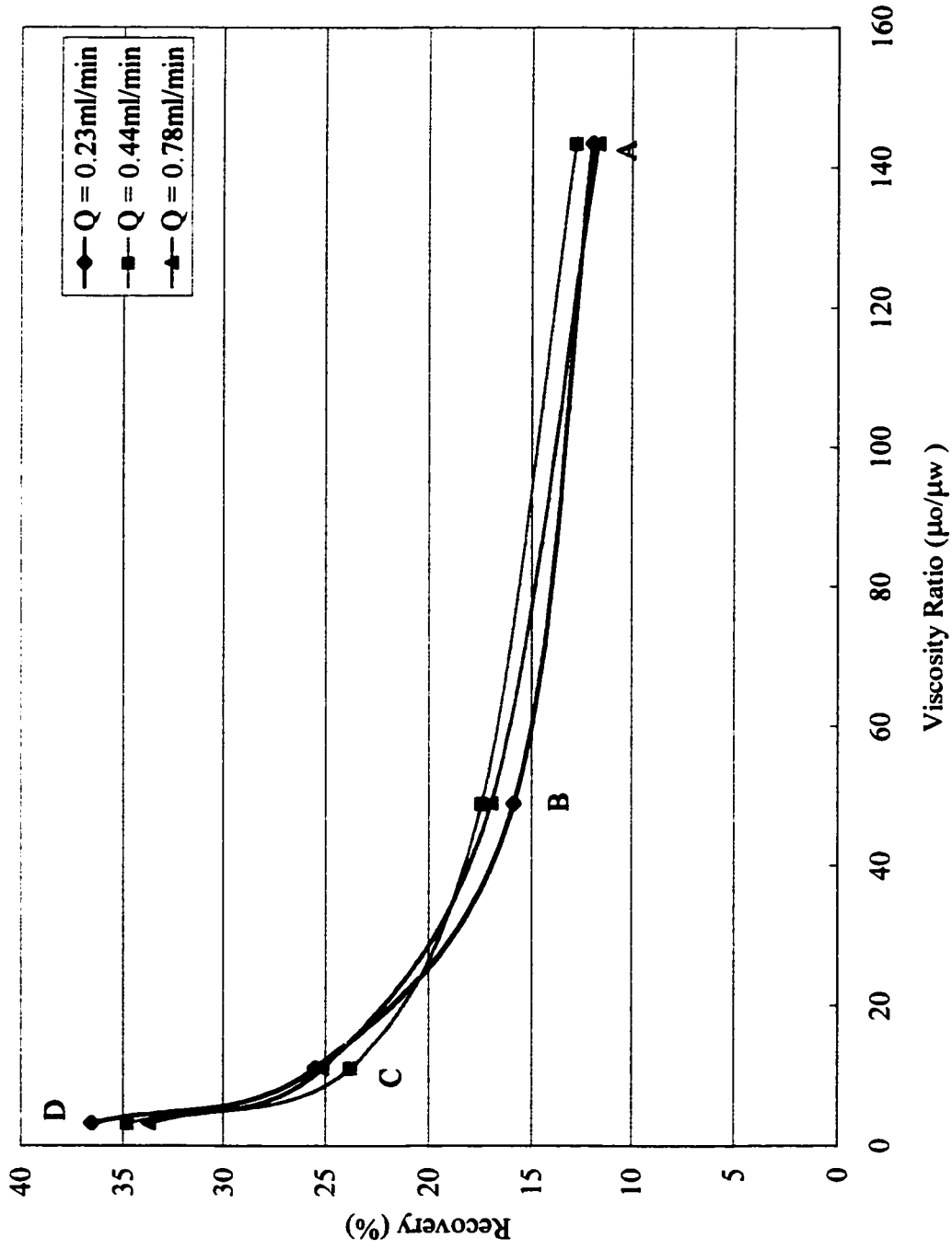


**Figure 3.14: Recovery vs. Viscosity Ratio (Horizontal mode - without connate water)**

### 3.2.2 Vertical upward flow mode

Experiments were conducted in the vertical upward flow mode where dyed glycerol solution displaced the heavy paraffin oil. The higher density displacing fluid tends to remain at the bottom of the cell gradually forming a large gravity tongue especially when the viscosity ratio and the flow rate are low. As a result, the recovery is high.

Figures 3.15 - 3.17 depict respectively the displacement patterns at glycerol concentrations of 0.00%, 30% and 75% at flow rates of 0.23ml/min, 0.44ml/min and 0.78ml/min. Although previous studies have shown the effects of the flow rate on the recovery efficiency, in the present study, due to the small variation in the flow rate the recovery is not significantly affected. Figures 3.16a and 3.17a show the effects of gravity on the displacement pattern. The densest fluid (glycerol solution) lingers at the bottom of the cell (edge where the fluid is injected) covering more area and displacing more oil; hence, the recovery is high compared to the results in other displacement modes. The displacement is fairly stable in the vertical upward flow mode and the recovery decreases as the viscosity ratio increases.

Figures 3.18 and 3.19 show the displacement pattern at different concentrations of the glycerol solution (different viscosity ratios) for a given flow rate. It can be seen that as the viscosity ratio decreases, the displacing fluid covers more area. The recovery is therefore high at low viscosity ratio. The effect of viscosity ratio can be observed on Figure 3.20 (plot of recovery versus viscosity ratio). From a viscosity ratio of 143.5 to 49, the recovery increases from 13.26% to 17.54% for the flow rate  $Q = 0.23\text{ml/min}$ , a difference of 4.28% in the recovery. From  $\mu_o/\mu_w = 143.5$  to 11.11, the recovery almost doubles, and triples when the viscosity ratio reaches 3.3. At high viscosity ratio, buoyancy forces are not strong enough to increase the recovery efficiency even at a low flow rate. The glycerol

**solution has a high density, so very strong buoyancy forces help to displace the paraffin oil. In the vertical upward flow mode, the buoyancy forces mainly govern the displacement especially at low viscosity ratio. The effect of viscous forces is less at a very low viscosity ratio; therefore, the flow rate does not affect the displacement pattern as shown in Figure 3.17.**

**The buoyancy forces are favourable in vertical upward flow mode leading to a high recovery. The vertical upward flow mode also offers a good visualization of the buoyancy forces.**

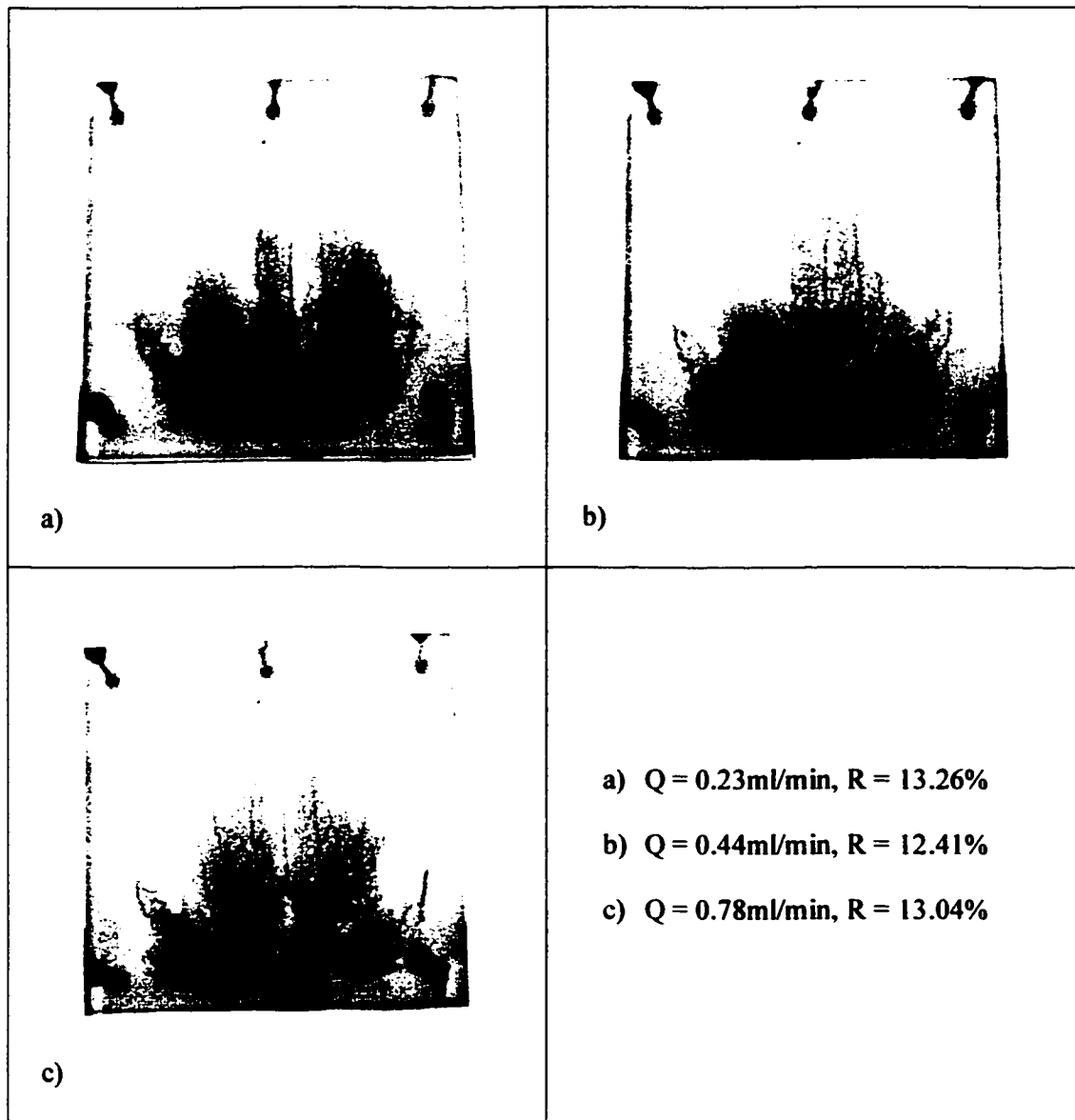


**Figure 3.15: Effects of flow rate on the vertical upward flow mode patterns at a given viscosity ratio  $\mu_o/\mu_w = 143.5$**

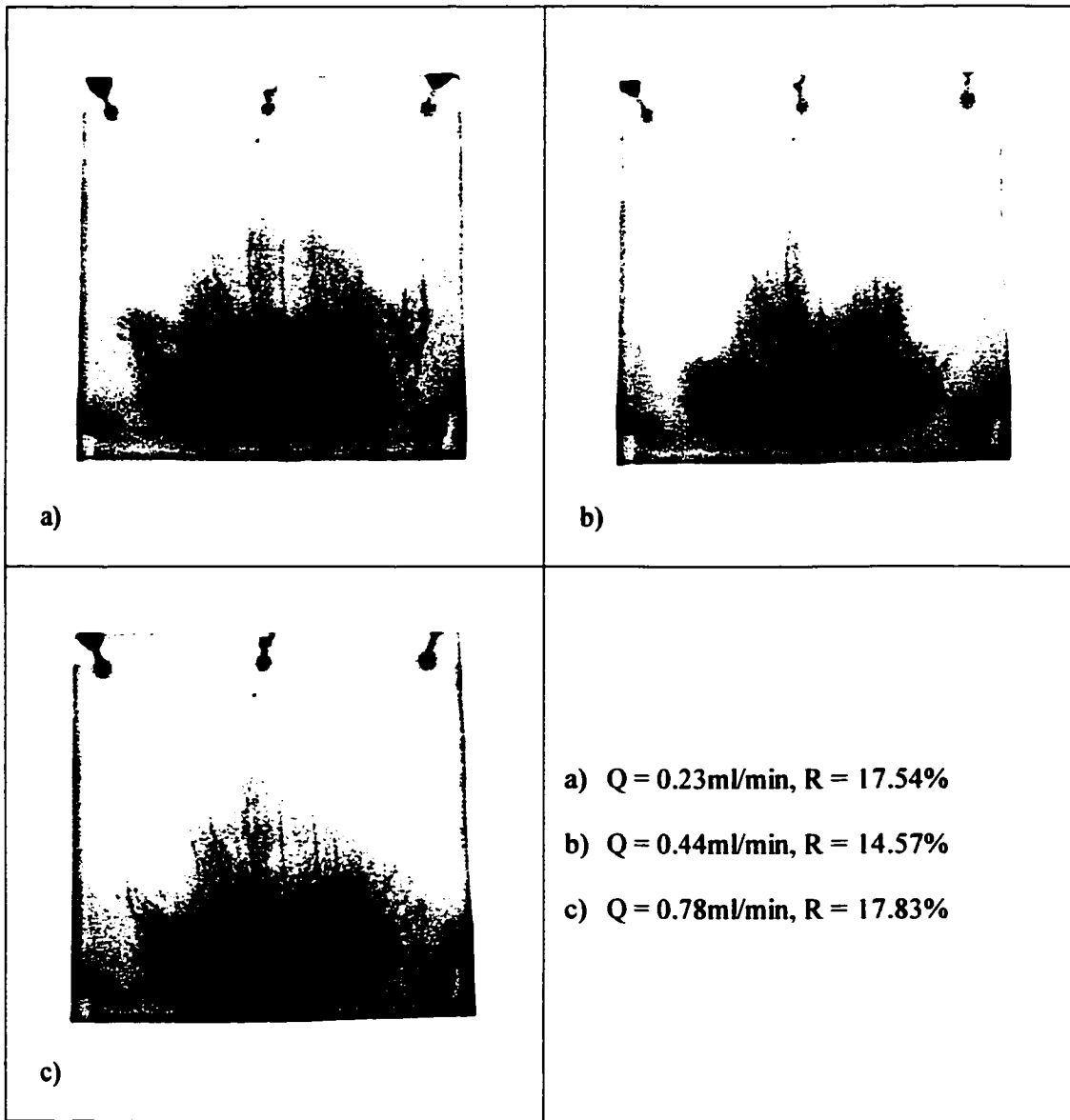


**Figure 3.16: Effects of flow rate on the vertical upward flow mode patterns at a given viscosity ratio  $\mu_o/\mu_w = 49.0$**

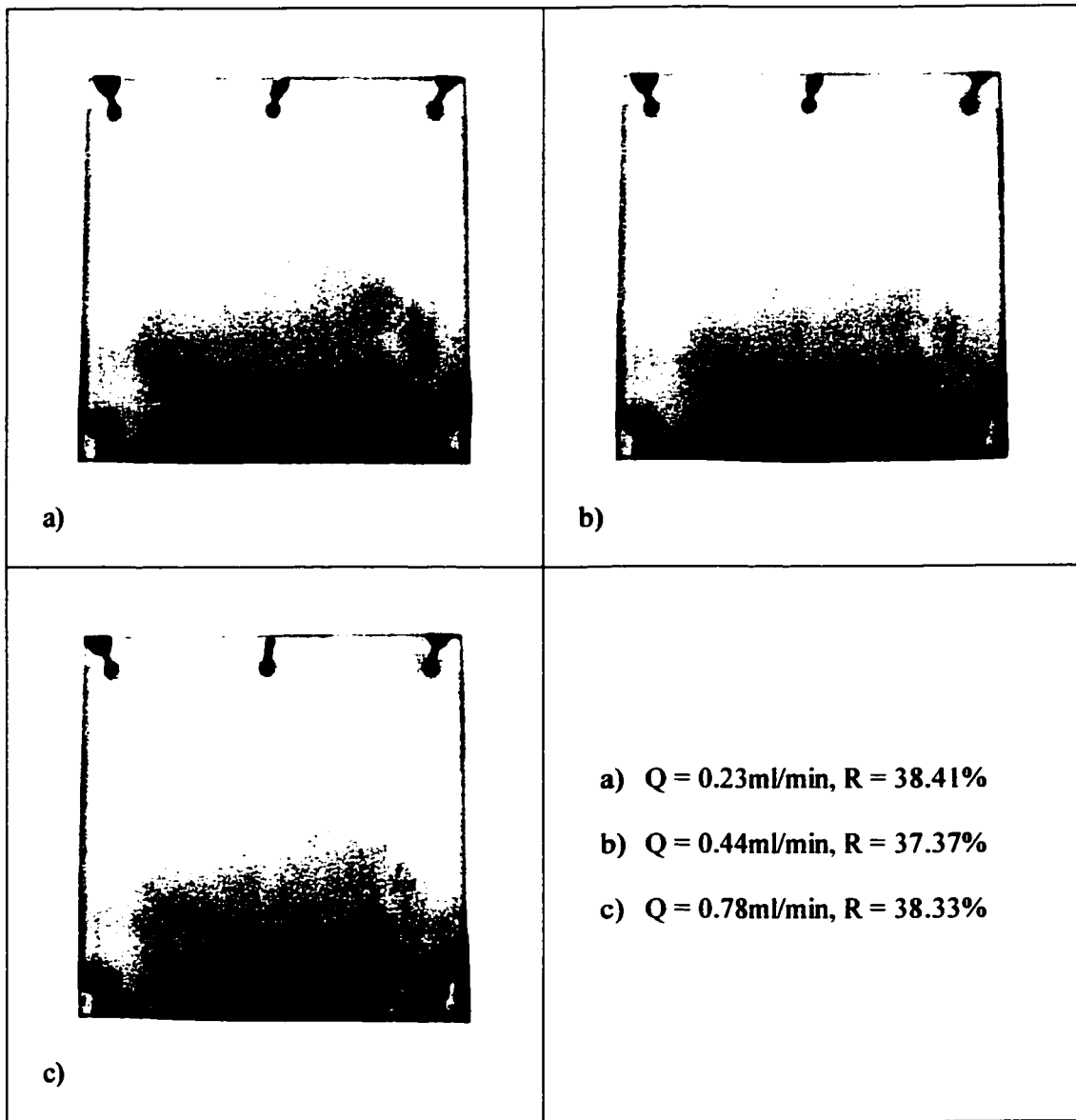


**Figure 3.17: Effects of flow rate on the vertical upward flow mode patterns at a given viscosity ratio  $\mu_o/\mu_w = 3.3$**

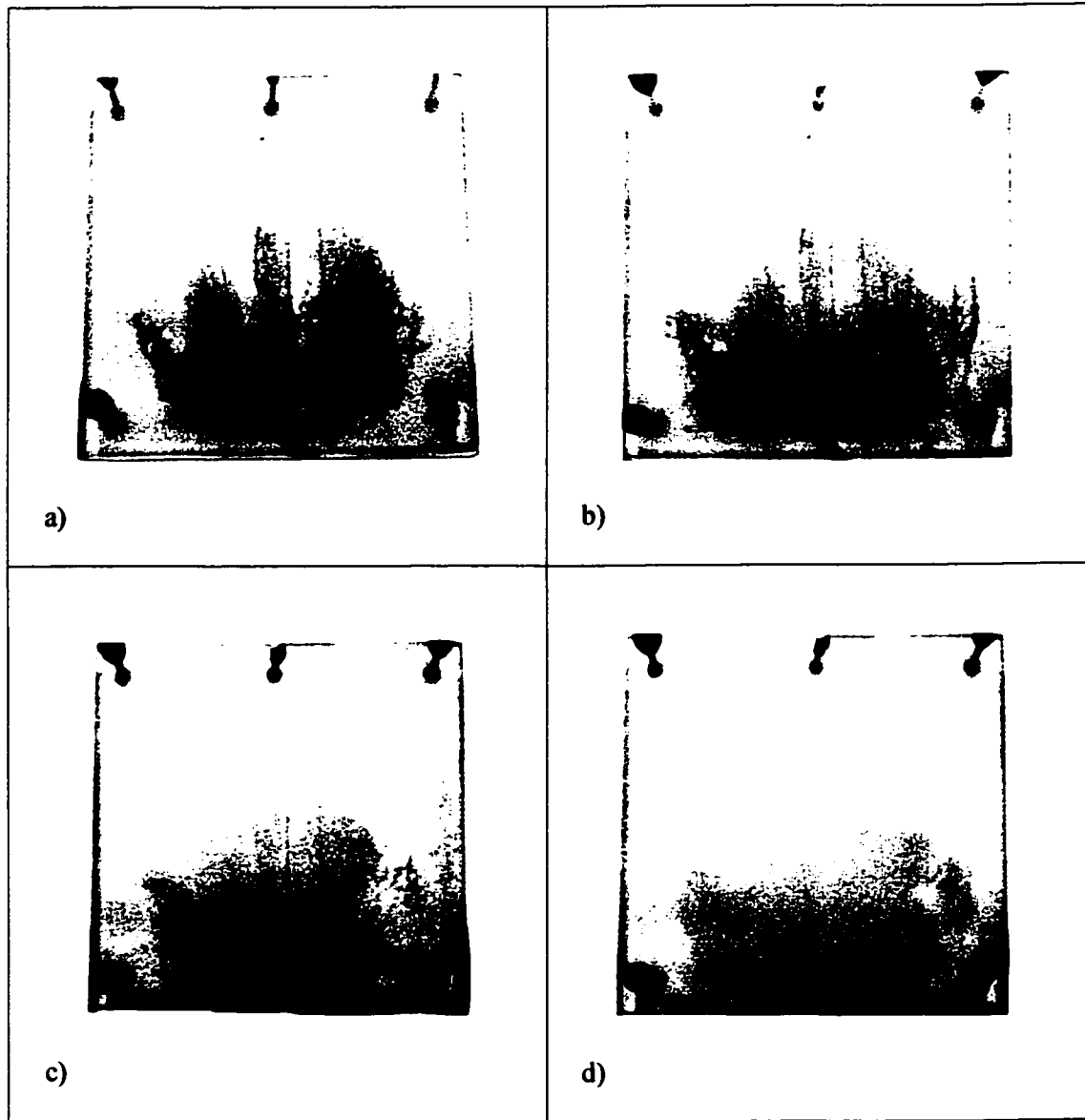


**Figure 3.18: Effects of viscosity ratio on the vertical upward flow mode patterns at a given flow rate  $Q = 0.23\text{ml/min}$ . a)  $\mu_o/\mu_w = 143.5$ , b)  $\mu_o/\mu_w = 49.0$ , c)  $\mu_o/\mu_w = 11.11$ , d)  $\mu_o/\mu_w = 3.3$**

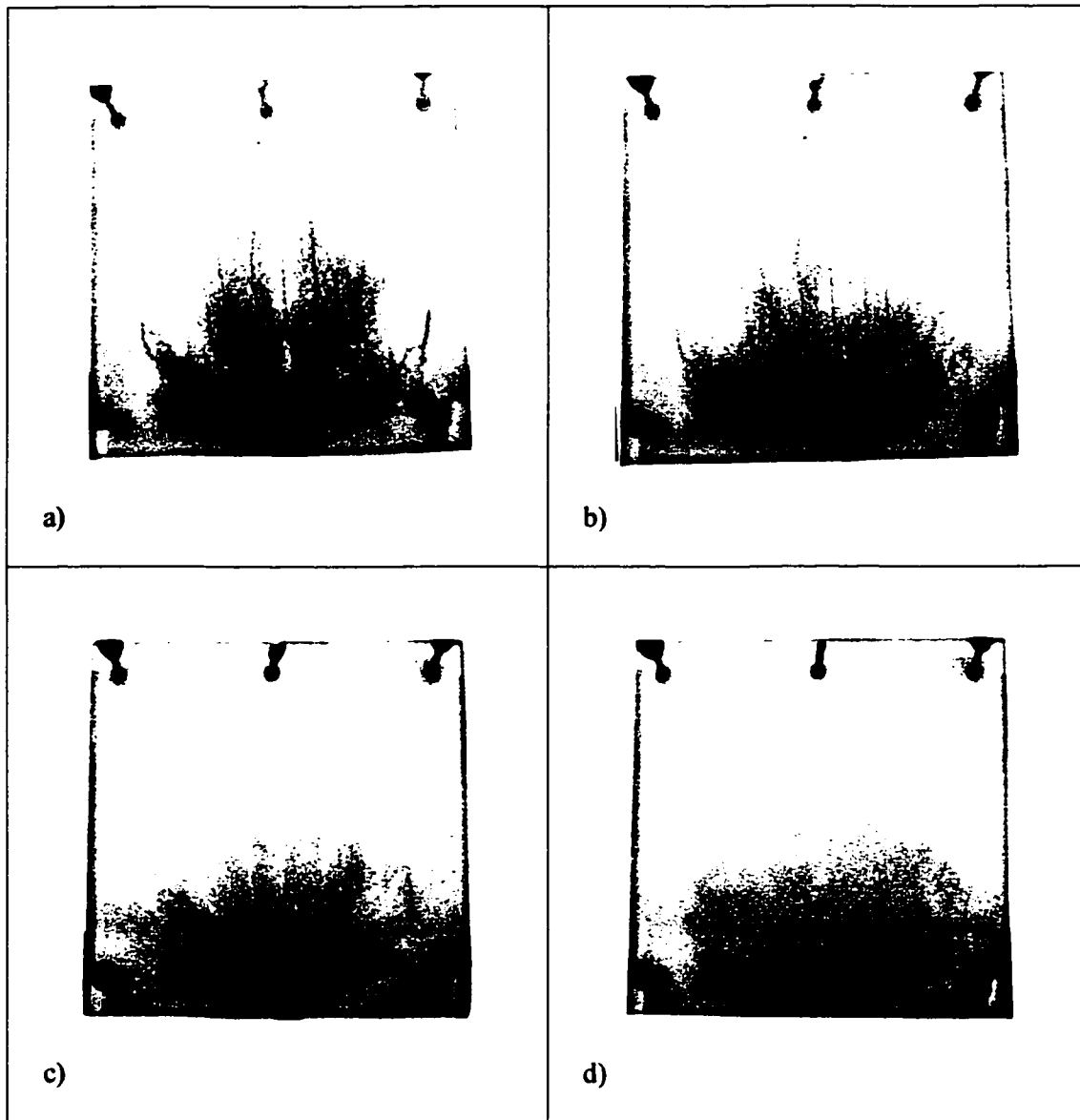


**Figure 3.19: Effects of viscosity ratio on the vertical upward flow mode at a given flow rate  $Q = 0.78\text{ml/min}$ . a)  $\mu_o/\mu_w = 143.5$ , b)  $\mu_o/\mu_w = 49.0$ , c)  $\mu_o/\mu_w = 11.11$ , d)  $\mu_o/\mu_w = 3.3$**

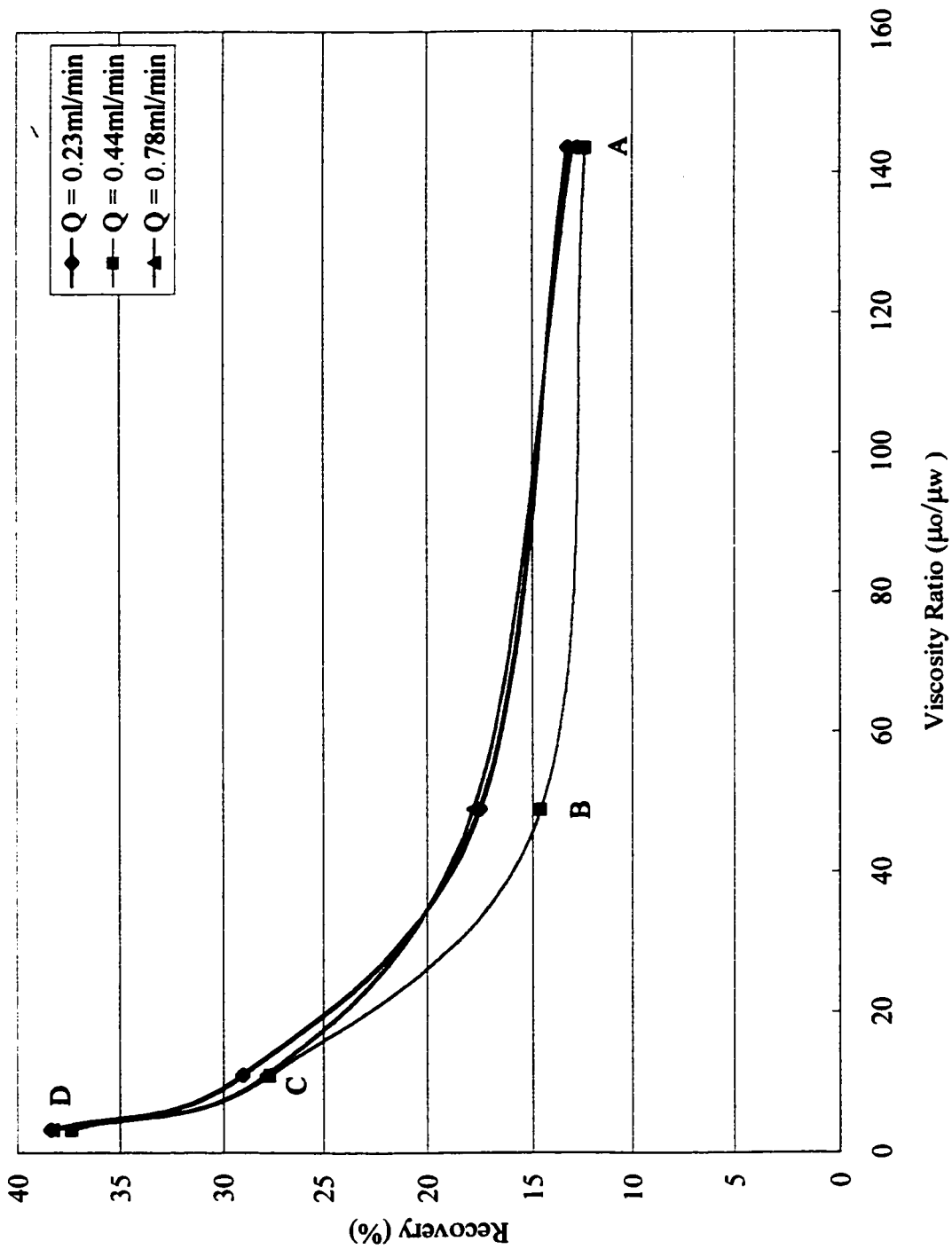


Figure 3.20: Recovery vs. Viscosity Ratio (Vertical upward mode - without connate water)

### **3.2.3 Vertical downward flow mode**

In vertical downward displacements, the cell is aligned in the vertical plane but the injection port is at the top of the cell and the recovery takes place at the bottom. Since the density of the displacing fluid is higher than that of the displaced fluid, the displacing fluid tends to sink naturally toward the bottom of the cell. Buoyancy forces are not strong enough to keep the glycerol solution at the top of the cell; this leads to a low recovery compared to other displacement modes. The displacement is unstable and a large number of fingers are formed. From Figures 3.21 - 3.23, the flow rate has little effect on the recovery efficiency. In the vertical downward flow mode, the injected fluid moves very fast leading to a premature breakthrough compared to the displacement in the vertical upward flow mode. This observation indicates the predominant effects of viscous forces in vertical downward displacement. Although viscous forces dominate the displacement process, buoyancy forces are still present but their effects are not significant.

The displacement patterns are different as the viscosity ratio increases. At a given flow rate ( $Q = 0.23\text{ml/min}$ ) it can be seen in Figures 3.24 and 3.25 that the displacing fluid covers more area when the viscosity ratio is decreased; hence, the recovery increases gradually. At high viscosity ratio, the number of tiny fingers increased indicating the presence of viscous forces. Only a gravity tongue is observed in Figures 3.24d and 3.25d. Upon decreasing the viscosity ratio, the fingers become closer to each other forming the gravity tongue as shown in Figures 3.24 and 3.25. The plot of the oil recovered versus the viscosity ratio (Figure 3.26) shows a decrease in the recovery when the viscosity ratio increases. The recovery drops from 32.01% to 10.41% for an increase in viscosity ratio from 3.3 to 143.5 for a given flow rate  $Q = 0.23\text{ml/min}$ . This plot confirms the effects of viscosity ratio on the recovery efficiency.

In the vertical downward flow mode displacement, buoyancy forces are unfavourable. The displacing fluid moves fast leaving more uncontacted area especially at high viscosity ratio. The greater the uncontacted area is, the less is the recovery. Viscous forces mostly dominate the vertical downward process; as a result, the recovery decreases as the viscosity ratio increases. Since experiments were carried out with only a small variation in the flow rate, the patterns and the recovery were not significantly affected. Nevertheless, the effects of the flow rate may be observed in some cases. The lower the viscosity ratio is, the more stable is the displacement and the higher is the oil recovery.

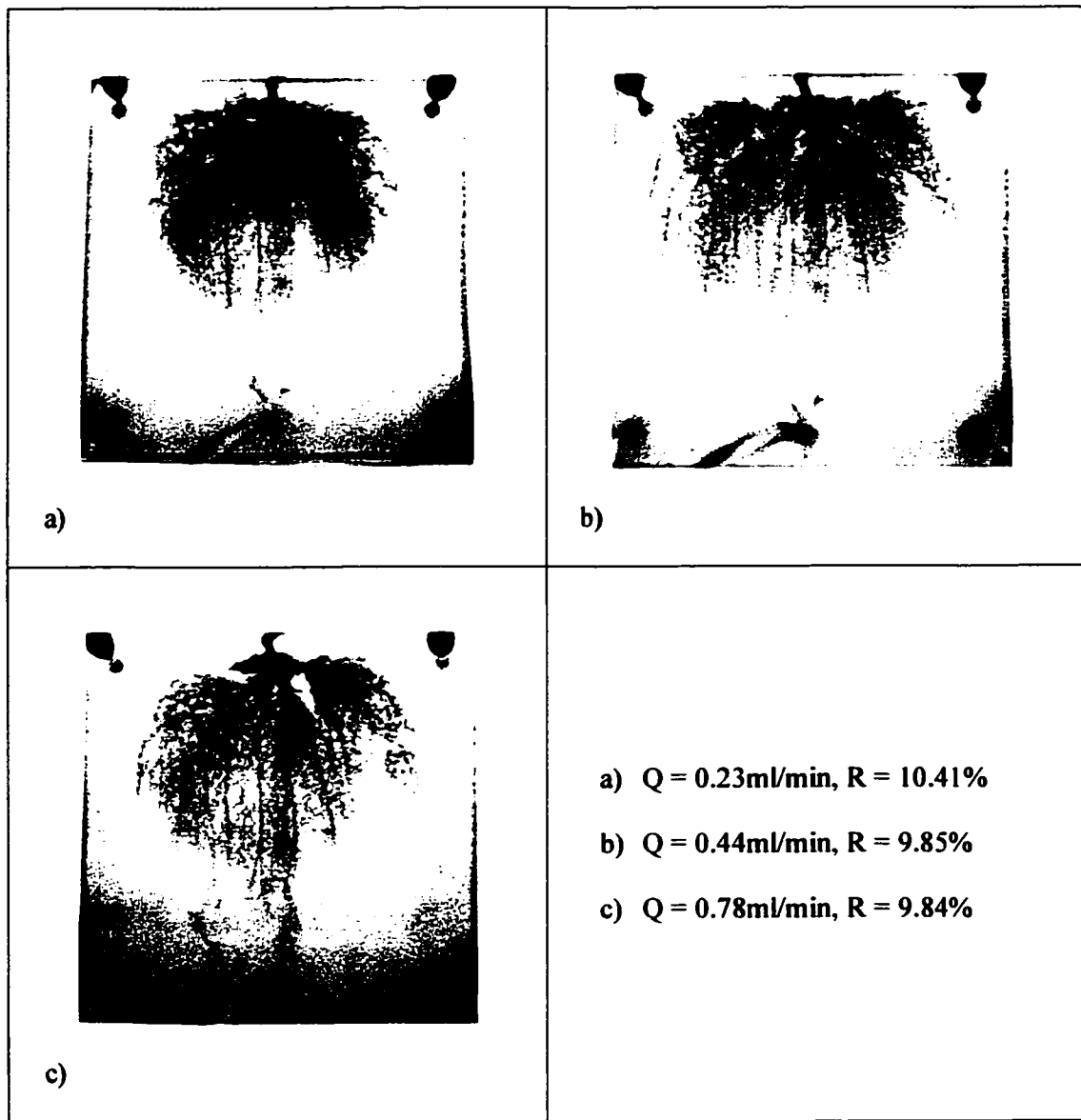


**Figure 3.21: Effects of flow rate on the vertical downward flow mode patterns at a given viscosity ratio  $\mu_o/\mu_w = 143.5$**

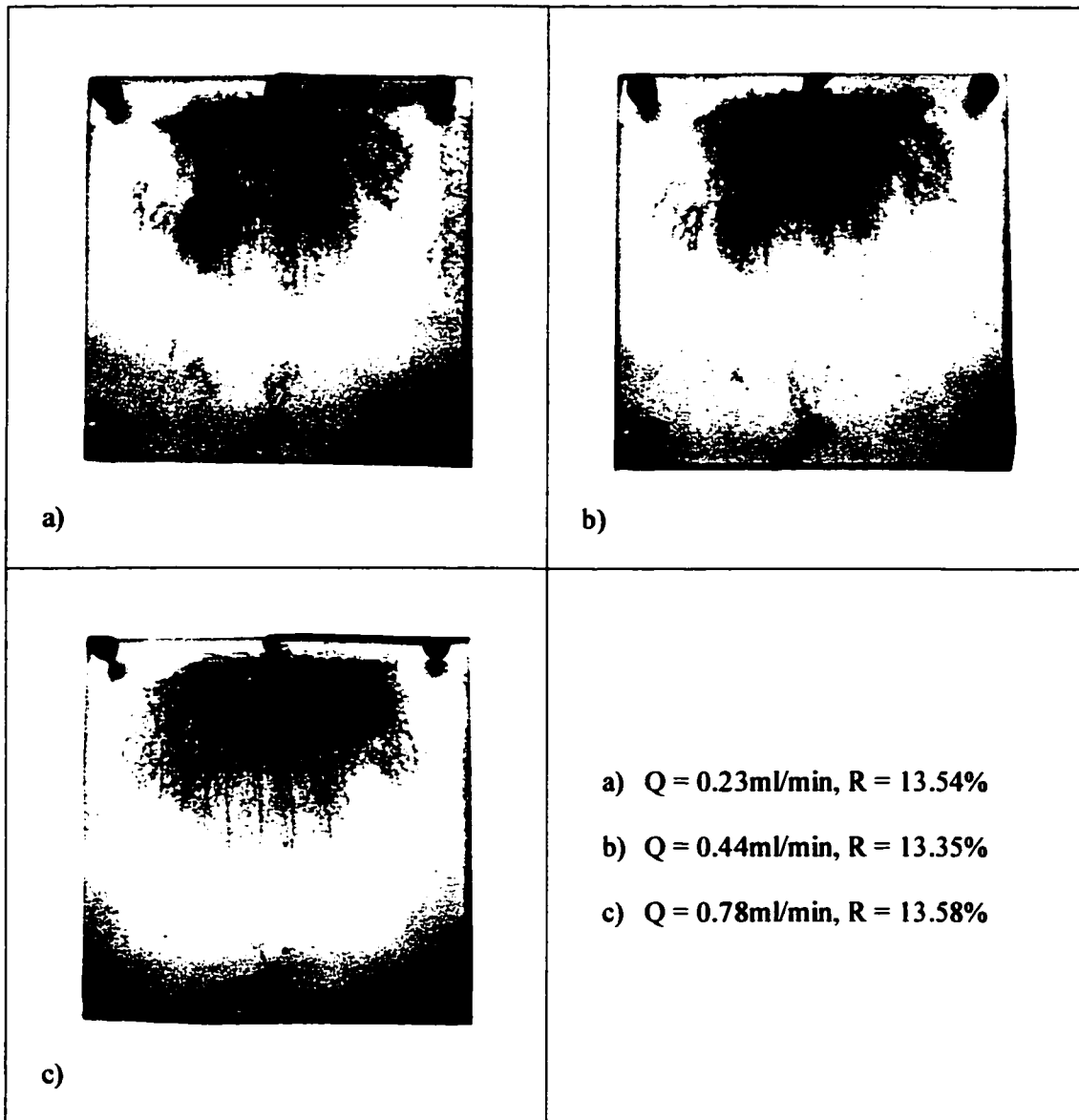


**Figure 3.22: Effects of flow rate on the vertical downward flow mode patterns at a given viscosity ratio  $\mu_o/\mu_w = 49.0$**

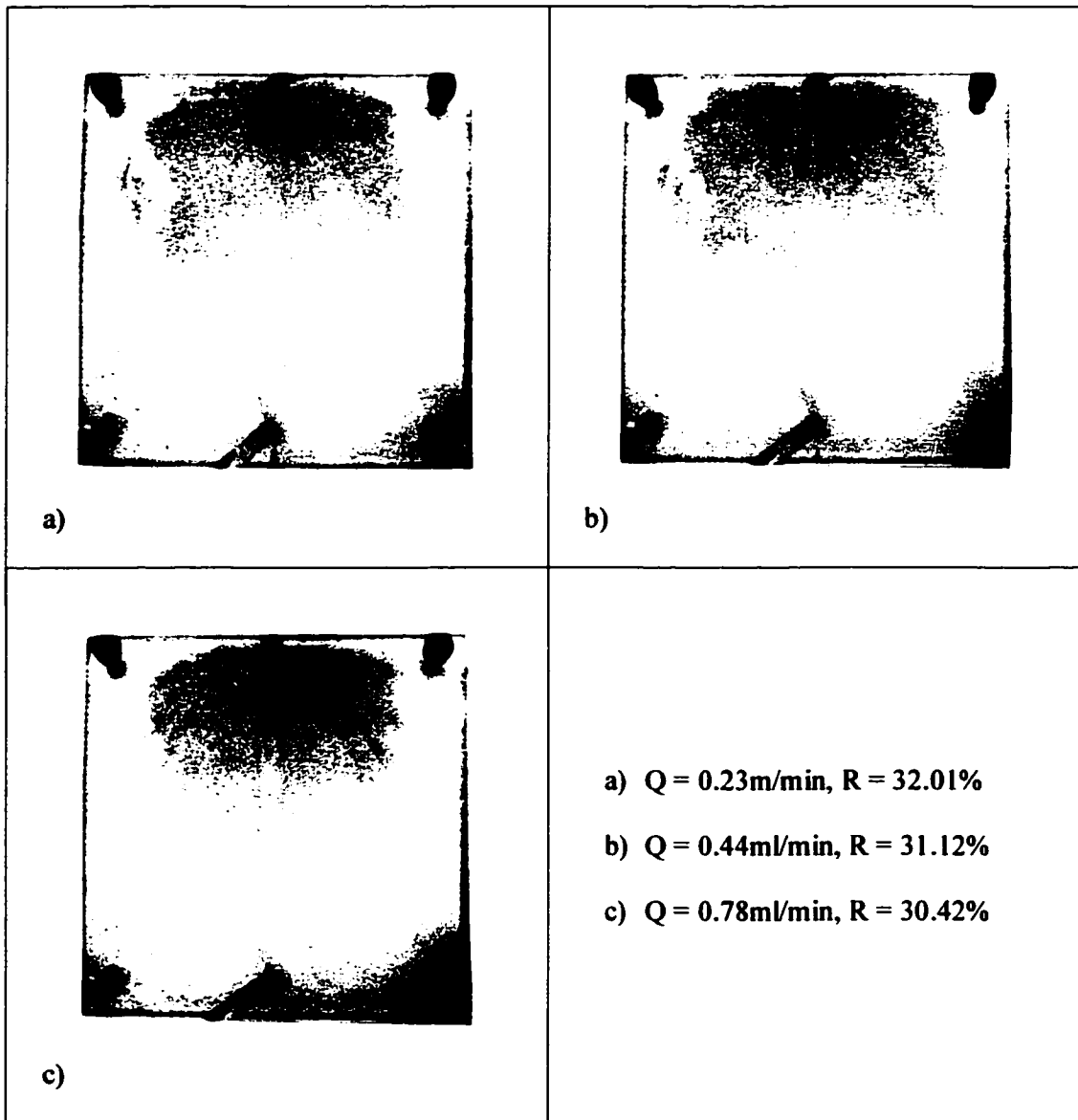


**Figure 3.23: Effects of flow rate on the vertical downward flow mode patterns at a given viscosity ratio  $\mu_o/\mu_w = 3.3$**

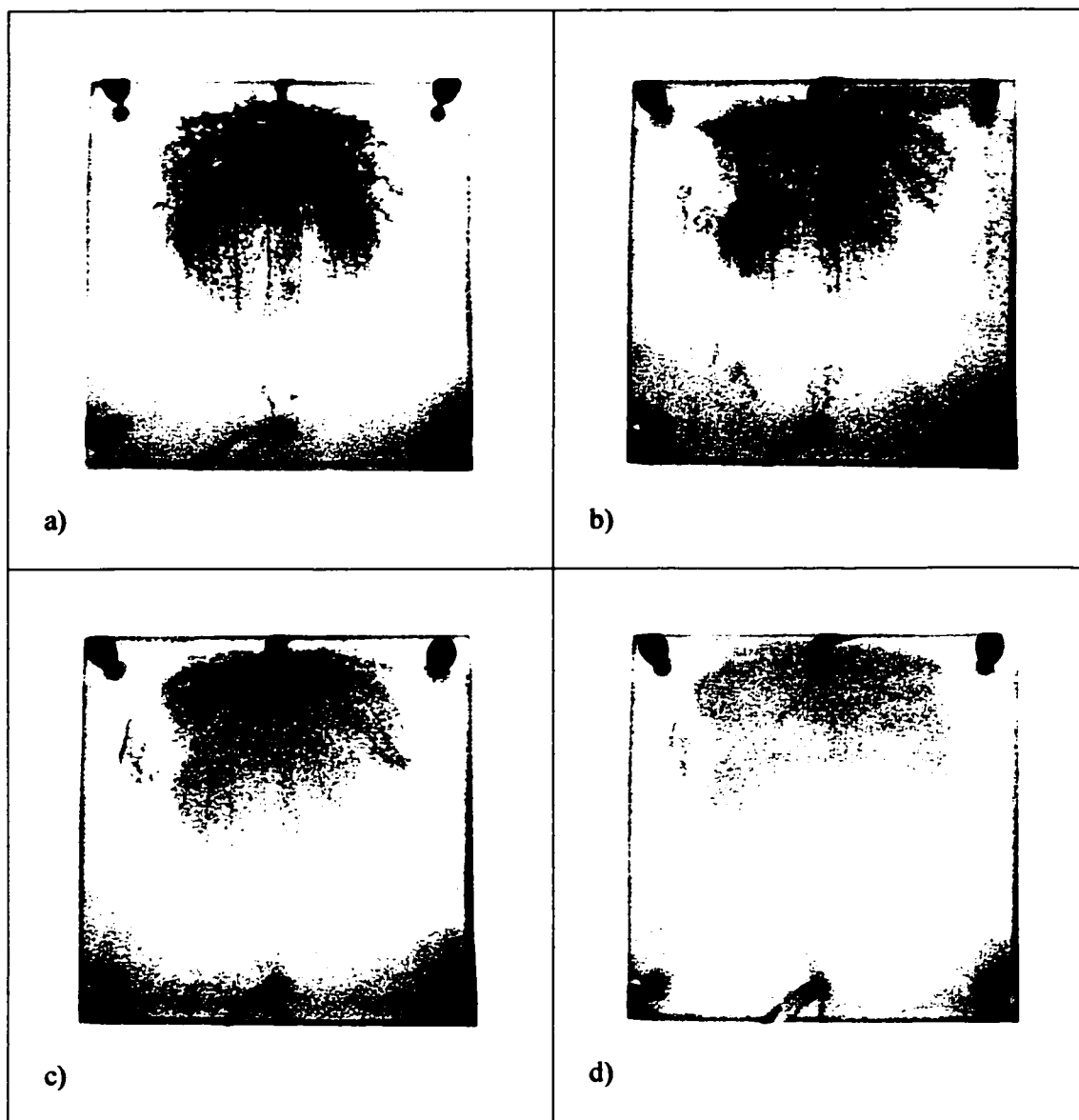


**Figure 3.24: Effects of viscosity ratio on the vertical downward flow mode patterns at a given flow rate  $Q = 0.23\text{ml/min}$ . a)  $\mu_o/\mu_w = 143.5$ , b)  $\mu_o/\mu_w = 49.0$ , c)  $\mu_o/\mu_w = 11.11$ , d)  $\mu_o/\mu_w = 3.3$**

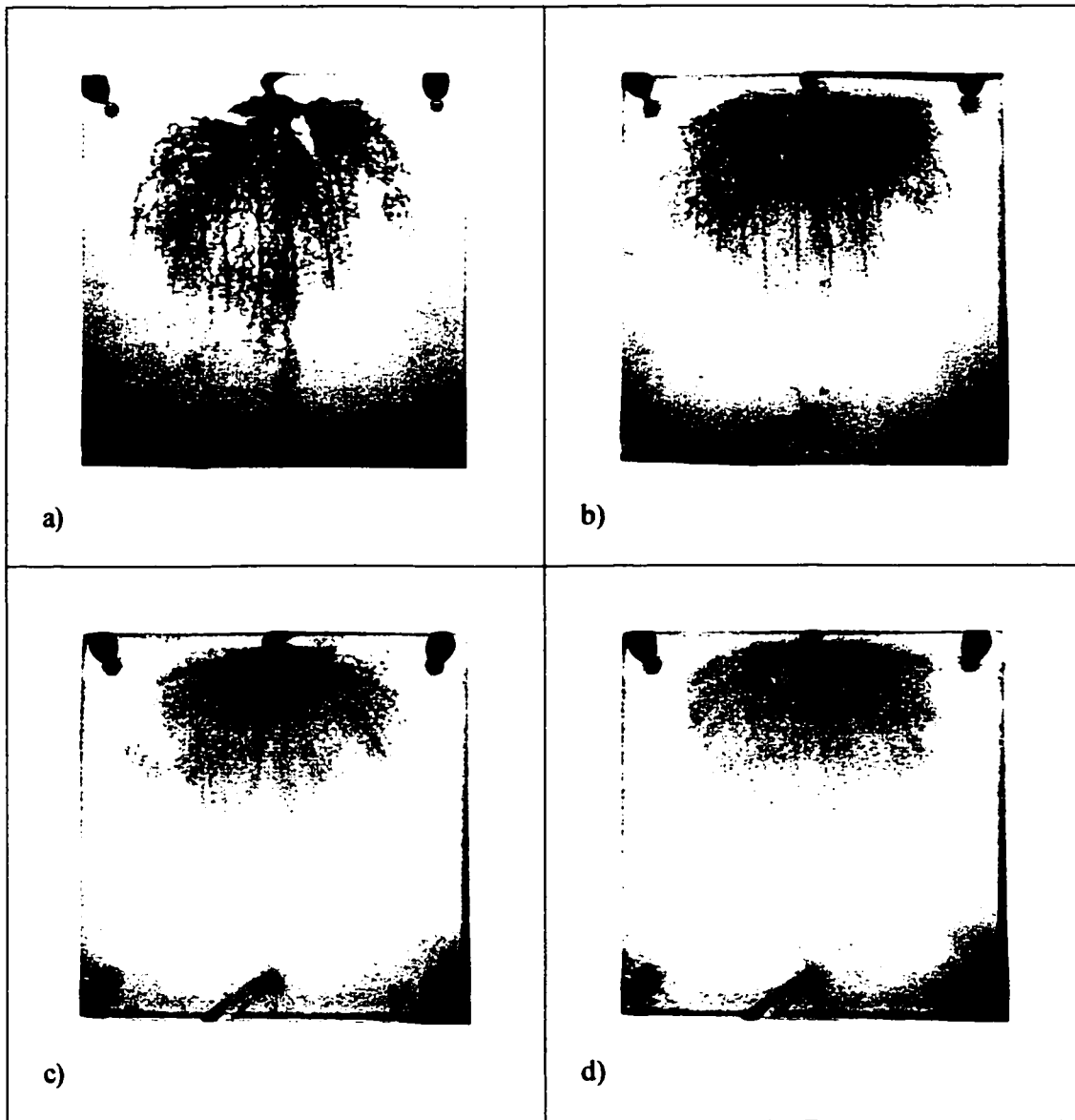


**Figure 3.25: Effects of viscosity ratio on the vertical downward flow mode patterns at a given flow rate  $Q = 0.78\text{ml/min}$ . a)  $\mu_o/\mu_w = 143.5$ , b)  $\mu_o/\mu_w = 49.0$ , c)  $\mu_o/\mu_w = 11.11$ , d)  $\mu_o/\mu_w = 3.3$**

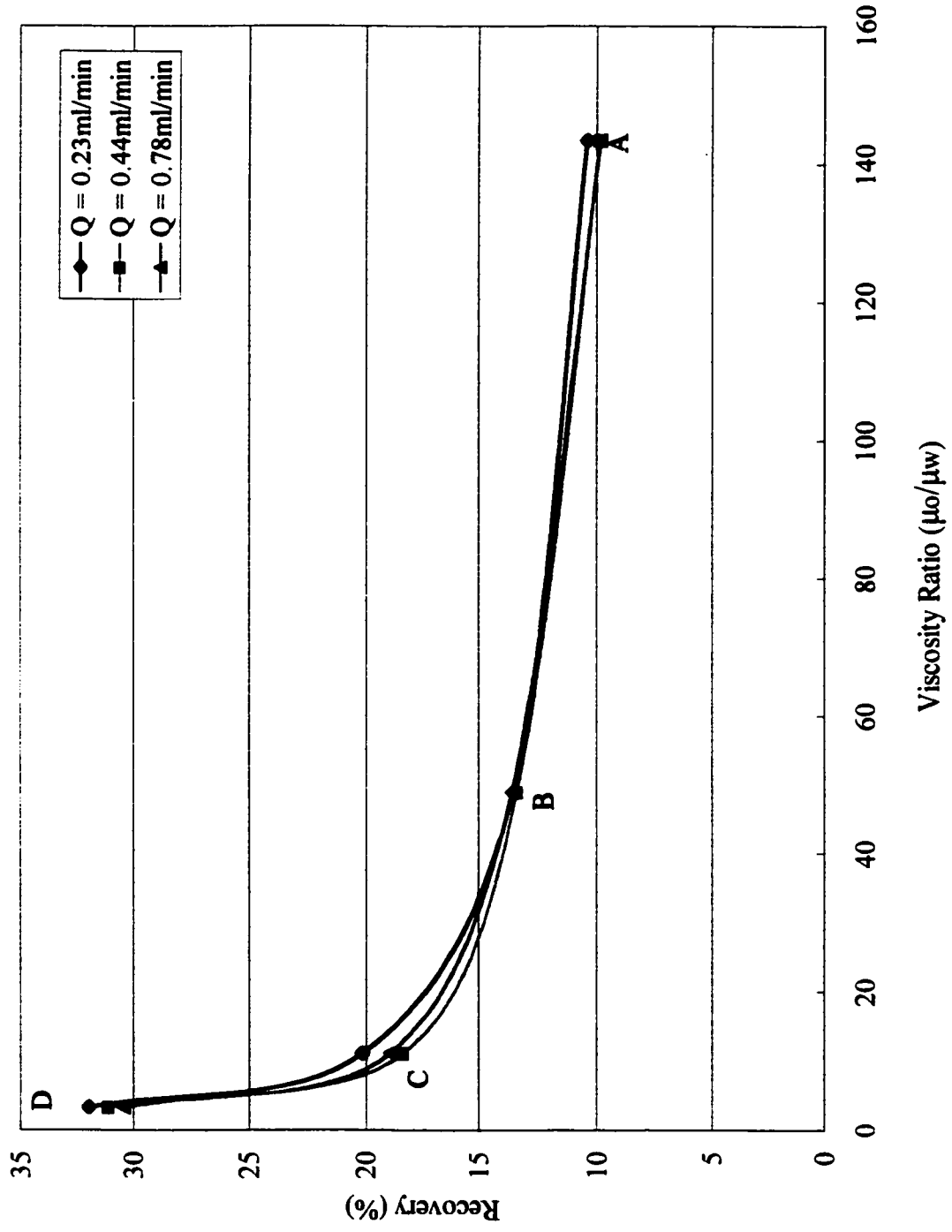


**Figure 3.26: Recovery vs. Viscosity Ratio (Vertical downward mode - without connate water)**

### **3.2.4 Transverse flow mode**

Figures 3.27 - 3.31 show the dyed glycerol solution displacing heavy paraffin oil in the transverse flow mode. Experiments were carried out without connate water. In a normal situation, gravity forces tend to move the fluid toward the bottom leading to an asymmetric displacement but the viscosity and the flow rate can affect this. Since the injection takes place at the central port of one edge and the recovery at the opposite edge, a gravity tongue may be observed no matter what the viscosity ratio and the flow rate are.

From Figure 3.27, at a viscosity ratio of 143.5 (i.e. pure water) and a flow rate of 0.23ml/min, many tiny fingers are developed; the displacement is also asymmetric. Viscous forces responsible for the displacement by fingering dominate the process at high viscosity ratio. As a consequence of this situation, more fingers are generated leading to a low recovery. Gravity effects can also be observed since the displacement is somewhat asymmetric (Figures 3.27a, 3.27b, 3.28a, 3.28b and 3.28c). When the flow rate increases, the gravity effect becomes less significant. Viscous forces then mainly govern the displacement leading to a premature breakthrough and a low recovery (Figure 3.27c).

When the viscosity ratio is low gravity forces tend to dominate the displacement process, and fewer fingers are formed. Figures 3.30 and 3.31 display the displacement patterns at the breakthrough condition for different viscosity ratios at a given flow rate. It can be seen that tiny fingers develop at a high viscosity ratio but as the viscosity ratio decreases these fingers become fewer in number. At a very low viscosity ratio,  $\mu_o/\mu_w = 3.3$ , only a single tongue is observed (Figures 3.30d and 3.31d); gravity forces stabilize the viscous forces even when the flow rate is high (Figure 3.29). The viscosity ratio affects significantly the recovery in a transverse flow mode displacement. From Figure 3.32 the

plot of the recovery versus the viscosity ratio, it is clear that a decrease in the viscosity ratio increases the recovery.

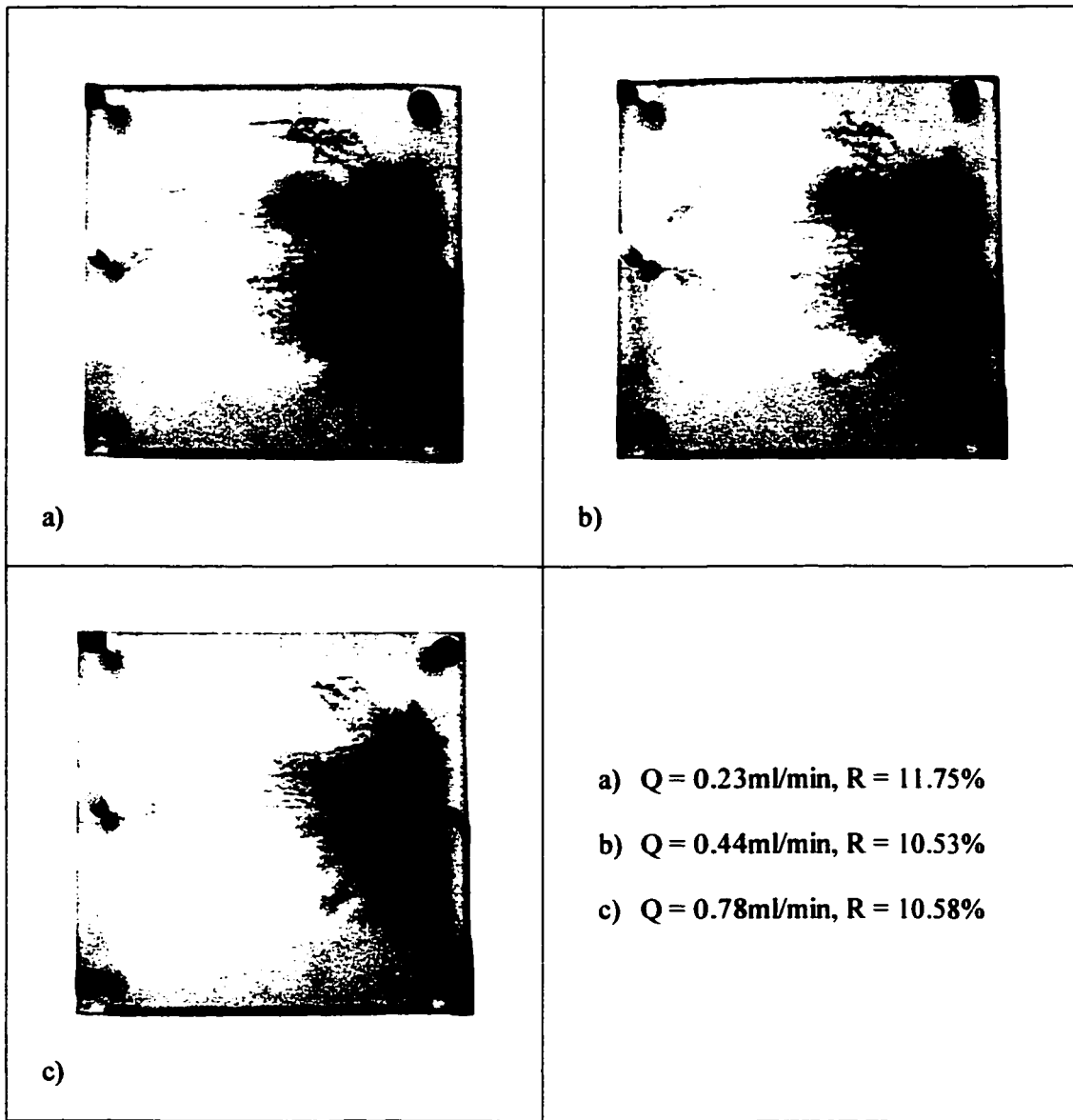


**Figure 3.27: Effects of flow rate on transverse flow mode patterns at a given viscosity ratio  $\mu_o/\mu_w = 143.5$**

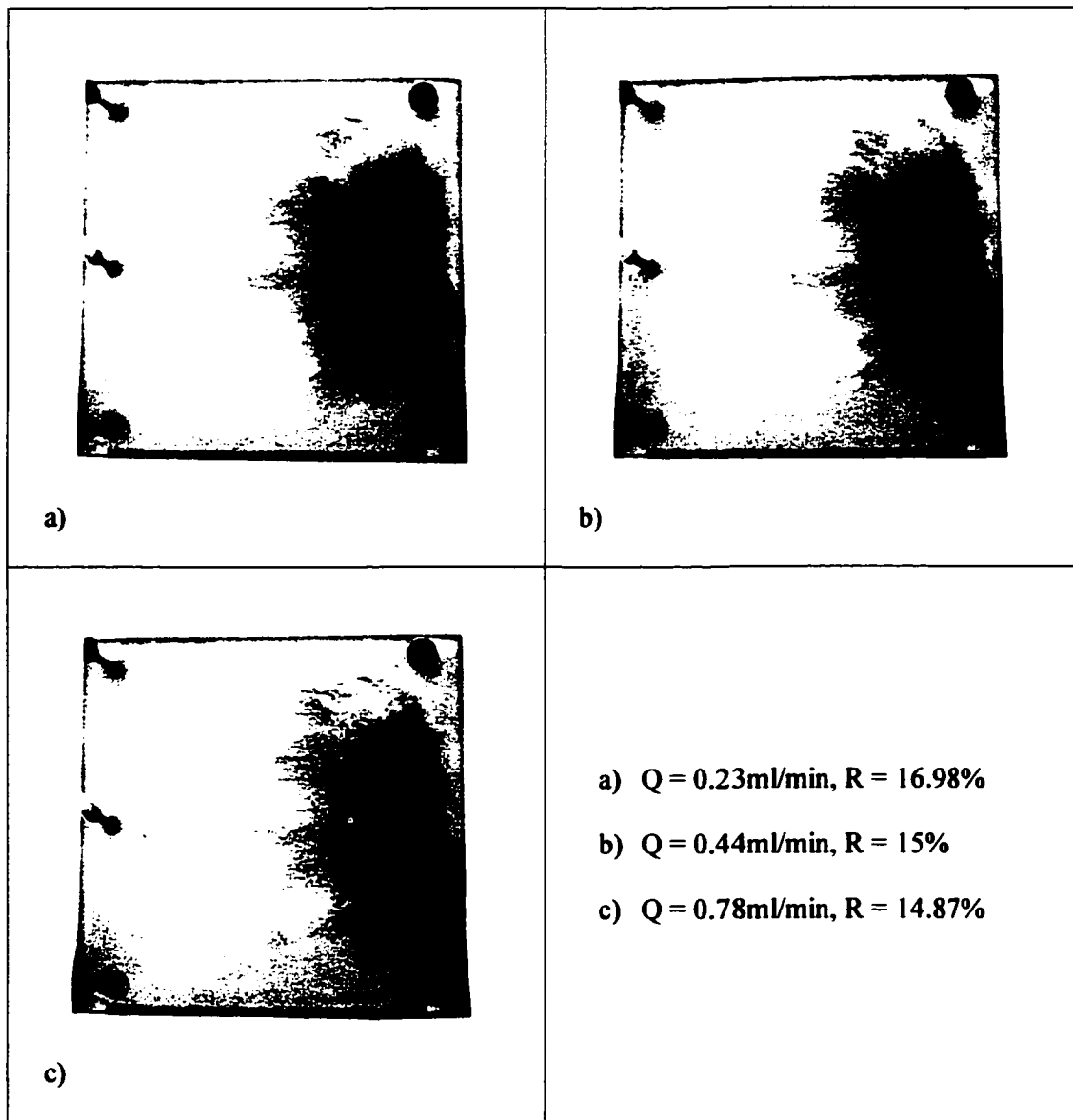


**Figure 3.28: Effects of flow rate on the transverse flow mode patterns at a given viscosity ratio  $\mu_o/\mu_w = 49.0$**

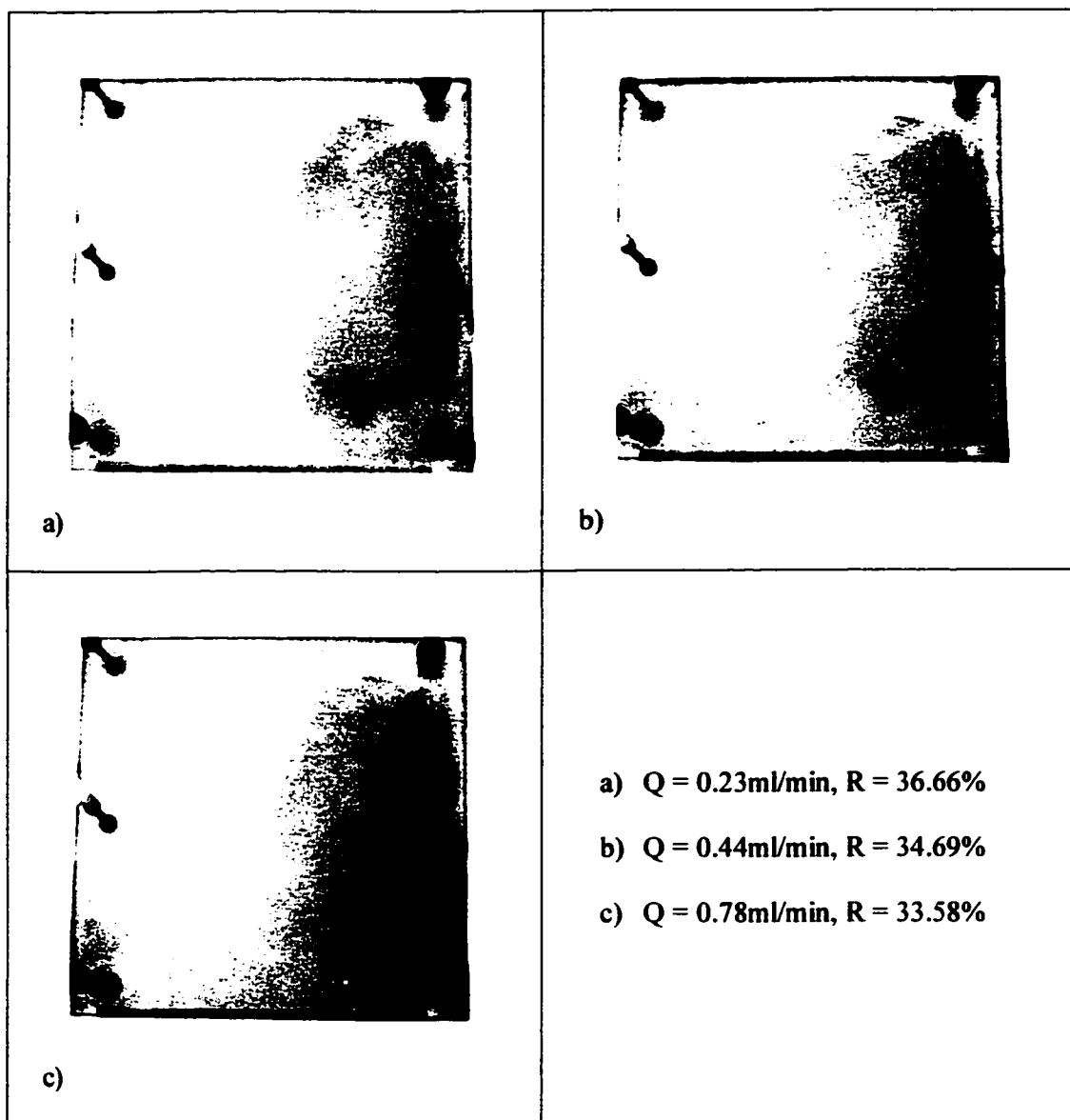


**Figure 3.29: Effects of flow rate on the transverse flow mode patterns at a given viscosity ratio  $\mu_o/\mu_w = 3.3$**

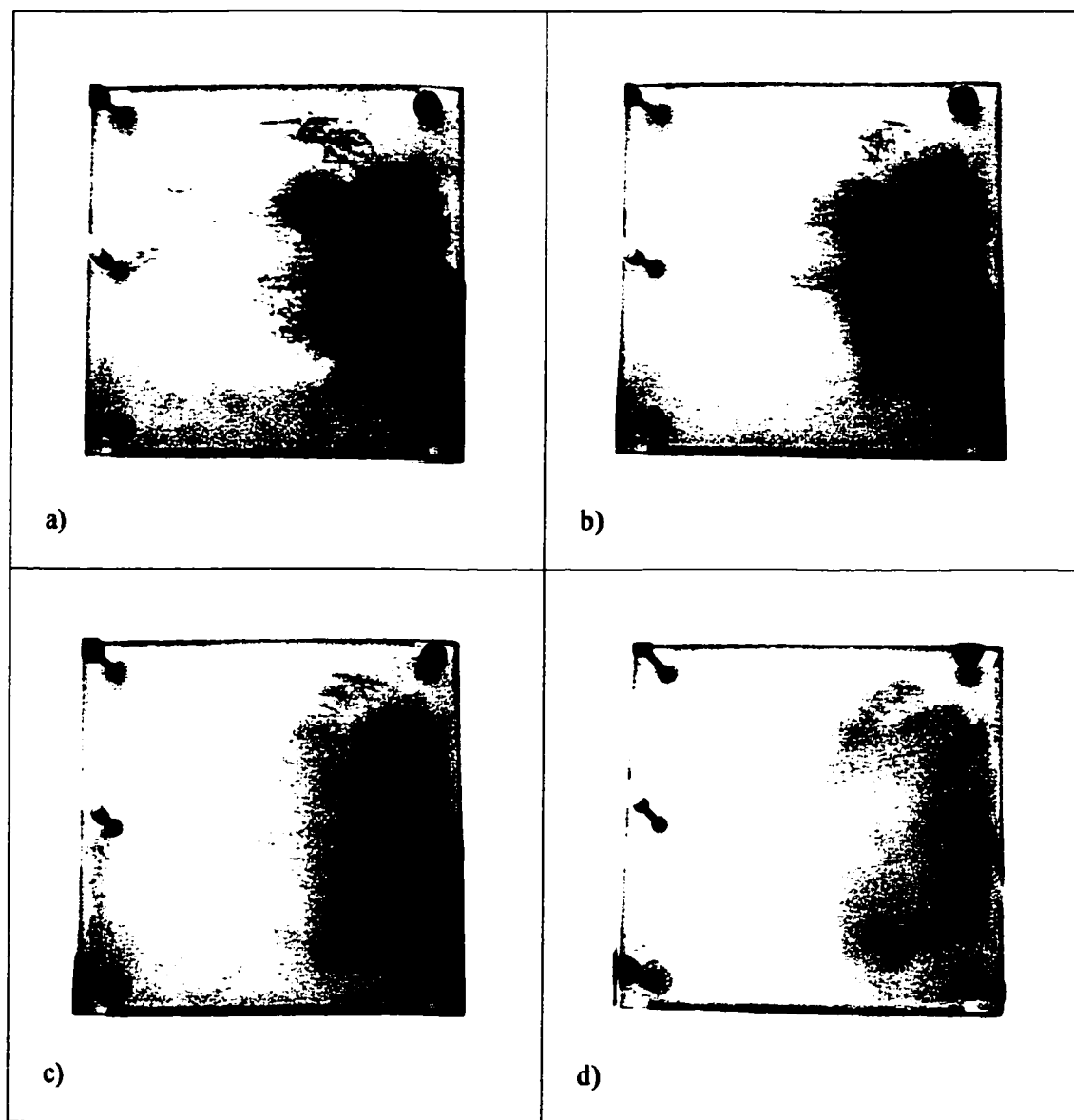


**Figure 3.30: Effects of viscosity ratio on the transverse flow mode patterns at a given flow rate  $Q = 0.23\text{ml/min}$ . a)  $\mu_o/\mu_w = 143.5$ , b)  $\mu_o/\mu_w = 49.0$ , c)  $\mu_o/\mu_w = 11.11$ , d)  $\mu_o/\mu_w = 3.3$**

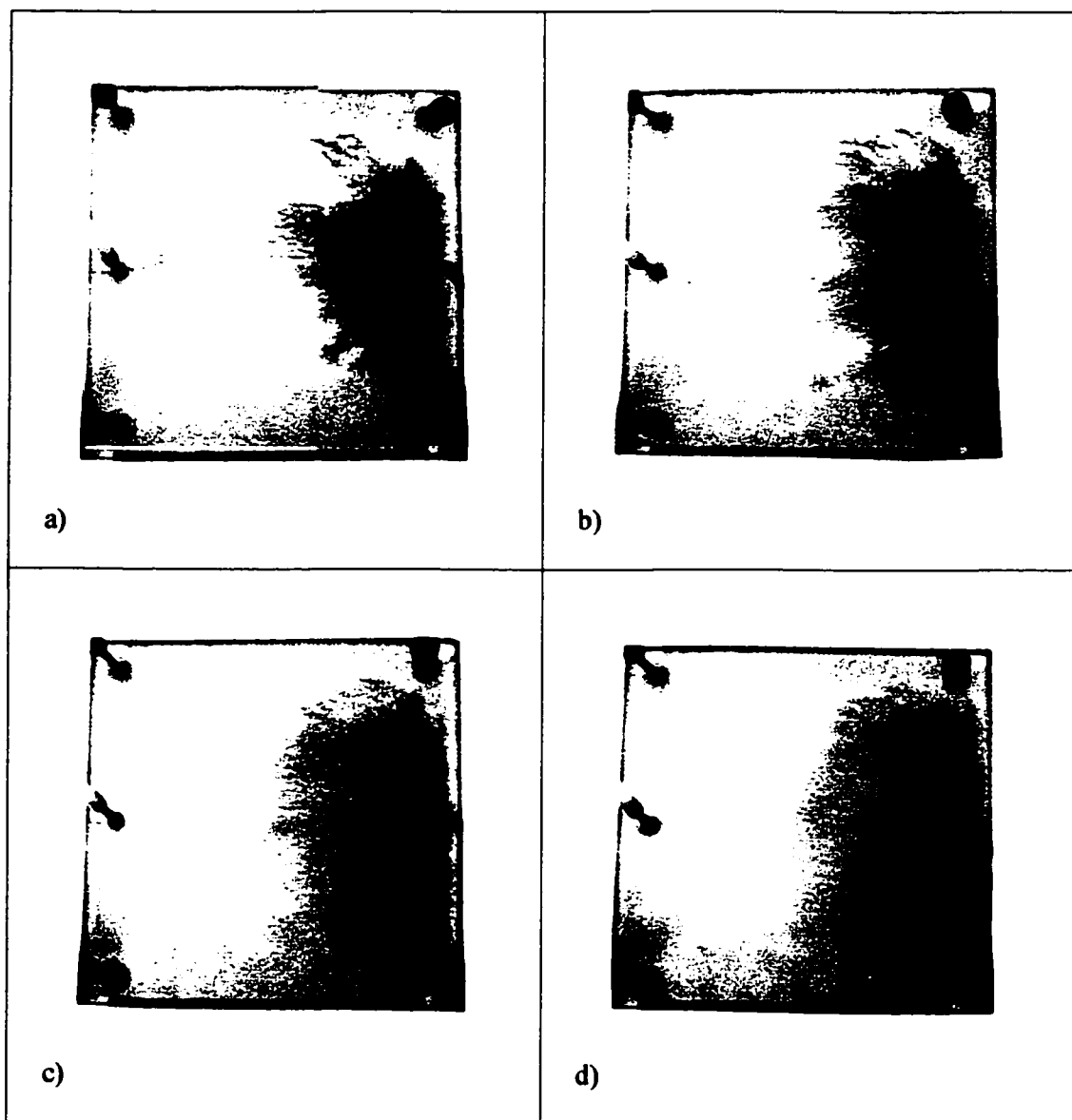


**Figure 3.31: Effects of viscosity ratio on the transverse flow mode patterns at a given flow rate  $Q = 0.78\text{ml/min}$ . a)  $\mu_o/\mu_w = 143.5$ , b)  $\mu_o/\mu_w = 49.0$ , c)  $\mu_o/\mu_w = 11.11$ , d)  $\mu_o/\mu_w = 3.3$**

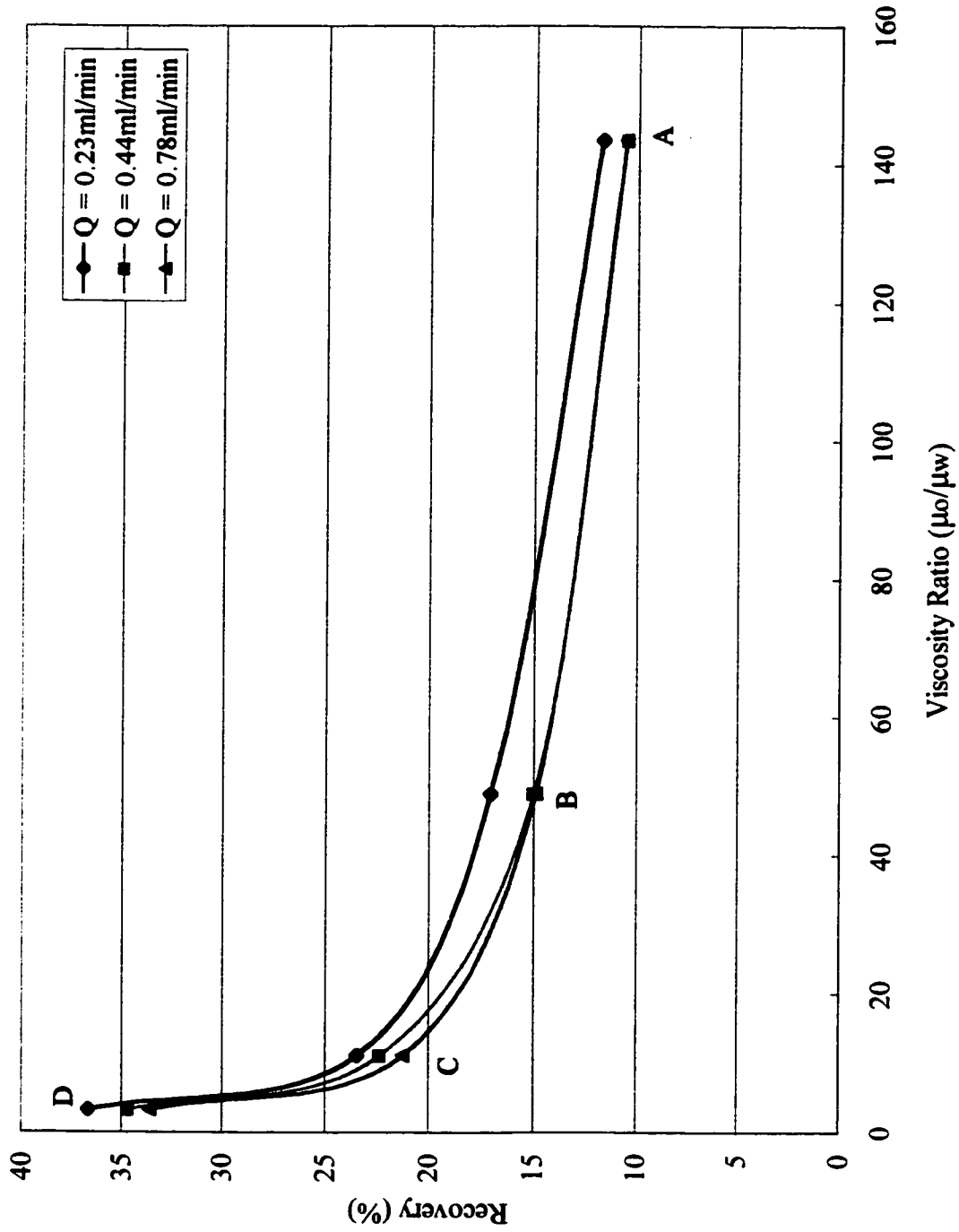


Figure 3.32: Recovery vs. Viscosity Ratio (Transverse mode - without connate water)

### **3.3 Displacements in the presence of connate water**

Experiments were carried out by displacing the heavy paraffin oil with the glycerol solution in the presence of a small amount of water within the cell (so-called connate water). In the natural reservoir simulation, the consolidated porous medium represents the reservoir rock and the remaining water the connate water. The cell properties may not be identical to those of the natural reservoir due to the complexity of the reservoir but the main interest for this study is the effect of one fluid displacing another one of different viscosity ratio assuming that the reservoir is an homogeneous system. During the displacement process, when the displacing fluid is in contact with connate water a new viscosity ratio should be defined at the tip of the fingers. For convenience, data analysis will be based on “apparent viscosity ratio” since it is difficult to evaluate the exact amount of connate water dispersed within the oil phase and the degree of mixing between the displacing fluid and connate water.

Figures 3.33 - 3.36 show the effects of flow rate on the displacement patterns for the different flow modes. Due to the very small variation in the flow rate, the displacement patterns look similar for all three flow rates. This observation applies to the four displacement modes. Within the range of flow rates studied, connate water seems not to significantly affect the fingering patterns in the horizontal, vertical upward, vertical downward and transverse flow modes. Therefore, the patterns are smooth. The displacing fluid and the water trapped between particles, the so-called connate water, are miscible. Due to the effect of dilution, the displacing fluid becomes less viscous (less dense), leading to an increase in the viscosity ratio. In the previous section, it had been found that the recovery decreases as the viscosity ratio increases. In a similar manner, in the presence of connate water the recovery decreases due to the effect of dilution. From Figure 3.37, a decrease in

the viscosity ratio generates more tiny fingers which, by coalescence, create a large and smooth pattern; hence, a high recovery for a low viscosity ratio such as  $\mu_o/\mu_w = 3.3$ .

Even if the amount of connate water was estimated in the literature to be approximately 5% of the pore volume, it may significantly affect the recovery efficiency. As can be seen in Figures 3.38 - 3.41, the plots displaying the relationship between the recovery and the viscosity ratio, an increase in the viscosity ratio leads to a decrease in the recovery. The high viscosity ratio has a negative effect on the recovery as the plots confirm. In addition, the presence of connate water reduces considerably the amount of oil recovered in an immiscible displacement in the porous medium.

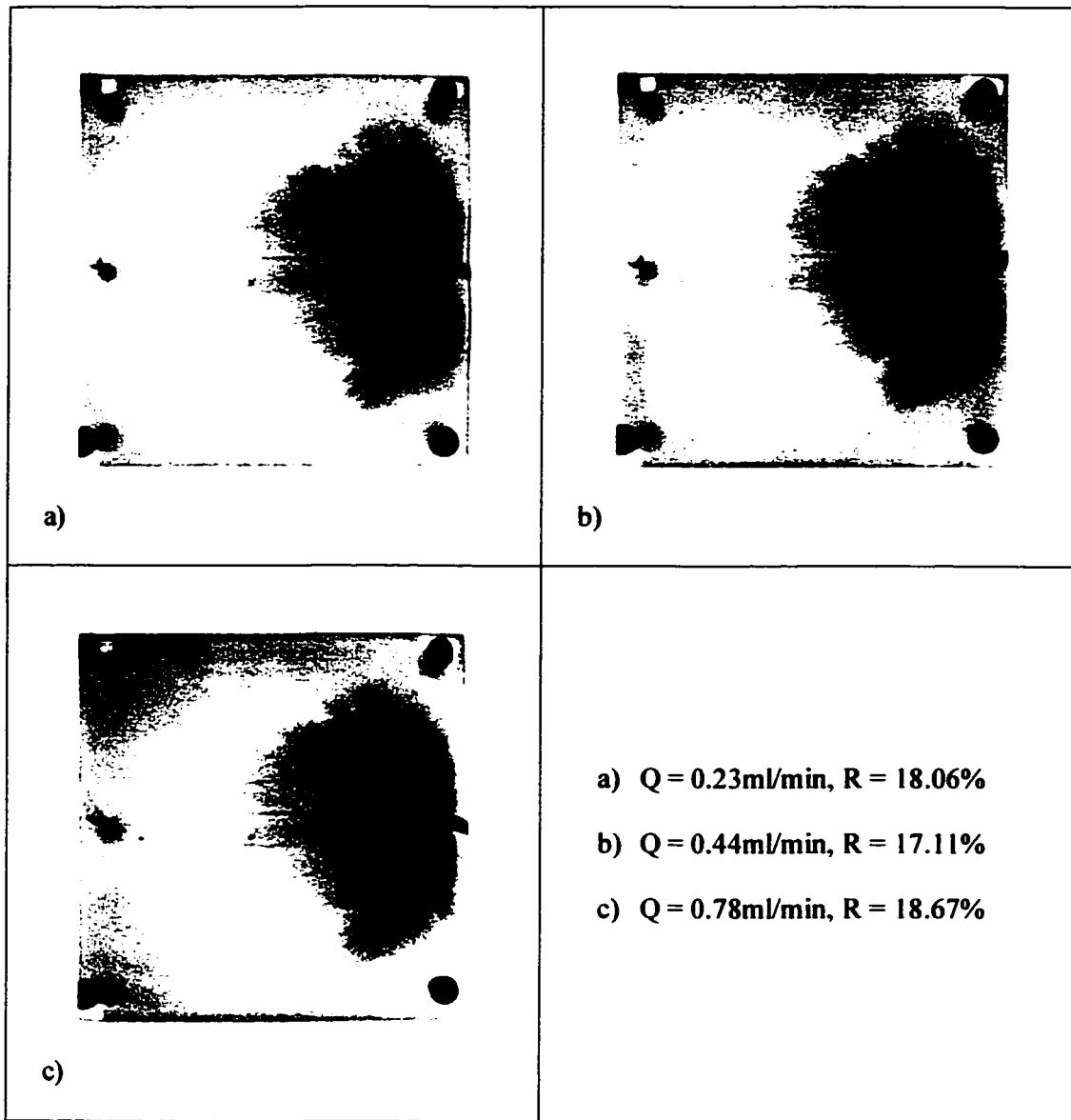


**Figure 3.33: Effects of flow rate on the horizontal flow mode patterns at a given viscosity ratio  $\mu_o/\mu_w = 49.0$**

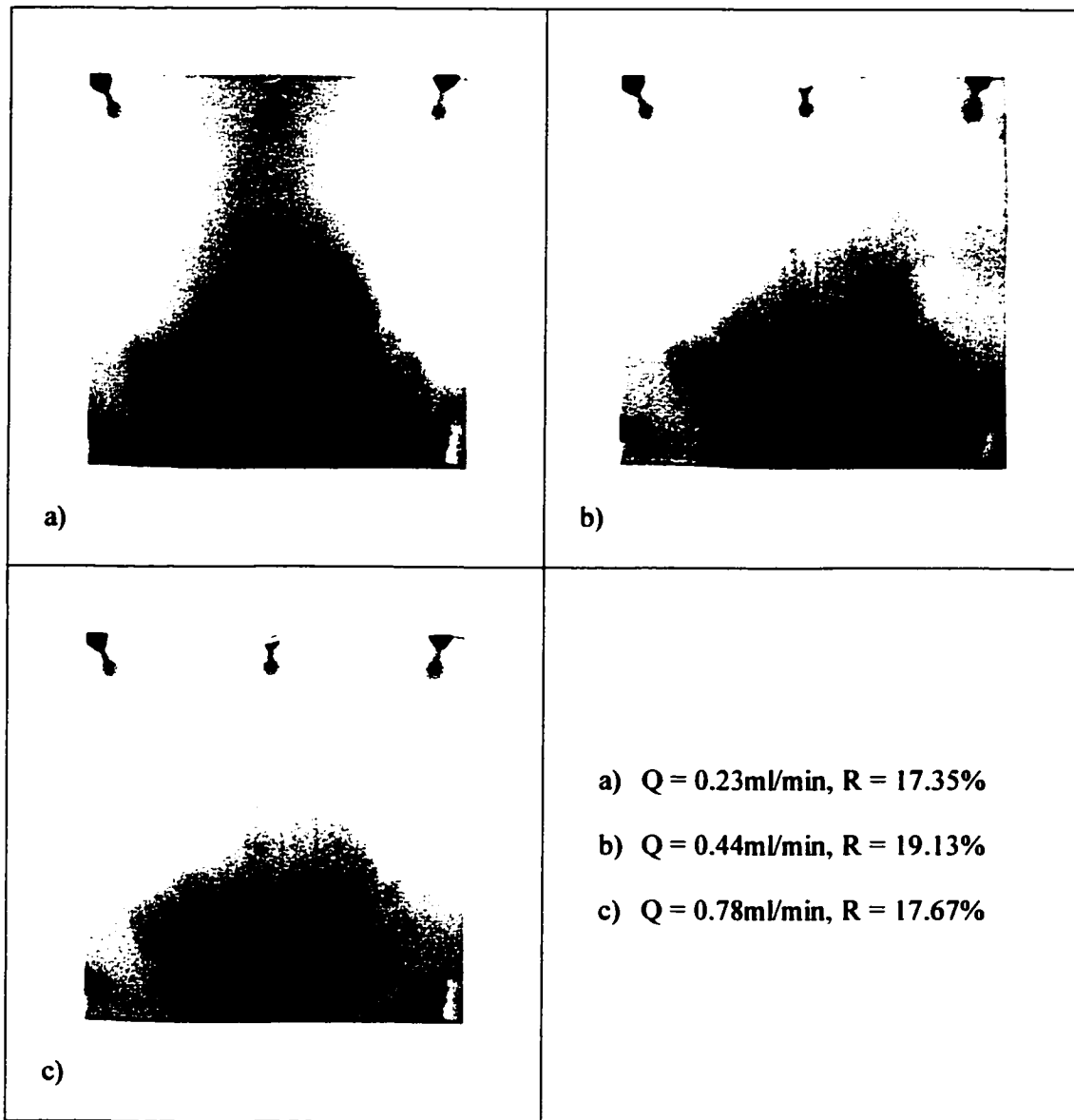


**Figure 3.34: Effects of flow rate on the vertical upward flow mode patterns at a given viscosity ratio  $\mu_o/\mu_w = 49.0$**

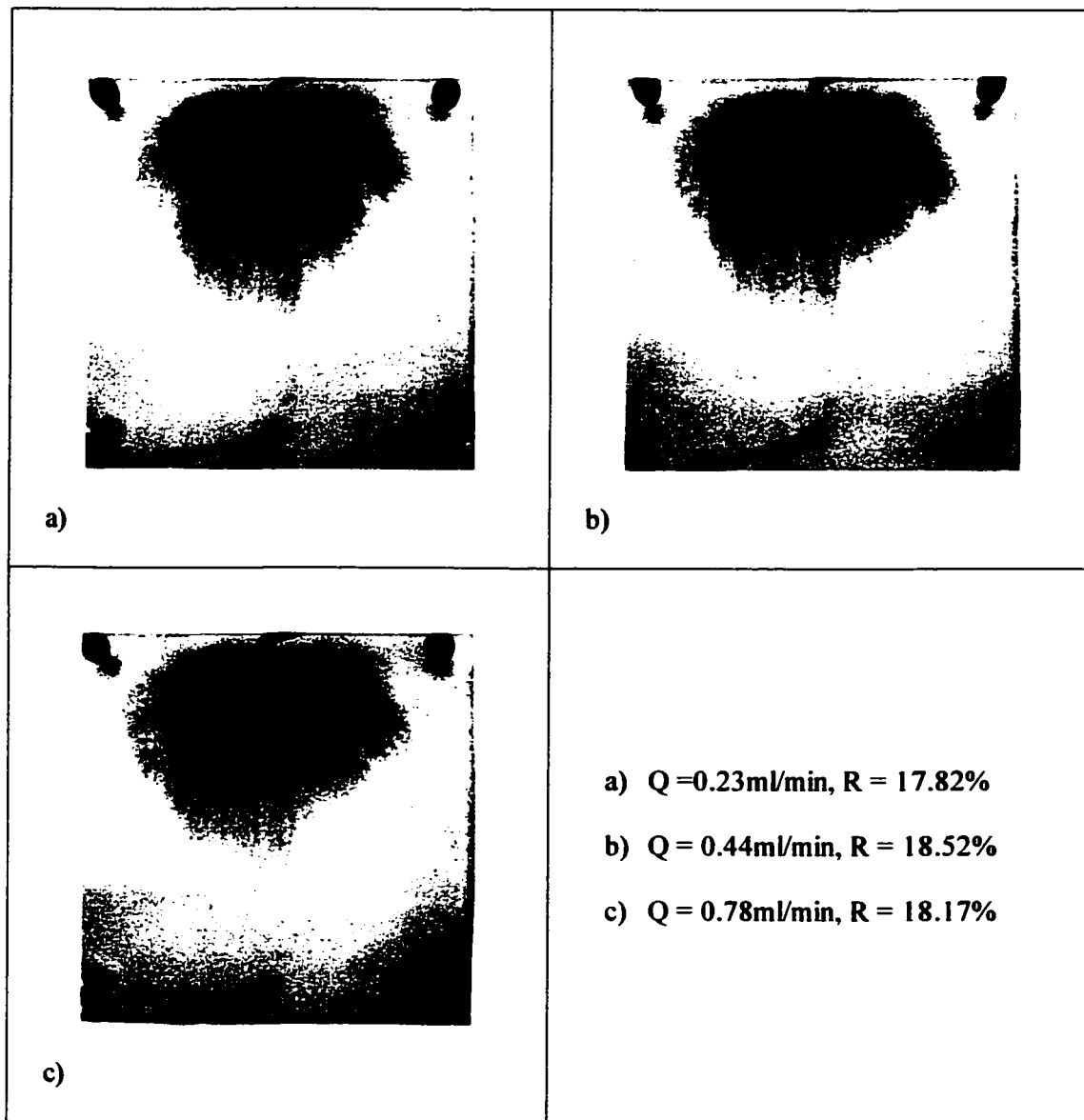


**Figure 3.35: Effects of flow rate on the vertical downward flow mode patterns at a given viscosity ratio  $\mu_o/\mu_w = 49.0$**

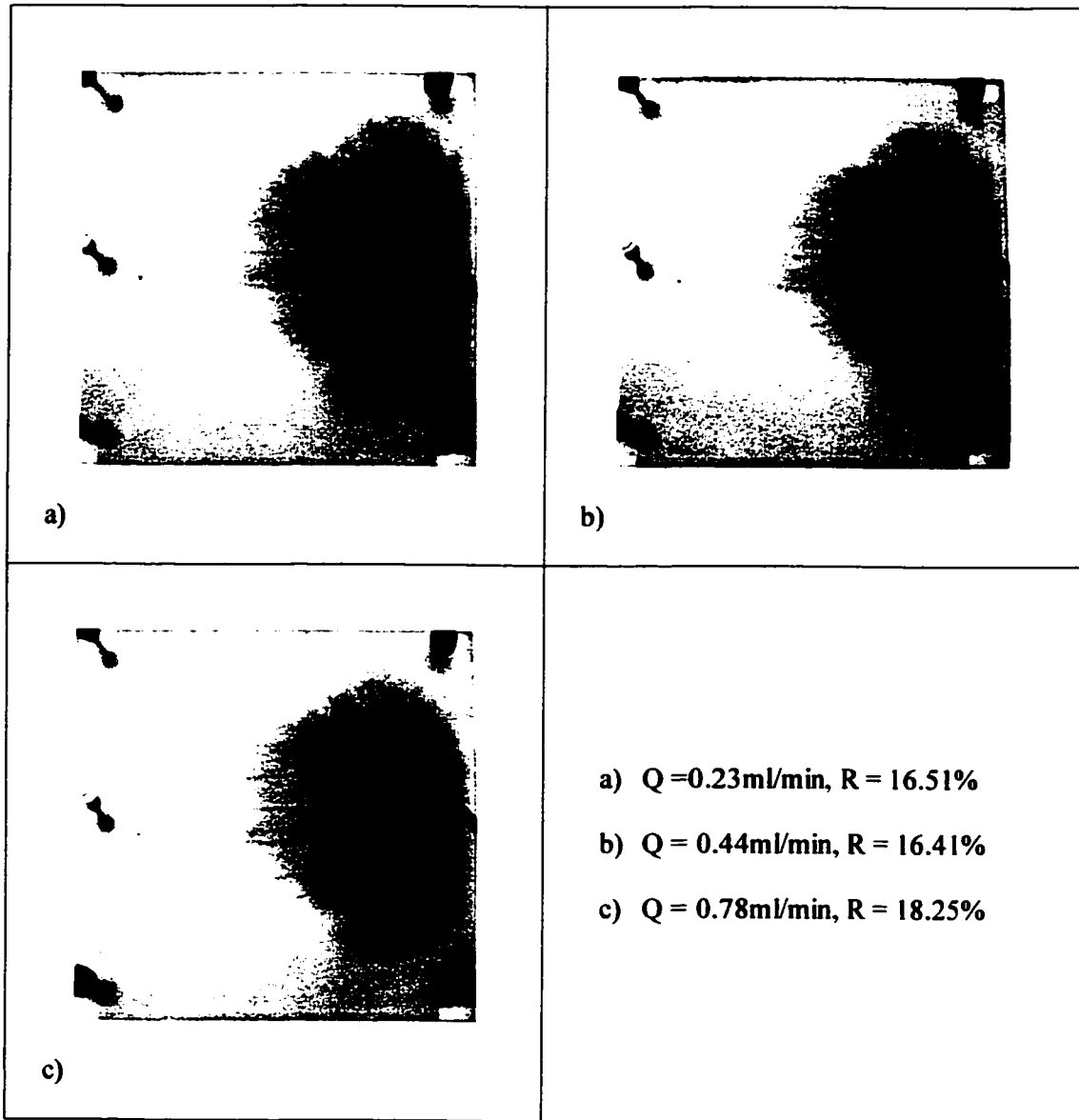


**Figure 3.36: Effects of flow rate on the transverse flow mode patterns at a given viscosity ratio  $\mu_o/\mu_w = 49.0$**

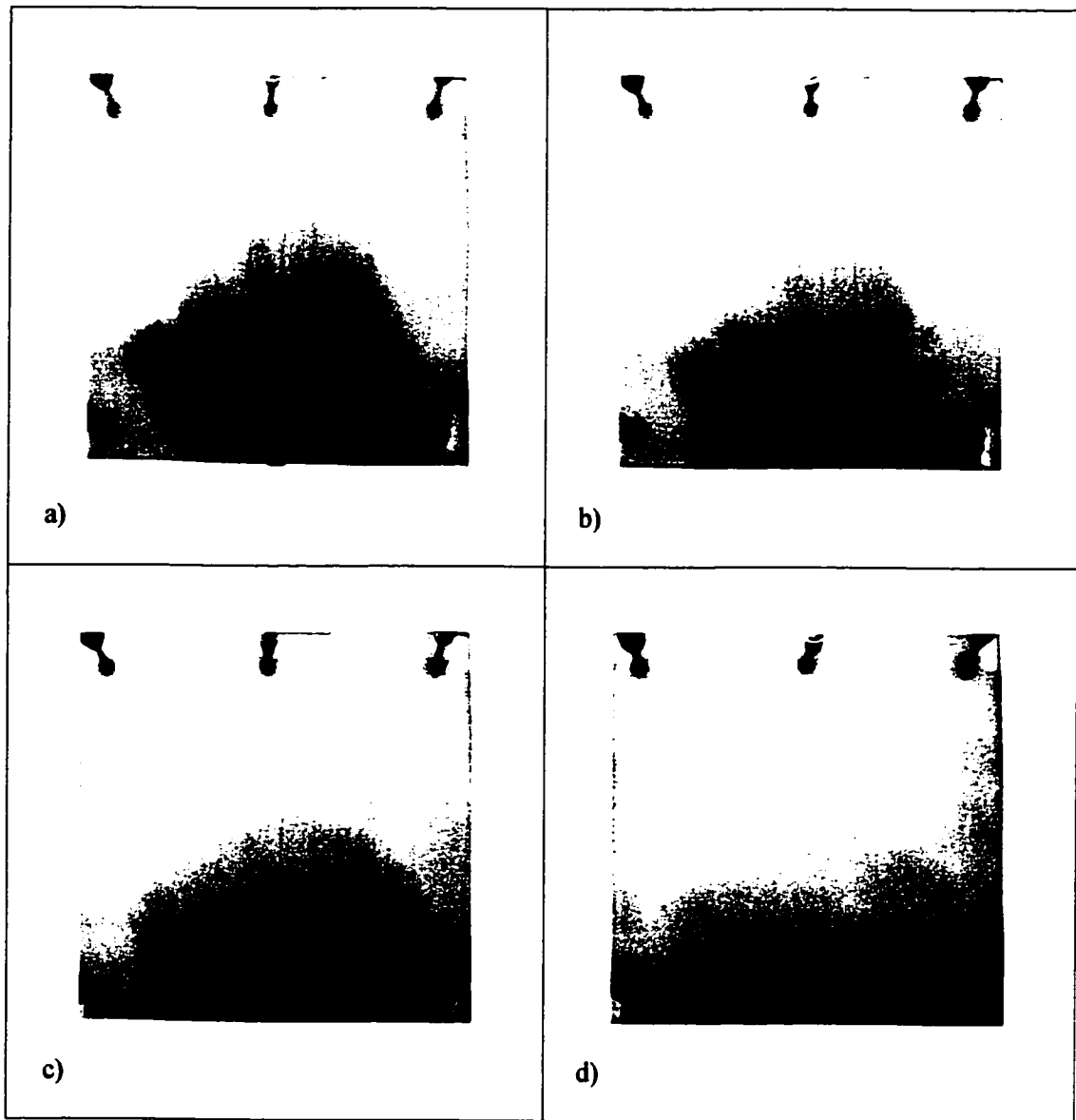


**Figure 3.37: Effects of viscosity ratio on the vertical upward flow mode patterns at a given flow rate  $Q = 0.78\text{ml/min}$ . a)  $\mu_o/\mu_w = 143.5$ , b)  $\mu_o/\mu_w = 49.0$ , c)  $\mu_o/\mu_w = 11.11$ , d)  $\mu_o/\mu_w = 3.3$**

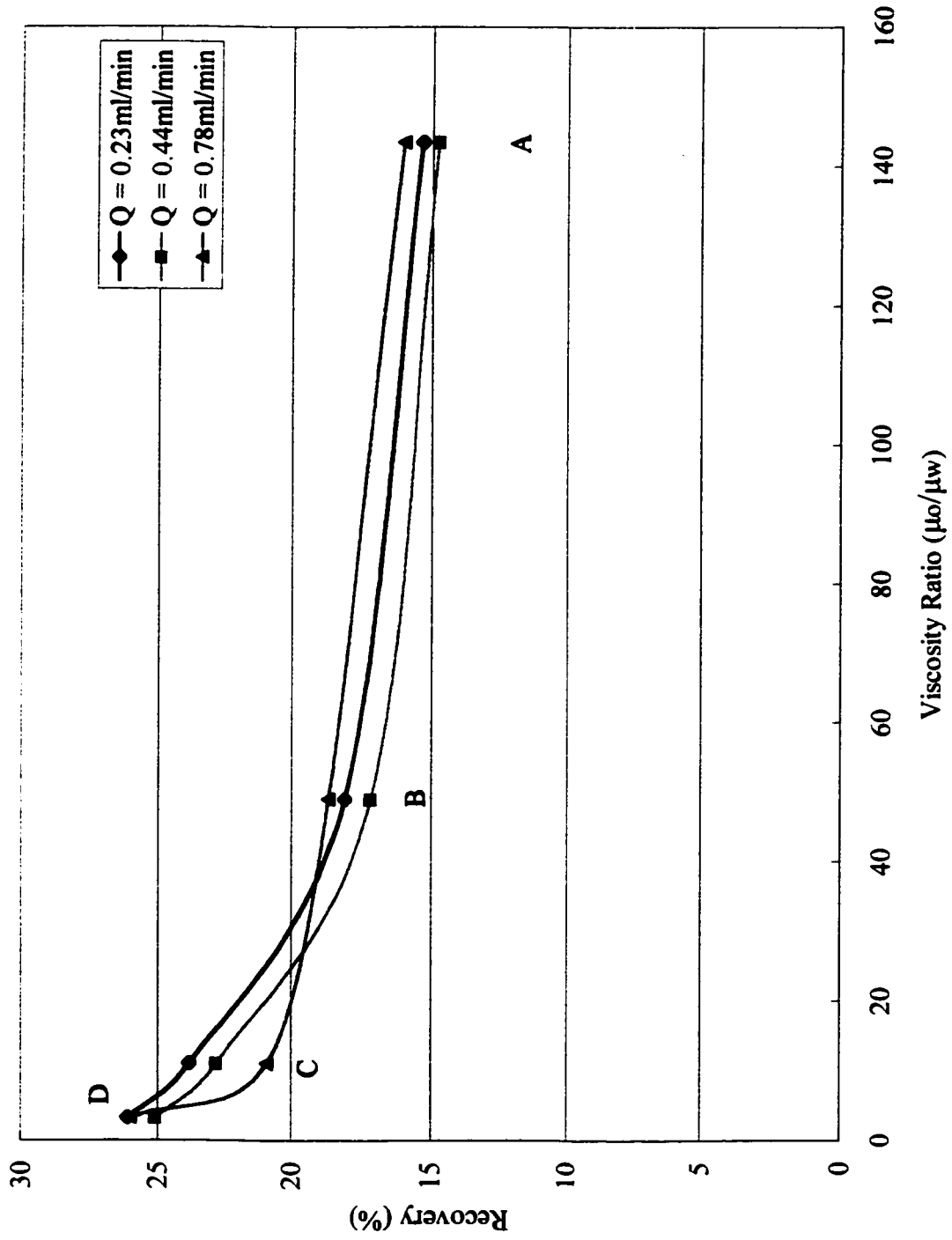
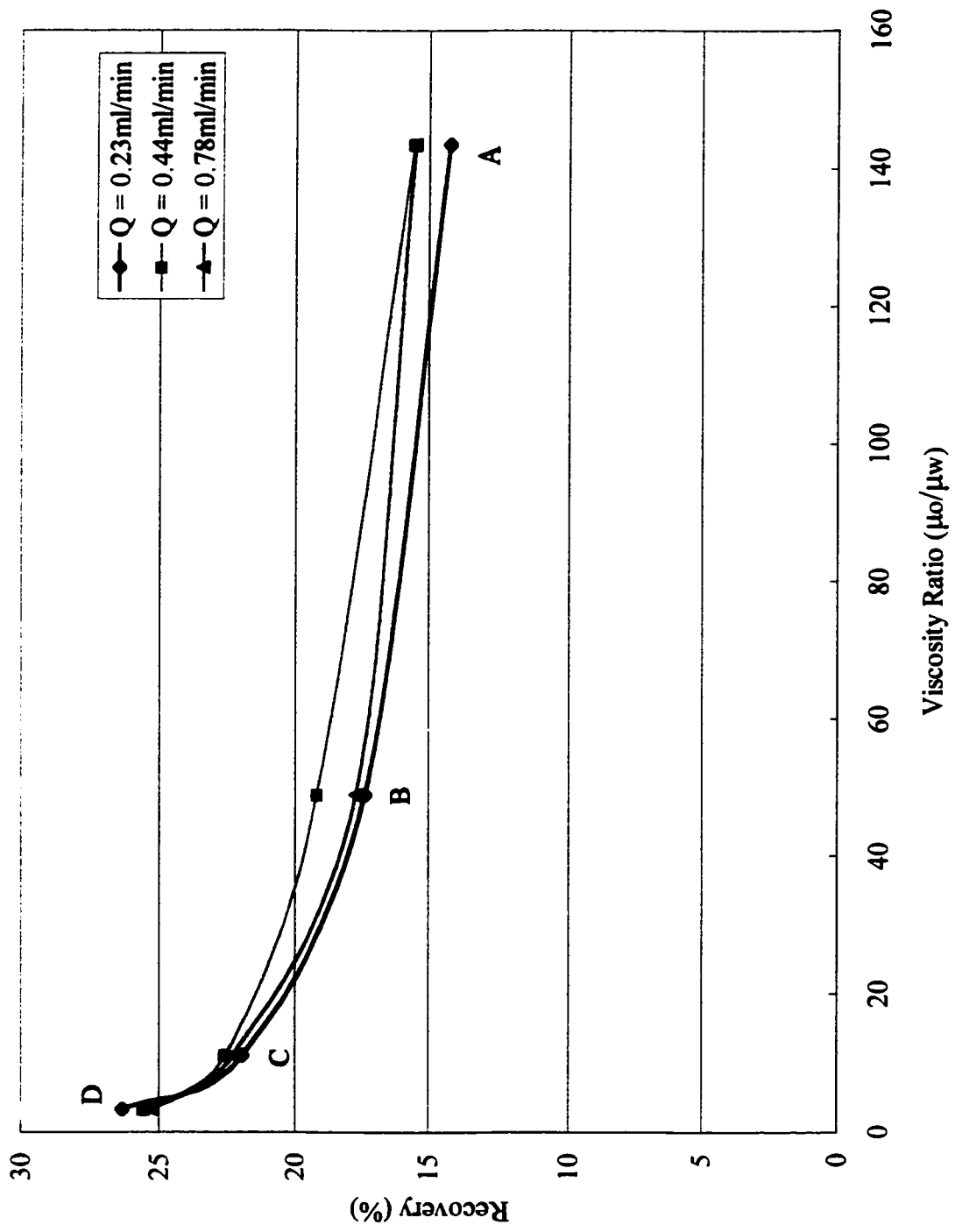


Figure 3.38: Recovery vs. Viscosity ratio (Horizontal mode - with connate water)



**Figure 39: Recovery vs. Viscosity Ratio (Vertical upward mode - with connate water)**

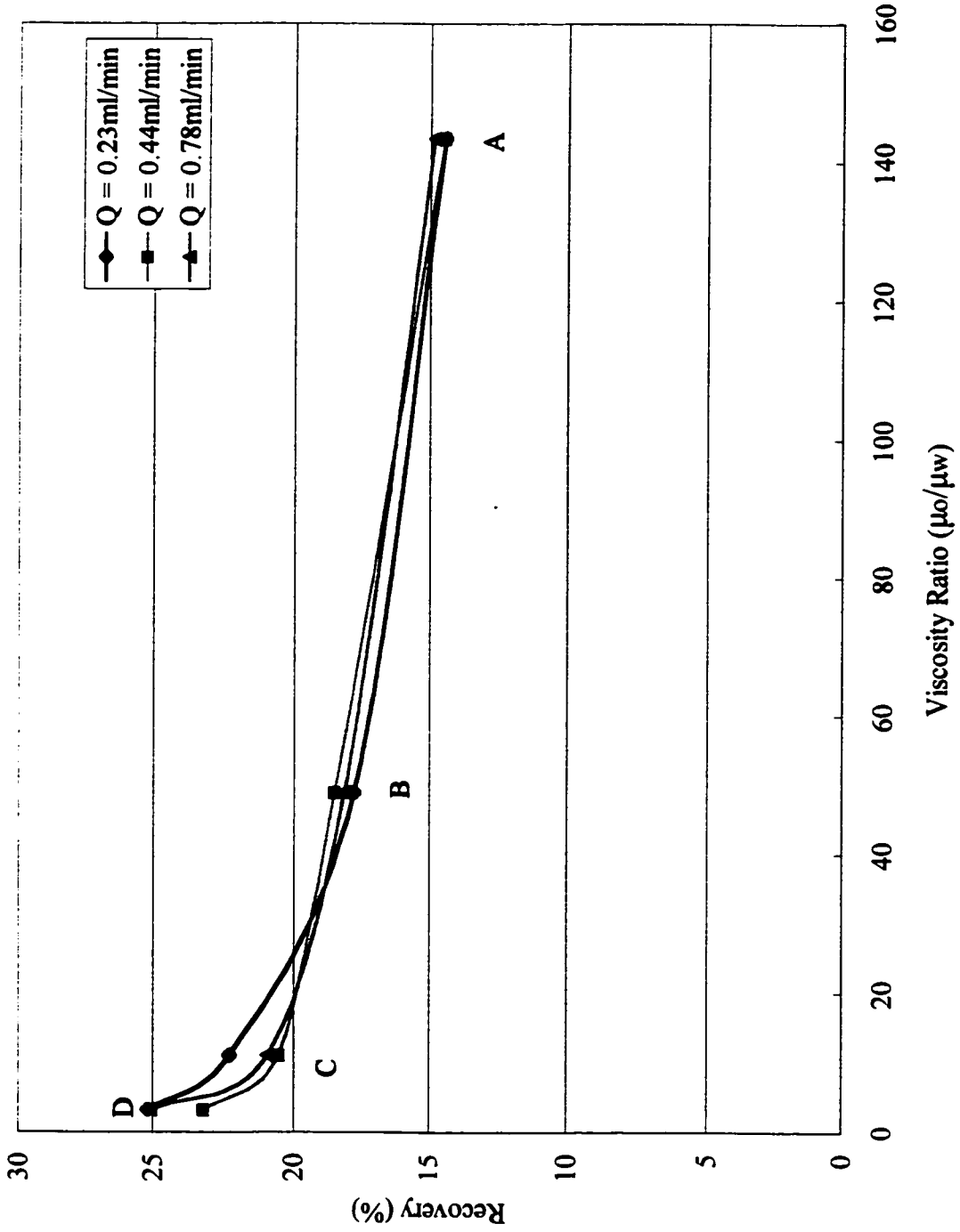


Figure 3.40: Recovery vs. Viscosity ratio (Vertical downward mode - with connate water)

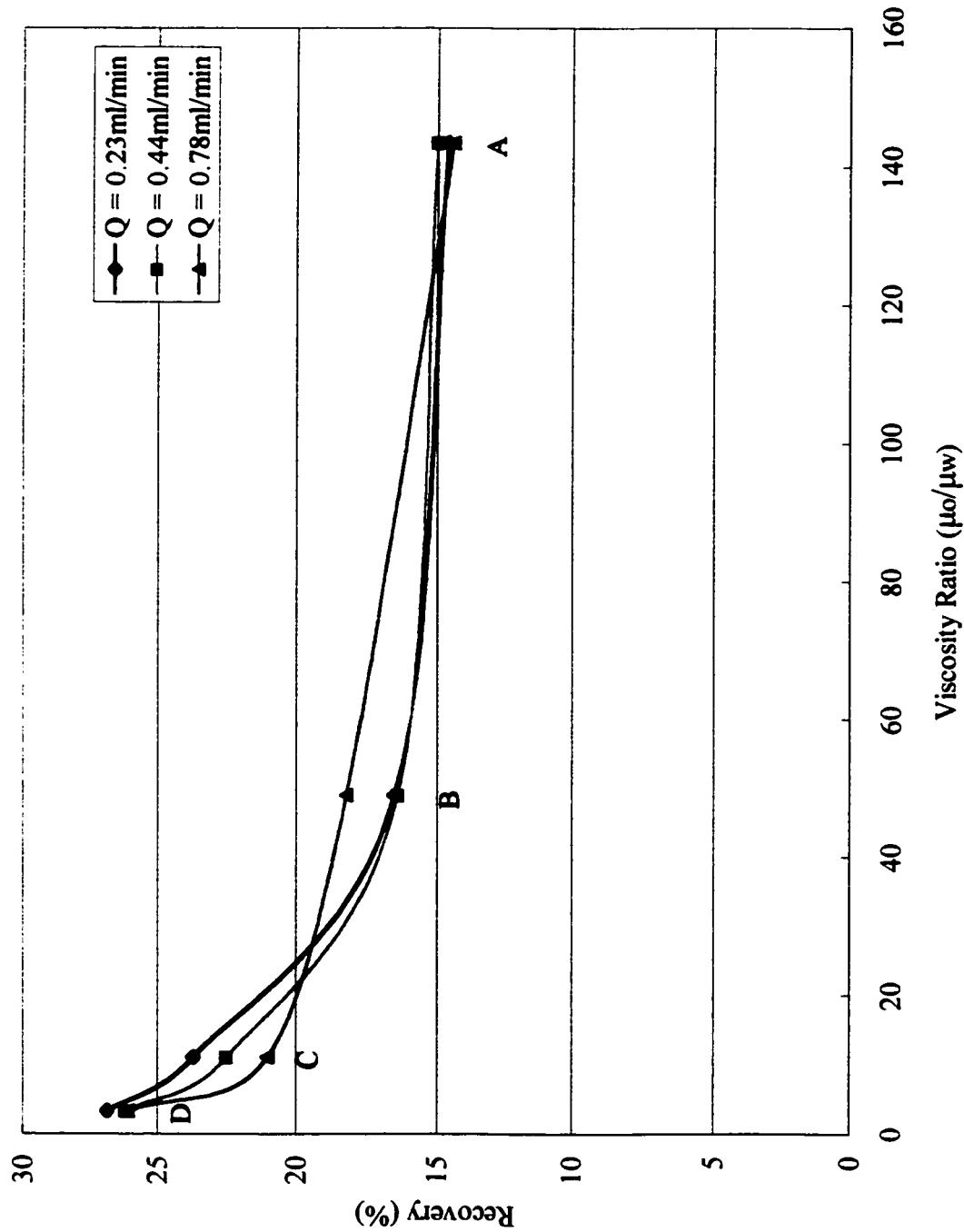


Figure 3.41: Recovery vs. Viscosity Ratio (Transverse mode - with connate water)

### **3.4 Effects of flow mode**

Figures 3.42 and 3.43 depict respectively the effects of flow mode on the fingering patterns at high and low viscosity ratios for the same flow rate in the absence of connate water. At high viscosity ratio, many tiny fingers are developed for all four flow modes and the displacing fluid covers less area. Consequently, the recovery is low. As can be seen in Table 2.4, the flow mode does not affect significantly the recovery at high viscosity ratio although the displacement pattern differs from one to another. The fractional recovery is somewhat higher in the vertical upward mode. By comparing Figures 3.42b and 3.42c, the effects of buoyancy forces can be observed. In the vertical upward mode, the displacing fluid of higher density tends to linger at the bottom of the cell covering a large area and displacing therefore a large amount of oil compared to the displacement in the vertical downward mode, which is dominated by viscous forces. In the transverse mode, viscous and gravity forces are both present. The displacement patterns are somewhat asymmetric, thereby confirming the presence of gravity forces.

The displacement at a low viscosity ratio is characterized by a high recovery especially in the vertical upward mode where gravity forces tend to stabilize the displacement. The lowest recovery is obtained in the vertical downward mode. In this case, the instability promoted by gravity leads to a premature breakthrough, which reduces the recovery efficiency. For all four flow modes, the higher the viscosity ratio is, the more strong viscous forces are and the less is the recovery efficiency. Viscous forces at high viscosity ratio mainly govern the displacement process.

When experiments are performed in the presence of connate water and at high viscosity ratio  $\mu_o/\mu_w = 143.5$  and  $Q = 0.23\text{ml/min}$ , the recovery is 15.33%, 14.22%, 14.4% and 14.6% for the horizontal, vertical upward, vertical downward and transverse modes

respectively. In the presence of connate water the flow mode seems not to affect significantly the fingering pattern and the fractional oil recovery. From Table 2.4, a similar effect is observed for the experiments performed at low viscosity ratio  $\mu_o/\mu_w = 143.5$  and  $Q = 0.23\text{ml/min}$  where the recovery is 26.1% (horizontal), 26.32% (vertical upward), 25.19%(vertical downward) and 26.87% (transverse). The explanation of this similarity in the results lies in the displacement patterns which are similar for all four flow modes for the same flow rate and same viscosity ratio (Figure 3.44).

### **3.5 Comparison with and without connate water**

Figures 3.2 and 3.6 from previous sections display the displacement patterns for experiments performed at the same flow rate and same viscosity ratio, in the absence and in the presence of connate water. Without connate water, the fingers are well defined and the displacing fluid covers up three-quarters of the cell's area indicating a high recovery. Conversely, only half of the area is covered when connate water is present. A tiny and thin finger moves fast and breaks through at the outlet port reducing the recovery efficiency. From Table 2.4, at high viscosity ratio, the recovery is independent of the presence of connate water. Unexpectedly, the recovery is somewhat higher when connate water is present, making the recovery unpredictable. In general, connate water has a negative effect on the recovery for all four flow modes especially at low viscosity ratio. It becomes necessary to include connate water when simulating a natural reservoir in the laboratory.

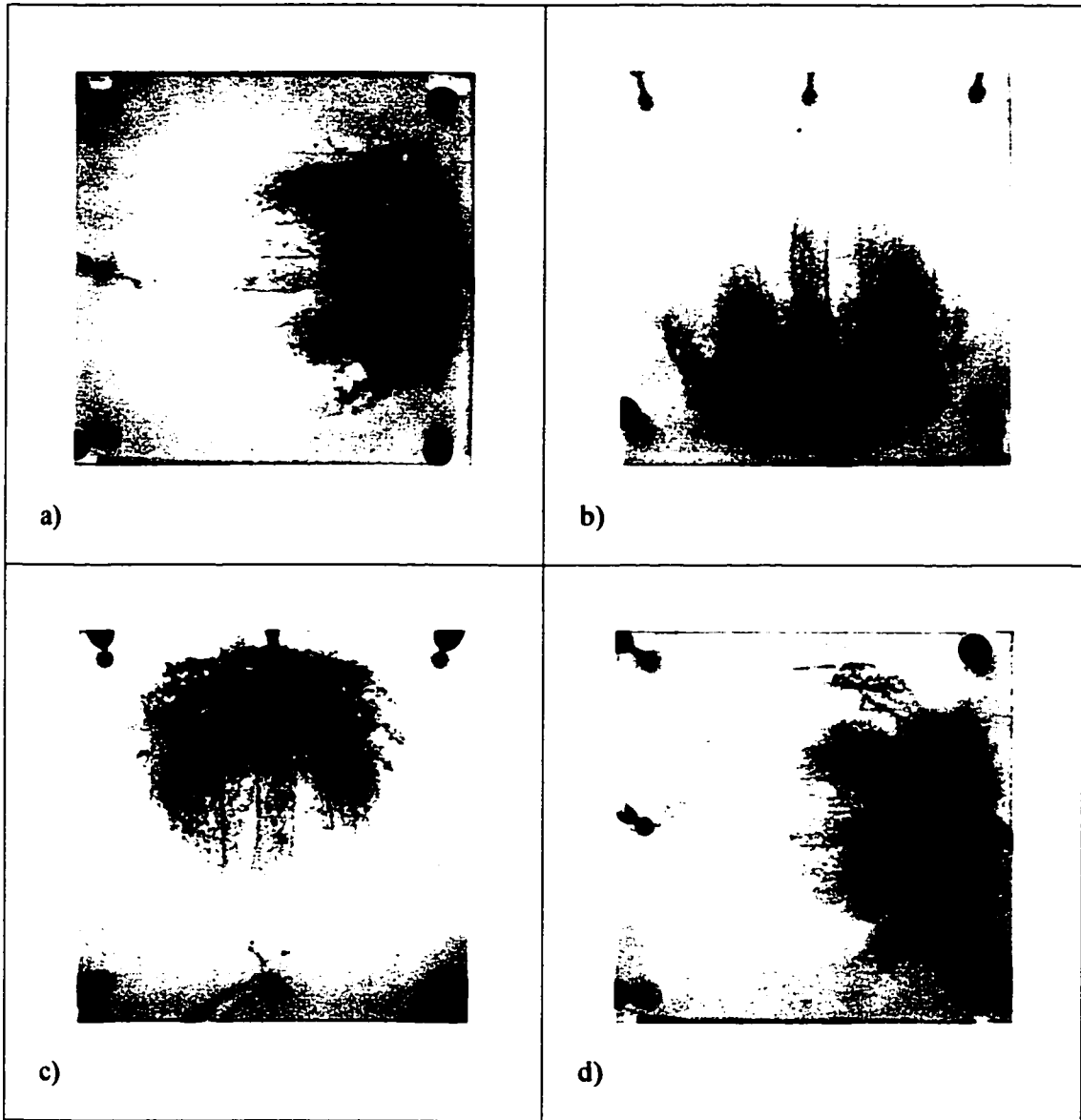


**Figure 3.42: Effects of flow mode in the absence of connate water for  $\mu_o/\mu_w = 143.5$  and  $Q = 0.23\text{ml/min}$ . a) Horizontal mode, b) Vertical upward mode, c) Vertical downward mode, d) Transverse mode**

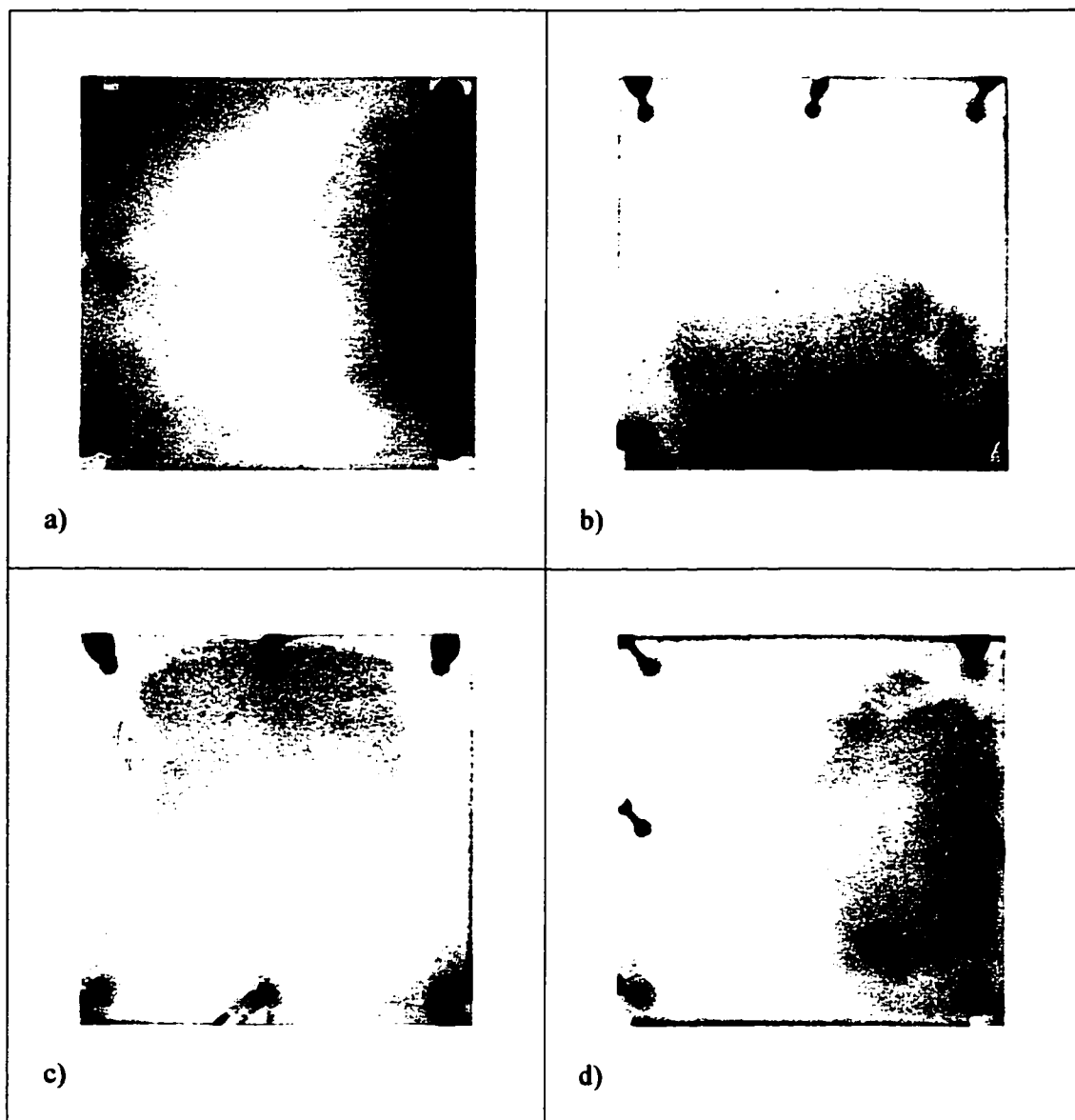


**Figure 3.43: Effects of flow mode in the absence of connate water for  $\mu_o/\mu_w = 3.3$  and  $Q = 0.23\text{ml/min}$ . a) Horizontal mode, b) Vertical upward mode, c) Vertical downward mode, d) Transverse mode**

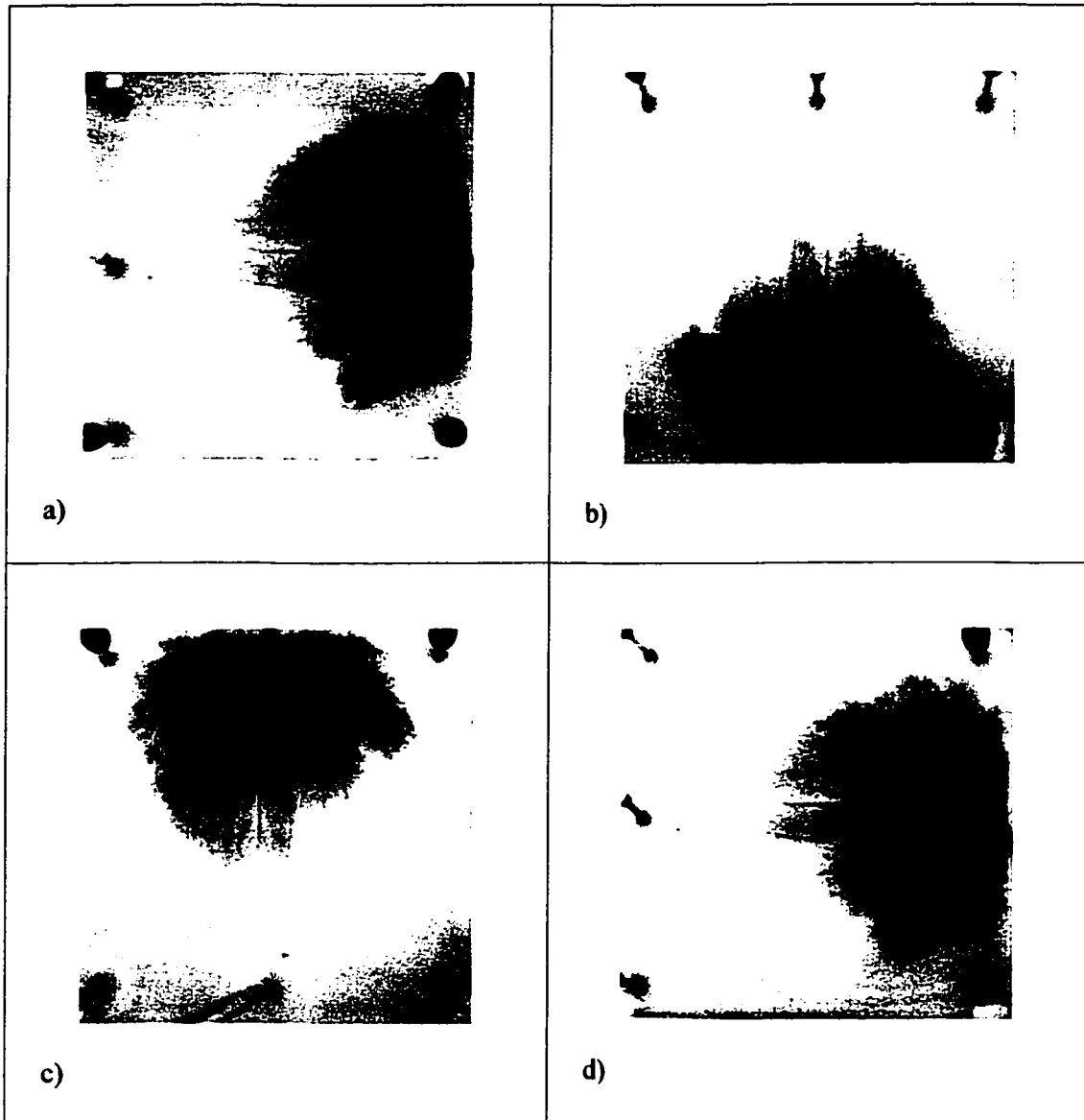


**Figure 3.44: Effects of flow mode in the presence of connate water for  $\mu_o/\mu_w = 143.5$  and  $Q = 0.23\text{ml/min}$ . a) Horizontal mode, b) Vertical upward mode, c) Vertical downward mode, d) Transverse mode**

## **CONCLUSIONS**

The displacement of oil by aqueous solutions conducted in a consolidated porous medium indicates a decrease in the recovery as the viscosity ratio increases for all four flow modes when experiments are performed in the presence of connate water as well as in the absence of connate water. In the absence of connate water, the highest recovery is obtained in the vertical upward mode especially at low viscosity ratio where the buoyancy forces stabilize the displacement process. In the vertical downward flow mode, the instability promoted by gravity leads to a low recovery compared to the other flow modes.

Although previous studies have shown the effects of the flow rate on the recovery, in the present study, due to the small variation in the flow rate, the recovery seems not to be significantly affected by the flow rate.

Comparison of the results obtained in the presence and in the absence of connate water shows that connate water has a negative effect on the recovery when the viscosity ratio is low. The synergistic effect between the viscosity ratio and the connate water reduces the oil recovery efficiency significantly.

## **RECOMMENDATIONS**

- 1. Explore the use of water-soluble surfactants (e.g., sodium dodecyl sulfonate) to reduce the oil/water interfacial tension (IFT) over a wide range, in particular to obtain ultra-low values less than 0.1mN/m. Ultra-low IFT values are known from the literature to be favourable to oil recovery. At low IFT values the oil becomes much more “miscible” (soluble) with water and the oil recovery increases.**
- 2. Explore the effects of certain metal ions in the connate water phase. Connate water in real petroleum reservoirs is known to contain  $\text{Na}^+$ ,  $\text{Ca}^{++}$  and other metal ions. These ions are known to adversely affect the effectiveness of surfactants in reducing the IFT to ultra-low values.**
- 3. Investigate the effects of “pulsating” flow, i.e., vary the water injection flow rate in a cyclic (sinusoidal) manner. There have been recent reports that pulsations can reduce the extent of fingering and thereby increase the oil recovery efficiency.**

## REFERENCES

Baig, C.G., Chun, Y.H., Cho, E.S. and Choi, C.K. (2000), "Experimental studies on the instabilities of viscous fingering in a Hele-Shaw cell", *Korean Journal of Chemical Engineering*, vol. 17, n<sup>o</sup>2, p 169-173.

Baker, R.O. and McClernon, L.L. (1998), "Estimation of volumetric sweep efficiency of miscible flood", *Journal of Petroleum Technology*, vol. 37, n<sup>o</sup>2, p 40-46.

Berger, B.D. and Anderson, K.E. (1981), *Modern petroleum: A basic primer of the industry*. Second Edition, PennWell Publishing Company, Tulsa, Oklahoma.

Christie, M.A., Muggeridge, A.H. and Barley, J.J. (1993), "3D simulation of viscous fingering and WAG schemes", *Society of Petroleum Engineering, Reservoir Engineering*, p 19-26.

Fanchi, J.R. and Christiansen, R.L. (1989), "Applicability of fractals to the description of viscous fingering", Paper SPE 19782 presented at the 64<sup>th</sup> Annual Technical Conference and Exhibition held in San Antonio, TX, p 105-120.

Fayers, F.J. and Newley, T.M.J. (1988), "Detailed validation of an empirical model for viscous fingering with gravity effects", *Society of Petroleum Engineering, Reservoir Engineering*, vol. 291, p 542-550.

Francis, W.S., Zemansky, M.W. and Young, H.D. (1987), *University physics*, Seventh Edition, Addison-Wesley Publishing Company.

Guo, T. and Neale, G.H. (1995), "Effects of buoyancy forces on miscible liquid-liquid displacement processes in a porous medium", *Powder Technology*, vol. 86, p 265-273.

**Han, D.K., Yang, C.Z., Zhang, Z.Q., Lou, Z.H. and Chang, Y.I. (1999), "Recent development of enhanced oil recovery in China", Journal of Petroleum Science and Engineering, vol. 22, p 181-188.**

**Homsy, G.M. (1987), "Viscous fingering in porous media", Annual Review of Fluid Mechanics, vol. 19, p 271-311.**

**Hornof, V. and Bernard, C. (1992), "Effect of interfacial reaction on immiscible displacement in Hele-Shaw cells", Experiments in Fluids, vol. 12, p 425-426.**

**Hu, M.C., Hornof, V. and Neale, G. (1985), "Visualization of unstable miscible radial displacements in a consolidated porous medium", Powder Technology, vol. 41, p 265-268.**

**Jenyon, M.K. (1990), Oil and gas traps: Aspects of their seismostratigraphy, morphology and development. John Wiley & Sons, New York.**

**Jerauld, G.R., Nitsche, L.C., Teletzke, G.F., Davis, H.T. and Scriven, L.E. (1984), "Frontal structure and stability in immiscible displacement" Society of Petroleum Engineers 12691, p 1-8.**

**Jha, K.N. (1982), "Enhanced oil recovery", Chemistry in Canada, vol. 34, p 19-26.**

**Koederitz, L.F, Harvey, A.H. and Honarpour, M. (1983), Introduction to petroleum reservoir analysis. Gulf Publishing Company, Houston, Texas.**

**Latil, M. (1980), Enhanced oil recovery. Editions Technip, Paris.**

**Manickam, O. and Homsy, G.M. (1995), "Fingering instabilities in vertical miscible displacement flows in porous media", Journal of Fluid Mechanics, vol. 288, p. 75-102.**

**Mayer-Gürr, A. (1976), Petroleum engineering. John Wiley & Sons, New York, vol. 3.**

**McCain Jr, W.D. (1990), The properties of petroleum fluids. Second Edition, PennWell Publishing Company, Tulsa, Oklahoma.**

**Nasr-El-Din, H., Hornof, V. and Neale, G. (1987), "Radial fingering in a water-wet porous medium", Revue de l'Institut Français du Pétrole, vol. 42, n°6, p 783-796.**

**Neale, G.H., Hornof, V. and Chiwetelu, C. (1981), "Importance of lignosulfonates in petroleum recovery operations", Canadian Journal of Chemistry, vol. 59, p 1938-1943.**

**Ni, L.W., Hornof, V. and Neale, G. (1986), "Radial fingering in porous medium", Revue de l'Institut Français du Pétrole, vol. 41, n°2, p 217-228.**

**Okandan, E. (1984), Heavy crude oil recovery. Martinus Nijhoff Publishers.**

**Page, C.A., Brooks, H.J. and Neale, G.H. (1993), "Visualization of the effects of buoyancy on liquid-liquid displacements in vertically-aligned porous medium cell", Experiments in Fluids, vol. 13, p 472-474.**

**Paterson, L., Hornof, V. and Neale G. (1982), "A consolidated porous medium for the visualization of unstable displacements", Powder Technology, vol. 33 p 265-268.**

**Paterson, L., Hornof, V. and Neale, G. (1984), "Water fingering into an porous medium saturated with oil at connate water saturation", Revue de l'Institut Français du Pétrole, vol. 39, n°4, p 517-522.**

**Perkins, T.K. and Johnston, Q.C. (1969), "A study of immiscible fingering in linear model", Journal of Society of Petroleum Engineers, vol. 9, p 39-45.**

**Peters, E.J., Broman Jr, W.H. and Broman, J.A. (1984), "A stability theory for miscible displacement", Society of Petroleum Engineering Journal, vol. 279, p 1-12.**

**Peters, E.J. and Cavalero, S.R. (1990), "The fractal nature of viscous fingering in porous media", Paper SPE 20491 presented at the 65<sup>th</sup> Annual Technical Conference and Exhibition held in New Orleans, LA, p 225-230.**

**Society of Petroleum Engineers. (1983), "Oil from earth".**

**Thibodeau, L., Guo, T. and Neale, G.H. (1997), "Effects of connate water on immiscible displacement processes in porous media", Powder Technology, vol. 93, p 209-217.**

**Thibodeau L. and Neale, G.H. (1998), "Effects of connate water on chemical flooding processes in porous media" Journal of Petroleum Science and Engineering, vol. 19, p 159-169.**

**Thirunavu, S.R. and Neale, G.H. (1995), "Effects of buoyancy forces on immiscible water/oil displacements in a vertically-oriented porous medium", Revue de l'Institut Français du Pétrole, vol. 50, n°4, p517-535.**

**Van Poolen, H.K. and Associates Inc. (1980), Fundamentals of enhanced oil recovery. PennWell Publishing Company, Tulsa, Oklahoma.**

**Wheeler, R.R. and Whited, M. (1985), From prospect to pipeline. Fifth Edition, Gulf Publishing Company, Houston, Texas.**

**Wolfson, R. and Pasachoff, J.M. (1987), Physics, Little, Brown and Company Boston, Toronto, p 382.**